AD-A121 111 SURFACE PHYSICS AND CHEMISTRY OF ELECTRICAL CONTACT PHENOMENA(U) SYRACUSE UNIV N Y DEPT OF CHEMICAL ENGINEERING AND MATERIALS SCIENCE R W VOOK 24 SEP 82 1/2

UNCLASSIFIED 1982-1-ONR N000014-79-C-0763 F/G 20/3 NL

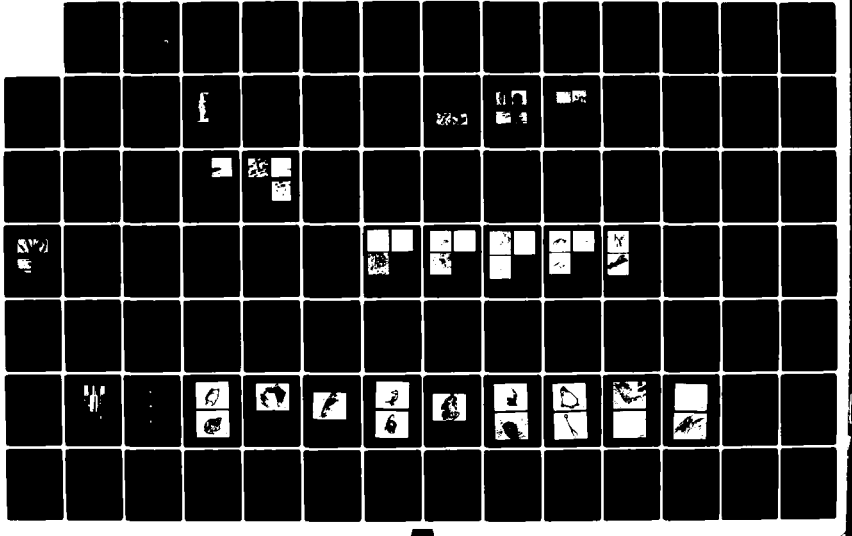

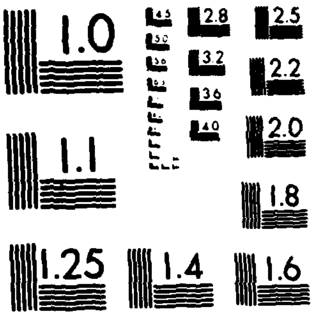

MICROCOPY RESOLUTION TEST CHART
NATIONAL BUREAU OF STANDARDS-1963-A

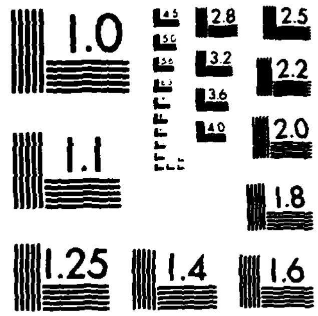

MICROCOPY RESOLUTION TEST CHART
NATIONAL BUREAU OF STANDARDS-1963-A

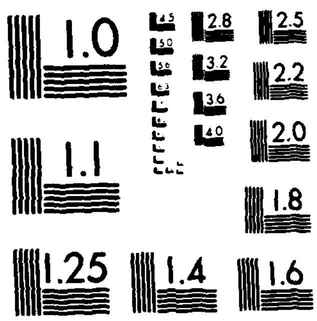

MICROCOPY RESOLUTION TEST CHART
NATIONAL BUREAU OF STANDARDS-1963-A

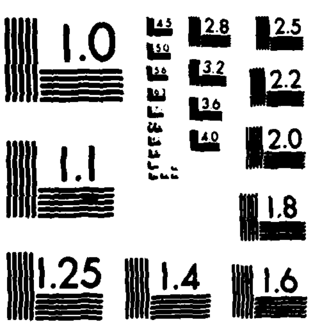

MICROCOPY RESOLUTION TEST CHART
NATIONAL BUREAU OF STANDARDS-1963-A

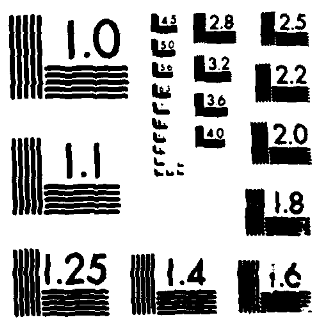

MICROCOPY RESOLUTION TEST CH
NATIONAL BUREAU OF STANDARDS-1963-A

SECURITY CLASSIFICATION OF THIS PAGE (When Data Entered)

REPORT DOCUMENTATION PAGE	READ INSTRUCTIONS BEFORE COMPLETING FORM
1. REPORT NUMBER: ONR-1982-1 (12)	2. GOVT ACCESSION NO.: AD-A121111 / 3. RECIPIENT'S CATALOG NUMBER:
4. TITLE (and Subtitle): Surface Physics and Chemistry of Electrical Contact Phenomena	5. TYPE OF REPORT & PERIOD COVERED: Final Report: 10/1/81-9/30/82
	6. PERFORMING ORG. REPORT NUMBER:
7. AUTHOR(s): Richard W. Vook	8. CONTRACT OR GRANT NUMBER(s): N00014-79-C-0763
9. PERFORMING ORGANIZATION NAME AND ADDRESS: Syracuse University, Dept. of Chemical Engineering and Materials Science, 409 Link Hall, Syracuse, NY 13210	10. PROGRAM ELEMENT, PROJECT, TASK AREA & WORK UNIT NUMBERS:
11. CONTROLLING OFFICE NAME AND ADDRESS: Dr. William Ruff, Mechanics, Materials Science Division 22217, Office of Naval Research, 800 N. Quincy, Arlington, VA	12. REPORT DATE: September 24, 1982
	13. NUMBER OF PAGES:
14. MONITORING AGENCY NAME & ADDRESS (if different from Controlling Office)	15. SECURITY CLASS. (of this report): Unclassified
	15a. DECLASSIFICATION/DOWNGRADING SCHEDULE:

16. DISTRIBUTION STATEMENT (of this Report)

Distribution List is attached to this report

This document has been approved for public release and sale; its distribution is unlimited.

17. DISTRIBUTION STATEMENT (of the abstract entered in Block 20, if different from Report)

DTIC ELECTE 4 NOV 1982 H

18. SUPPLEMENTARY NOTES

19. KEY WORDS (Continue on reverse side if necessary and identify by block number)

Friction, wear, electrical contact resistance
Auger electron spectroscopy
Scanning electron microscopy and x-ray energy spectroscopy

20. ABSTRACT (Continue on reverse side if necessary and identify by block number)

Rotating electrical contacts have been characterized with respect to friction, wear electrical contact resistance, current carrying capacity, and the elemental chemical composition of the surfaces of the slip ring, brush wire ends, and wear particles. Previous work in which both the slip ring and the brush wire were made of Cu was extended to Ag wire brushes running on a Cu slip ring. The transfer of metal from brush to slip ring and vice versa as well as to the wear particles was studied for contacts lubricated by 1 atm of humidified CO_2 as a function of current. The results are embodied in 6 papers attached to this report. (con't.)

DD FORM 1 JAN 73 1473 EDITION OF 1 NOV 65 IS OBSOLETE

82 10 04 166

Unclassified

SECURITY CLASSIFICATION OF THIS PAGE (When Data Entered)

AD A121111

DTIC FILE COPY

20. The most interesting results were the observation that wear occurred chiefly on the harder Cu component and that the "molecular ball bearing" hypothesis for lubrication by H_2O-CO_2 molecules could be applied to both Cu-Cu and Ag-Cu sliding contacts.

FINAL REPORT

October 1, 1981 - September 30, 1982

SURFACE PHYSICS AND CHEMISTRY OF ELECTRICAL CONTACT PHENOMENA

by

Dr. Richard W. Vook
(Phone: 315-423-3466)
Professor of Materials Science
Syracuse University, Syracuse, NY 13210

Research supported by the Office of Naval Research on
Contract No. N00014-79-C-0763
September 23, 1982

ONR-1982-1

TABLE OF CONTENTS

SUMMARY

This report covers research dealing with the application of modern surface science and microstructural analysis techniques to the physical, chemical and mechanical properties of current-carrying, rotating electrical contacts operating in controlled environments. In all cases fine wire brushes were used to transmit current to a rotating OFHC Cu slip ring. In previous years our efforts were devoted to systems in which the brush wires were also made of Cu. During the past year, however, fine Ag wires were used in the brushes in order to be able to study the transfer of material from brush to slip ring and vice versa, as well as the formation of wear debris. It was found that at low currents, the principal wear mechanism was abrasive wear resulting in an overwhelming preponderance of the harder Cu material in the wear particles. Thus the softer Ag wire brushes preferentially wear the Cu slip ring rather than vice versa. A model explaining this unexpected result was developed. In the high current regime, partial melting occurs and the wear particles become mixed, approximately 50% Cu and 50% Ag. At extremely high currents, melting and subsequent welding phenomena are so severe that intense arcing results from the resulting stick-slip phenomena. The results of these experiments have clarified many of the complex mechanisms involved in electrical contact processes.

I. REPORT

A. Research highlights

In the earlier work involving current carrying Cu wire brushes in contact with a rotating Cu slip ring, two kinds of experiments were carried out. One involved rotating in an ultra high vacuum (Appendix I). In these experiments the initial electrical contact resistance decreased until a stable value was obtained; the interfacial impurity content decreased as the contaminants were buried in the surface layers; and the friction increased until cold welding occurred. The wear particles consisted principally of rolled up layers, indicative of abrasive wear followed by rolling in the interface between brush and slip ring, where the particles were trapped for a period of time.

In the other set of experiments (Appendices II and III), rotation was carried out in a humidified CO_2 environment at pressures of 1×10^{-4} torr and 1 atm respectively, the former giving results intermediate between the UHV and the 1 atm. cases. In the latter case the electrical contact resistance decreased as the contact spots were "run in", the friction decreased to a stable value, and the concentration of surface contaminants decreased to almost zero. Some residual S remained on the surface as a result of impurities in the CO_2 source, but no oxygen and very little carbon was detected after rotation. The results clearly show that rotation in gaseous H_2O-CO_2 does not contaminate the surface. Oxides, for example, are not formed. Rather, just as in the UHV case, impurities tend to be buried in the surface layers as a result of bulk-surface intermixing caused by the mechanical disturbance of the surface as the slip ring rotates under the brush. Auger depth profiling confirmed this result. Moreover, wet CO_2 was found to be an excellent lubricant for the Cu-Cu interface.

These results led to a qualitative model for this system. Namely that perfectly clean Cu surfaces can slide against each other with low friction and low electrical contact resistance in the presence of 1 atm of humidified CO_2. The H_2O-CO_2 molecules act like "molecular ball bearings," largely preventing adhesive wear from occurring. Wear takes place only when this intermediate layer is momentarily broken and cold welding occurs, resulting eventually in a wear particle which rolls for a while in the interfacial region between brush and slip ring before falling away. The low values of electrical contact resistance may arise from an electron tunneling phenomenon through the H_2O-CO_2 layer or simply from an electron scattering mechanism, as has been previously observed in the adsorption of gases on current carrying metal films. Other mechanisms are also possible. In the former case an estimate of the thickness of the H_2O-CO_2 film led to a value of approximately 6 Å. This value indicates a layer one to three molecules thick.

One phenomenon which could not be investigated in the Cu-Cu system was the transfer of material back and forth across the brush-slip ring interface and to the wear particles. For this reason, work involving a Cu slip ring and Ag wire brushes was carried out. The experiments of this past year dealt almost exclusively with this system. The results so far are given in Appendices IV, V, and VI.

Only a few experiments were carried out in UHV because stick-slip and arcing phenomena occurred almost immediately after rotation began. Thus the bulk of the experiments were carried out in 1 atm of humidified CO_2. As in the Cu-Cu case, the electrical contact resistance for Ag-Cu decreased to values in the range of 0.1 to 0.3 mΩ, irregardless of the d.c. current in the range

of 0 - 40 A. The coefficient of friction decreased to a more or less steady value of 0.25. Thus wet CO_2 was found to be a good lubricant for both the Ag-Cu and Cu-Cu interfaces. This result is not surprising on the basis of the "molecular ball-bearing" hypothesis because chemical reactions at the Ag and Cu surfaces apparently do not occur at any significant rate in an H_2O-CO_2 atmosphere.

The principal focus of the work on Ag-Cu sliding electrical contacts was on metal transfer phenomena. It was found that Ag and Cu were transferred back and forth between the two contacts. Thus Ag was transferred to the Cu slip ring in the normal adhesive wear manner. However, Cu was also transferred to the Ag wire brush ends. This latter result was surprising in light of the fact that Cu is harder than Ag. A tentative explanation of this phenomenon in terms of prow formation was given (Appendix VI).

In the 0-40 A current range, four wear mechanisms were detected: abrasive, adhesive, polishing, and melting. Measurements were made using a 40g contact force and after 6000 revolutions. It was shown that abrasive wear dominated in the current range up to a few amperes. Almost all the wear particles in this region were pure Cu or Cu-rich. Moreover AES investigations showed that only a small, approximately constant amount of Ag was transferred to the Cu slip ring in this current range. Thus, as mentioned earlier, the softer Ag wire brush (consisting of 342 0.005" diameter Ag wires) preferentially wears away the harder Cu slip ring.

A maximum in the fraction of Cu and Cu-rich wear particles in the debris occurs in the 1-10 A range, probably because the temperatures generated in the interface are sufficient to desorb the H_2O-CO_2 molecules, thereby allowing the

the abrasive wear mechanism to become more effective. At currents up to 40 A, melting phenomena become increasingly important resulting in intermixing of Cu and Ag in the wear particles. Moreover transfer of Ag to the Cu slip ring increases very rapidly with increasing current beyond 10 A. At 50 A melting and subsequent solidification, resulting in welding and a stick-slip behavior, are by far the dominant processes. As a result severe arcing occurs and the wear debris has a large component which consists of spherical particles that were formed from melting and solidification phenomena. The results of these experiments have led to important insights into the nature of the processes associated with sliding electrical contacts.

B. Equipment used

The experiments were performed in a stainless steel UHV system in which a rotating slip ring was turned by means of a magnetically coupled rotary feedthru. This feedthru was turned by a motor, the current to which as well as the angular velocity of the feedthru were measures of the friction encountered at the brush-slip ring interface. Electrical contact resistance at each interface was measured in situ by a potentiometric technique. The surface elemental concentration was determined by Auger electron spectrocopy. The cylindrical mirror analyzer was interfaced to a Hewlett-Packard 9825A desktop computer for data storage, analysis, and plotting. The surface of the slip ring was sputter etched by means of an argon sputter ion gun. Wear particles were collected in a tray located beneath the sliding interface. These wear particles were investigated ex situ by scanning electron microscopy and x-ray energy spectroscopy along with the slip ring and brush wire end surfaces. On occasion the wear particles were studied also by x-ray diffraction and transmission/reflection high energy

electron diffraction techniques. Another small UHV system was designed and constructed for use on long duration sliding electrical contact tests. It was completed just in time for the contract to end.

C. Personnel and activities

Dr. Richard W. Vook, Professor of Materials Science, acted as Principal Investigator on the project. During the past year he was assisted by Dr. Bhoj Singh (who left us at the end of October 1981) and Dr. Arindam Banerjee, who joined us on December 1, 1982. Dr. Banerjee was on leave as a Lecturer in the Physics Department of the Indian Institute of Technology in New Delhi, India. Some very important research in the area of friction and wear is being carried out at this Institute, involving mainly coatings on cutting tools. Mr. B. H. Hwang who worked on the project last year, received his M.S. in Solid State Science and Technology in June of 1981. Mr. M. Garshasb, a graduate research assistant, joined the project in June of 1981. He is presently working on his Ph.D. in Solid State Science and Technology. Two other visiting research scientists, Mr. J. A. Zhang and Mr. L. R. Zhang, worked as unpaid participants on the project during the past year. They were on leave from the Peking Institute of Posts and Telecommunications, where each is a Lecturer.

The work that was carried out led to the numerous presentations and publications listed in the next two sections.

II. PUBLICATIONS OF ONR SUPPORTED RESEARCH: 1978 - PRESENT

1. "Elemental Surface Composition of Slip Ring Copper as a Function of Temperature," R. W. Vook, B. Singh, E.-A. Knabbe, J. H. Ho, and D. K. Bhavsar, Electrical Contacts, 1979 (I.I.T. Chicago), 17-21 (1979)
and
IEEE Transactions on Components, Hybrids, and Manufacturing Technology, Vol. CHMT-3, 9-12 (1980).

2. "AES Study of Sulfur Segregation on Polycrystalline Copper," B. Singh, R. W. Vook and E.-A. Knabbe. Read at the 26th AVS Symposium held in New York,Oct. 1-5, 1979, Jour. of Vac. Sci. and Tech., 17, 29-33 (1980).

3. "In Situ AES Characterization of Rotating Electrical Contacts," B. Singh and R. W. Vook, Electrical Contacts, 1980 (I.I.T. Chicago), 53-58 (1980).
and
IEEE Transactions on Components, Hybrids, and Manufacturing Technology, Vol. CHMT-4, 36-40 (1981).

4. "Interfacial Characterization of Copper Slip Ring-Wire Brush Contacts," B. Singh and R. W. Vook, Proceedings of the 8th International Vacuum Congress at Cannes, France, Vol. II, Vacuum Technology and Vacuum Metallurgy, 441-444, 1980,(Suppl. a la Revue << Le Vide, les Couches Minces >> #201).

5. "Characterization of Copper Slip Ring-Wire Brush Electrical Contacts", B. Singh, B. H. Hwang and R. W. Vook, Accepted for publication in Vacuum 32 (1982) 23.

6. "In Situ AES Characterization of Wet CO_2 Lubricated Sliding Copper Electrical Contacts," B. H. Hwang, B. Singh, R. W. Vook and J. G. Zhang, Accepted for publication in Electrical Contacts 1981 (I.I.T. Chicago) (1981) p. 273. Wear 78 (1982) 7.

7. "Microstructural Characterization of Rotating Cu-Cu Electrical Contacts in Vacuum and Wet CO_2 Environments," B. Singh, J. G. Zhang, B. H. Hwant, and R. W. Vook. Electrical Contacts - 1981 (I.I.T. Chicago) p. 279. Wear 78 (1982) 17.

8. "Characterization of Ag Wire Brush-Cu Slip Ring Electrical Contacts Rotating in Wet CO_2," R. W. Vook, J. G. Zhang, A. Banerjee, M. Garshasb, and L. R. Zhang. Electrical Contacts - 1982 (I.I.T. Chicago) p. 193 (1982). To be published in I.E.E.E. Transactions on Components, Hybrids, and Manufacturing Technology.

9. "Wear Debris Analysis in Rotating Ag-Cu Electrical Contacts," A. Banerjee, J. G. Zhang, M. Garshasb, L. R. Zhang, and R. W. Vook. Accepted (Aug. 1982) for publication in Wear.

10. "Electric Current Effects in Wear Phenomena at a Rotating Cu-Ag Interface," A. Banerjee, M. Garshasb, L. R. Zhang, J. G. Zhang, and R. W. Vook. Submitted to Wear.

III. LECTURES, SEMINARS, PRESENTATIONS FOCUSING ON ONR SUPPORTED RESEARCH

1.	Jan. 15-16, 1979	Third DARPA workshop on Advanced Current Collection, Coral Springs, Florida, "Surface Physics of Electrical Contact Phenomena."
2.	Sept. 10-12, 1979	25th Holm Conference on Electrical Contacts, I.I.T. Chicago, "Elemental Surface Composition of Slip Ring Copper as a Function of Temperature."
3.	Oct. 2-5, 1979	American Vacuum Society Symposium, New York, NY, "AES Study of Sulfur Surface Segregation on Polycrystalline Copper."
4.	Oct. 24-26, 1979	Fourth DARPA workshop on Advanced Current Collection , Pittsburgh,PA, "Slip Ring and Film Evaporation,"
5.	Sept. 22-26, 1980	Eighth International Vacuum Congress-Vacuum Technology and Vacuum Metallurgy, Cannes, France, "Interfacial Characterization of Copper Slip Ring-Wire Brush Contacts.
6.	Sept. 29-Oct 1, 1980	26th Holm Conference on Electrical Contacts, I.I.T. Chicago, "In Situ AES Characerization of Rotating Electrical Contacts" Written presentation only.
7.	Jan. 6, 1981	Fifth DARPA Advanced Current Collection workshop, Pittsburgh, PA, "SEM/AUGER Studies at Syracuse University."
8.	Sept. 21-23, 1981	27th Holm Conference on Electrical Contacts, I.I.T. Chicago, "In Situ AES Characterization of Wet CO_2 Lubricated Sliding Electrical Contacts."
9.	Sept. 23-25, 1981	Advanced Current Collection Conference, Chicago, "Microstructural Characterization of Rotating Cu-Cu Electrical Contacts in Vacuum and Wet CO_2 Environments."
10.	Sept. 13-15, 1982	28th Holm Conference on Electrical Contacts, I.I.T. Chicago, "Characterization of Ag Wire Brush-Cu Slip Ring Electrical Contacts Rotating in Wet CO_2."

APPENDIX I

Microstructural Characterization of Rotating Cu-Cu Electrical Contacts in Vacuum and Wet CO_2 Environments

by

B. Singh, J. G. Zhang, B. H. Hwang, and R. W. Vook

Wear 78(1982)17-28

Wear, 78 (1982) 17 - 28

MICROSTRUCTURAL CHARACTERIZATION OF ROTATING Cu–Cu ELECTRICAL CONTACTS IN VACUUM AND WET CO_2 ENVIRONMENTS*

B. SINGH, J. G. ZHANG, B. H. HWANG and R. W. VOOK

Department of Chemical Engineering and Materials Science, Syracuse University, Syracuse, NY 13210 (U.S.A.)

(Received November 5, 1981)

Summary

The chemical, electrical and wear properties of the rotating interface between OFHC copper slip rings and two high purity copper wire brushes were investigated *in situ* in ultrahigh vacuum (UHV) and in 1 atm wet CO_2. The chemical composition of the slip ring surface was determined by Auger electron spectroscopy. The contact resistance was measured by a potentiometric four-point probe technique while the wear properties of the interface and the morphology of the debris were studied by frictional force, scanning electron microscopy (SEM), transmission electron diffraction (TED) and X-ray diffraction (XRD) measurements. Rotation in UHV of a conventionally cleaned (CC) slip ring produced a much cleaner surface. The contact resistance of both brush interfaces decreased and the frictional force increased with increasing number of revolutions. After many revolutions the brush and slip ring welded. The decrease in contact resistance with the number of slip ring revolutions more or less paralleled the decrease in total impurities. Rotation in wet CO_2 of a CC slip ring and brushes also produced much cleaner surfaces. In contrast, initially argon ion sputter-cleaned surfaces became slightly contaminated (mainly carbon and sulfur) when rotated. The contact resistance at both interfaces and the coefficient of friction decreased with increasing number of slip ring revolutions, finally reaching steady state values.

After each experiment, SEM examination of vacuum rotated surfaces showed deep ridges and broken pieces of material on the slip ring surface and badly deformed brush wire ends. Wet CO_2 rotated surfaces were relatively smooth and shallow ridges were seen. SEM examination of wear particles collected during rotation indicated that they may have come from both the slip ring and brush wire materials and were rolled in the regions between the brush and slip ring. XRD and TED from individual particles showed a randomly oriented polycrystalline microstructure. The particles collected from the wet CO_2 experiments were much smaller in size than those collected

*Paper presented at the Advanced Current Collection Conference, Chicago, IL, U.S.A., September 23 - 25, 1981.

Elsevier Sequoia/Printed in The Netherlands

in vacuum experiments. In wet CO_2, the contact resistance was interpreted as being predominantly due to an electron tunneling mechanism through the CO_2–H_2O molecular layer at the interface. As expected, the thickness of the layer appeared to vary with the contact pressure. Friction would then arise largely when the molecular layer was occasionally broken, allowing intimate contact and temporary welding of the brush and slip ring surfaces. Subsequent fracture of these welds during continued rotation would initiate the formation of wear particles.

---

1. Introduction

Over the last 20 years, considerable effort has been made theoretically [1, 2] and experimentally [3 - 5] to reduce friction, wear and contact resistance between dynamic interfaces. Attempts have hitherto been made to devise conditions to yield minimum contact resistance and minimum friction and wear between the brushes and slip ring. The brush and slip ring materials and the contact load and environment are the most influential parameters affecting these properties. There are various techniques and surface tools available for the study of the atomic nature of the wear surfaces [6]. In this paper, Cu–Cu dynamic contact interfaces are characterized in vacuum and in 1 atm of wet CO_2 by measuring contact resistance, frictional force, chemical composition and mechanical wear. A morphological and microstructural study of the debris formed during sliding contact provided important information about their origins and evolution. While there are various techniques [7, 8] available for a morphological analysis of the wear debris, the techniques of scanning electron microscopy (SEM), X-ray diffraction (XRD) and transmission electron diffraction (TED) were used in the present study.

2. Slip ring–brush arrangement and experimental procedure

The brush–slip ring arrangement has already been described in greater detail elsewhere [9, 10]. A stainless steel ultrahigh vacuum (UHV) system of low (10^{-10} Torr) range capability was used to characterize rotating electrical contacts. Figure 1 shows the arrangement of the copper slip ring which rotates in contact with two copper wire brushes. The slip ring is axially attached to a magnetically coupled rotary feedthrough, which is turned by an a.c. motor coupled to it by a rubber belt. The slip ring is of cylindrical shape, 2.5 cm in diameter, composed of OFHC (99.98%) copper. The brushes each consist of 362 99.999% Cu wires, each 0.127 mm in diameter. The brushes are clamped to two rectangularly shaped stainless steel electrodes, each having a smooth hinge in the middle. The brushes are arranged at 180° to each other, making an approximately 40° - 45° angle with the normal to the slip ring surface and axially displaced (1 - 1.5 cm) to make separate tracks on the slip ring. The

Fig. 1. Photograph of the slip ring brush assembly: M, magnetically coupled rotary feedthrough; H, brush holder; R, slip ring; B, brush; S, spring; F, vacuum flange.

whole brush–slip ring assembly is mounted on a specimen manipulator capable of X, Y, Z displacements. The UHV system includes an Auger cylindrical mirror analyzer, a 3 keV sputter ion gun and a 90° magnetic sector partial pressure analyzer.

Before each experiment, the surfaces of the slip ring and the brush wire ends were mechanically polished with a series of emery papers ending with grit 600A and then rinsed ultrasonically (brush retracted) in acetone and ethanol. The contact resistances between the two brushes and the slip ring (grounded) were recorded on a dual-pen recorder. Experiments were performed with three brush direct currents: 50 mA, 5 A and 30 A in vacuum and 30 A in wet CO_2. With the brushes retracted, the speed of the rotating slip ring was monitored with an optical tachometer. During the experiment,

the rotational speed of the slip ring was measured at regular time intervals together with the input power to the motor.

The Auger electron spectrometer which was used to examine the surface tracks was fully controlled by a Hewlett Packard 9825A desktop computer and multiprogrammer. Typical Auger traces covering a 50 - 1300 eV range were directly digitalized with an energy increment of 0.65 eV or less. Computerized values of peak-to-peak heights of the Auger electron spectroscopy (AES) signals of various elements were obtained with a precision of 1 in 2000. These Auger spectra were taken using a primary beam energy of 3 keV, a modulation amplitude of 1 V (peak to peak) and a 25 μA beam current.

A wet CO_2 environment in the vacuum system was obtained by running CO_2 from the cylinders (commercial grade, 99.8%) through a doubly distilled H_2O–CO_2 solution in a stainless steel trap and finally through a UHV leak valve [11]. The pressure of wet CO_2 in the vacuum system during the course of the rotation experiments was approximately atmospheric. Auger spectra from the wet CO_2 rotated slip ring surface were taken only after the wet CO_2 was pumped down to the high 10^{-8} Torr region, a process which took about 2 days. A molybdenum sheet tray was placed inside the vacuum chamber under the brush–slip ring assembly to collect wear particles during contact rotation.

After the experiment was over, the slip ring assembly and wear debris were removed from the chamber. The normal force on each brush was measured. The average frictional force was determined from the decrease in rotational speed of the slip ring by comparing it with a calibration involving known torques applied to the slip ring in a separate experiment in air. SEM pictures were taken of both the slip ring surface tracks, brush contact surfaces and of wear particles. XRD photographs were obtained from relatively large particles (about 0.5 mm) and TED photographs were taken from small particles (about 0.05 mm or less).

3. Results

3.1. Contact resistance and friction measurements

Figure 2 shows the contact resistance for both the upper and the lower interfaces and the average coefficient of friction as a function of the number of slip ring rotations or linear track length covered. The contact resistance decreased with increasing number of slip ring revolutions. The curves are more or less parallel to each other, indicating that the initial conditions determine whether a curve is "high" or "low". These initial conditions include such variables as contact force, lead resistance, brush wire orientation with respect to slip ring, surface impurities etc. The contact resistances in the wet CO_2 experiments are consistently higher than those in the vacuum experiments and result in much smoother curves. This high contact resistance could be due to the lower normal force, smaller contact area and the addi-

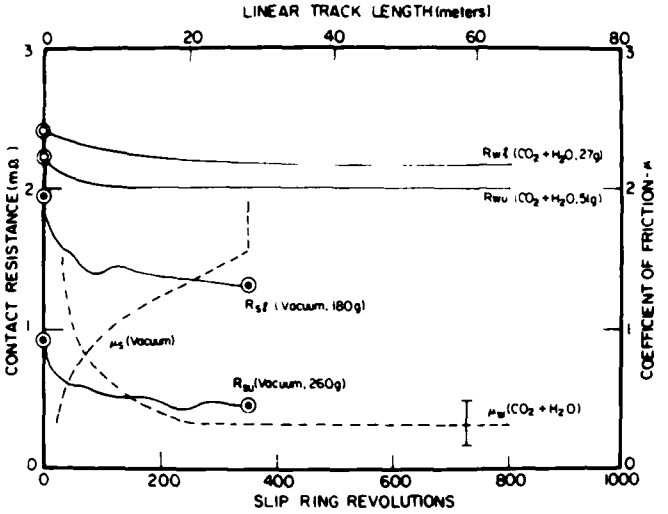

Fig. 2. Contact resistance and average coefficient of friction *vs.* number of slip ring revolutions. Subscripts s, w, u and l denote strong spring, weak spring, upper brush interface and lower brush interface respectively.

tional resistance introduced by the thin wet CO_2 layer at the interface. The circled points indicate the contact resistance before the slip ring started rotating and after it stopped. For wet CO_2, the slip ring rotation did not stop, but the experiment was terminated after about 5 - 10 min of rotation when the resistance attained steady state values. The resistance of the interfaces clearly depended on the magnitude of the contact force. In vacuum experiments, the frictional force increased substantially as the rotation proceeded and finally after many hundreds of revolutions the motor stopped rotating because of excessive friction and ultimate cold welding. The average coefficient μ of friction was calculated from the ratio of the frictional force to the measured normal force and is shown in Fig. 2 for both the vacuum and wet CO_2 experiments. For the vacuum experiment it increased by a factor of more than 4 while for wet CO_2 it decreased to about 0.35 where it remained relatively stable.

3.2. Auger electron spectroscopy measurements

In the vacuum experiments, the elemental surface compositions of both the upper and lower tracks on the slip ring were obtained by AES before and immediately after the contact resistance measurements. However, in the wet CO_2 experiments Auger spectra were taken about 2 days after the contact rotation because the system had to be pumped down to the high 10^{-8} Torr region before operating the Auger spectrometer. The brushes were retracted during the AES measurements and the slip ring was continuously rotated. This procedure gave the average impurity concentrations on the whole track.

TABLE 1

Elemental concentrations (at.%) on slip ring tracks for rotation in vacuum (contact force, 235 gf) and wet CO_2 (contact force, 51 gf)

Elements	*Vacuum*		*Wet CO_2*		
	Before rotation	*After rotation*	*Before sputtering*	*After sputtering*	*After rotation*
Cu	47.5	97.1	39.9	99.4	88.0
S	0.8	0.1	0.0	0.0	4.7
C	42.1	2.0	40.9	0.6	7.3
O	7.1	0.4	14.2	0.0	0.0
Balance (Cl, N, Ar)	2.5	0.4	5.0	0.0	0.0

The peak-to-peak heights of all Auger signals were normalized [12, 13] to atomic per cent concentrations. The elemental surface concentrations on the slip ring for two typical experiments in vacuum and wet CO_2 are given in Table 1. The copper, sulfur, carbon and oxygen concentrations are listed together with the impurity balance. In vacuum rotated experiments the conventionally cleaned (CC) interface became cleaner, while in the wet CO_2 experiments the sputter-cleaned interface became only slightly contaminated. The impurities picked up were sulfur and carbon. Argon ion sputter depth profiles of the slip ring surface showed that these impurities were rapidly removed by small amounts of ion etching.

To understand the cause of the high concentration of sulfur, an additional experiment was performed in which the brush–slip ring assembly was replaced by a flat OFHC copper sample. The sample was first sputtered clean (to 98 at.% Cu, 0.2 at.% S) and then heated to 585 °C for 30 min where 9 at.% of sulfur segregation was detected [14]. Sulfur was removed by argon ion sputter depth profiling techniques and its concentration was monitored as a function of sputtering time. After it was almost completely removed (0.2 at.%), the clean sample was exposed to 1 atm of wet CO_2, resulting in a surface concentration of 7 at.% of sulfur. The sulfur concentration was again removed by sputter depth profiling. The results are shown in Fig. 3. It is clear that the adsorbed sulfur is removed much faster than the bulk segregated sulfur. Thus the high concentration of sulfur on the slip ring surface was due to an impurity in the wet CO_2 supply and not to bulk segregation.

3.3. Scanning electron microscopy

After each experiment, the brush–slip ring assembly and wear particles collected during rotation were removed from the vacuum chamber and examined by SEM. For the same period of rotation, the quantity and size of the debris collected in vacuum experiments were larger than those in the wet CO_2 experiments. The average length of vacuum wear particles was about 0.3 - 0.5 mm while for wet CO_2 the length of the wear particles was about

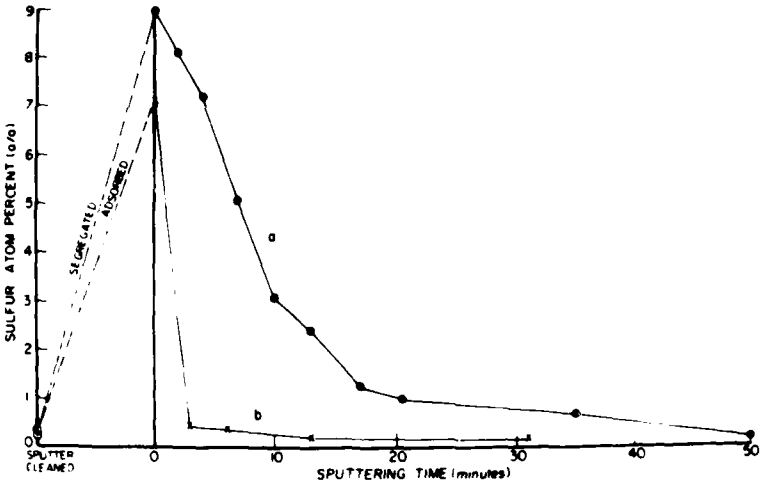

Fig. 3. Sputter depth profile of sulfur on a flat OFHC copper sample: curve a, segregated on heating at 585 °C for 30 min; curve b, adsorbed on exposure to 1 atm wet CO_2 at room temperature for 15 min.

Fig. 4. SEM photograph of copper wear particles collected during slip ring rotation in contact with brushes in wet CO_2.

Fig. 5. SEM photograph of copper wear particles collected during slip ring rotation in contact with brushes in wet CO_2.

0.03 - 0.08 mm. SEM photographs of several particles from the wet CO_2 experiments are shown in Fig. 4. Figure 5 shows details of the structure of two typical wear particles collected in a wet CO_2 experiment. The morphology of these particles suggests that they are rolled layers or rolled particles. Figure 6 shows a particle collected from a vacuum experiment. XRD was carried out on large individual particles by mounting them on a glass fiber and by using a transmission pinhole technique. The very small

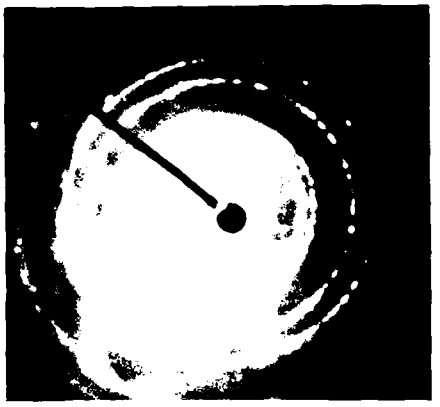

Fig. 6. SEM photograph of copper wear particle collected during slip ring rotation in contact with wire brushes in vacuum. Particles of silver paint on the substrate should be noted.

Fig. 7. TED photograph of a small wear particle collected while the slip ring rotated in contact with a wire brush in wet CO_2.

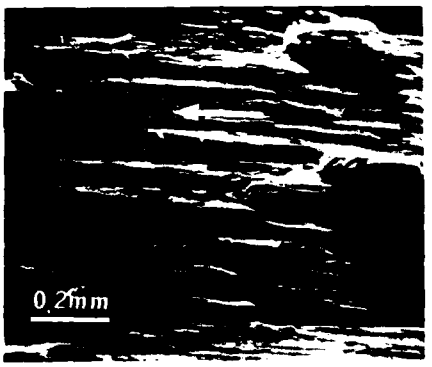

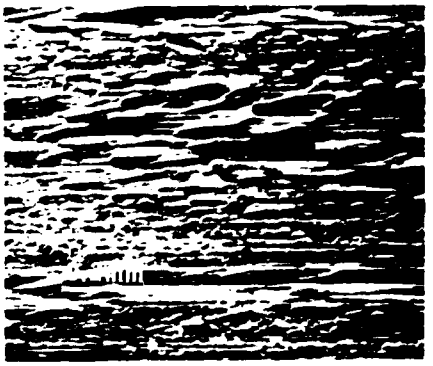

Fig. 8. SEM photograph of OFHC copper slip ring, upper track, showing broken wire pieces (W) and deep ridges. The arrow indicates the direction of relative brush motion (high vacuum).

Fig. 9. SEM photograph of OFHC copper slip ring, upper track, showing shallow ridges. The arrow indicates the direction of relative brush motion (wet CO_2).

particles were difficult to mount in such a way and therefore their individual diffraction patterns were studied by TED. The results from XRD studies of large particles were identical with those obtained by TED from small particles. Figure 7 shows a TED pattern obtained from a small particle. The absence of preferred orientation is apparent.

Figures 8 and 9 show typical SEM pictures of brush tracks on slip rings rotated in vacuum and in wet CO_2 respectively. The surface from the vacuum

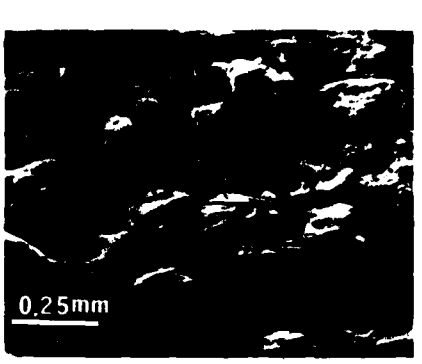

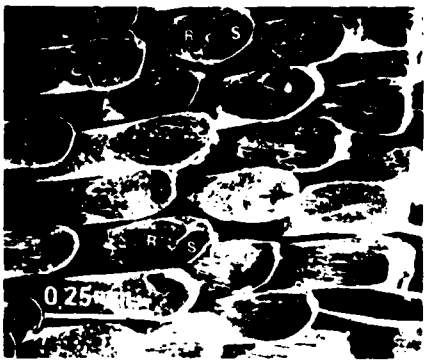

Fig. 10. SEM photograph of wear surfaces on upper brush copper wires (contact force, 235 gf). The arrow indicates the direction of relative motion of the slip ring (high vacuum).

Fig. 11. SEM photograph of wear surfaces on upper brush copper wires (contact force, 51 gf). The arrow indicates the direction of relative motion of the slip ring (wet CO_2).

experiment shows deep grooves and high ridges and several pieces of brush wire wear particles adhering to the surface. The wet CO_2 rotated surface shows shallow grooves and low ridges with a few occasional deep ridges. Also, no wear particles are observable. The ridges shown in these micrographs lie parallel to the directions of travel. SEM pictures of brush ends are shown in Figs. 10 and 11 for vacuum and wet CO_2 experiments. The vacuum contact brush wire ends appear very rough and abruptly broken, while the wet CO_2 contact brush wire ends are much smoother and of round shape. In Fig. 11, two regions S and R are clearly seen on the wire ends. The smooth (S) regions touched the slip ring and the rough (R) and long streaked regions were produced by the initial emery paper polishing before insertion in the UHV chamber. These latter regions apparently did not touch the slip ring during rotation.

4. Discussion

The elemental surface compositions of OFHC copper slip rings that rotate in contact with two high purity copper wire brushes in vacuum and in 1 atm of wet CO_2 are presented. In vacuum, the initial CC surfaces (50 at.% Cu) became almost completely clean (98 at.% Cu) after several hundred rotations. Carbon was the major impurity observed. As the surface became cleaner with continued rotation, adhesion, friction and occasional cold welding started to develop. The occasional and erratic stick–slip resulted in large momentary fluctuations in the contact resistance. Finally the adhesion became so large that the motor rotating the slip ring could not overcome the frictional torque and cold welding occurred.

For rotation in wet CO_2, the surface also became clean except for the development of slight sulfur and carbon contamination. The studies involving a flat OFHC copper sample (see Section 3.2) suggest that the sulfur came from an impurity in the CO_2 gas and not as a result of bulk segregation [14]. The carbon concentration was of the same order as that observed in the vacuum experiments. Thus running in wet CO_2 contributed no additional carbon to the surface. In wet CO_2, the rotational speed of the slip ring increased and became steady after a few hundred rotations. Cold welding did not occur. These results indicated that the wet CO_2 environment provided good lubrication [3, 4]. The AES composition of the wet CO_2 surface was taken only when the wet CO_2 was pumped down to the 10^{-8} Torr region which usually took about 30 h. This result means that the H_2O–CO_2 mixture was not very tightly bound to the surface. It is well known that CO_2 is not chemisorbed on copper and its maximum heat of physical adsorption [15] on metals is about 9 kcal mol^{-1}. Water, in contrast, has a heat of adsorption of about 22 - 24 kcal mol^{-1} and is notoriously difficult to remove at room temperature [16]. Thus CO_2 is pumped out much faster than H_2O, which was also observed by the mass spectroscopy analysis of the residual gas. It is thus expected that the H_2O molecules aid in the adsorption of CO_2.

The thickness of the H_2O–CO_2 interfacial layer would be expected to depend on the contact pressure. This result is in agreement with the contact resistance measurements, where the higher normal forces have lower contact resistances. Thus the interfacial resistance appears to arise from a combination of quantum mechanical tunneling through the CO_2–H_2O layer as well as occasional direct brush–slip ring contact, resulting in adhesion and fracture of plastically deformed surface regions. The net effect is that wear particles are formed. A determination of the approximate layer thickness h can be made from an empirical relation [17] $R_f = \rho_t \xi H/F$, where ρ_t is the tunnel resistivity, $\xi \approx 0.7$ is a pressure factor and H is the contact or penetration hardness, based on a tunneling conduction mechanism together with an experimental relationship between ρ_t and h [18]. The results are approximate but indicate that the H_2O–CO_2 layer is about 6 Å thick for a 2.2 mΩ film resistance R_f and 80 gf normal force F. This result is reasonable since it implies a layer of CO_2–H_2O one to three molecules thick. The thickness of the layer also depends on the orientation of the molecules with respect to the substrate as well as with respect to each other. It is thus concluded that the contact resistance at the Cu–Cu interface in wet CO_2 is not due to contamination by carbon or other impurities, but rather arises from the presence of this H_2O–CO_2 layer at the interface. The low contact resistance in vacuum arises from direct metal–metal contact. It decreases during rotation because the initial surface impurities are buried during rotation or possibly partially removed by the fallen wear particles and also because the surface contact area increases.

Formation of the wear particles and the ridges on the slip ring surface are of much interest. In vacuum, deep ridges arise from brush end ploughing and/or random localized welding of brush wire ends to the slip ring during

rotation, resulting in tensile plastic deformation of the weld and then final fracture of the weld material or wire. Continued rotation may pull out some of these broken wire ends or material from the protruded ridges. These pieces then roll over between the brush–slip ring interface and eventually fall away from the interface. Clearly, the wear particles in the vacuum case would be larger in size than those produced on occasional localized metal–metal contact through the thin CO_2–H_2O layer where the weld area is likely to be smaller. This result is what has been observed experimentally. The average length of the vacuum wear particles is 0.3 - 0.5 mm and their diameter is 0.09 - 0.12 mm. The wet CO_2 wear particles have average lengths of 0.03 - 0.08 mm and diameters of 0.02 - 0.04 mm.

The morphologies of the wear particles are more or less the same. Some are made of thin layers rolled as sheets and some with more compacted but still rolled surfaces. There appears to be some relationship between the size of the wear particles, the ridges and the diameter of the brush wires. The average height of the broken wire pieces shown in Fig. 8 (vacuum) is about 0.09 - 0.13 mm, which is close to the diameter of the wires of the brush. It is thus reasonable to suppose that these pieces are parts of the broken wire which cold welded to the slip ring surface as it became cleaner in vacuum. In Fig. 9 (wet CO_2), the lengths of the well-defined ridges vary from about 0.02 to 0.2 mm. The estimated unfolded length of the layer making up the particle in the upper left corner of Fig. 5 is about 0.09 mm, which is within the range of the length of the ridges in Fig. 9. Therefore, it is possible that this particle originally came from the slip ring surface rather than from the wire of the brush. The variation in the length of the ridges could be due to variations in contact force at individual wire ends of the brush. The ridges may be formed by the ploughing action of the wire ends through the surface material of the slip ring. Continued rotation in the case of wet CO_2 tends to smooth these ridges, resulting in burnishing. The vacuum rotated surface has deep and sharp ridges because erratic cold welding prevented burnishing from occurring.

Acknowledgments

The authors would like to express their appreciation to I. R. McNab, J. L. Johnson, P. Reichner, J. J. Schreurs, P. K. Lee and E. Rabinowicz for helpful discussions, the Westinghouse Research and Development Center for the loan of certain equipment, and the Office of Naval Research for financial support under Contract N00014-79-C-0763.

References

1 P. Reichner, Pressure–wear theory for sliding electrical contacts, *Proc. Conf. on Electrical Contacts, 1980*, Illinois Institute of Technology, Chicago, IL, 1980, pp. 25 - 32.

2 C. M. Adkins III and D. Kuhlmann-Wilsdorf, Development of high-performance metal fiberbrushes. II: testing and properties, *Proc. Conf. on Electrical Contacts, 1979*, Illinois Institute of Technology, Chicago, IL, 1979, pp. 171 - 186.

3 P. Reichner, Metallic brushes for extreme high current applications, *Proc. Conf. on Electrical Contacts, 1979*, Illinois Institute of Technology, Chicago, IL, 1979, pp. 191 - 197.

4 J. L. Johnson and O. S. Taylor, High current brushes. Part VI: machine environment tests, *Proc. Conf. on Electrical Contacts, 1979*, Illinois Institute of Technology, Chicago, IL, 1979, pp. 129 - 135.

5 E. Rabinowicz and P. Chan, Wear of silver-graphite brushes against various ring materials at high current densities, *Proc. Conf. on Electrical Contacts, 1979*, Illinois Institute of Technology, Chicago, IL, 1979, pp. 123 - 127.

6 D. H. Buckley, The use of analytical surface tools in the fundamental study of wear, *Wear, 46* (1978) 19 - 53.

7 J. K. Beddow, S. T. Fong and A. F. Vetter, Morphological analysis of metallic wear debris, *Wear, 58* (1980) 201 - 211.

8 A. W. Ruff, Characterization of debris particles recovered from wearing systems, *Wear, 42* (1977) 49 - 62.

9 B. Singh and R. W. Vook, *In situ* AES characterization of rotating electrical contacts, *Proc. Conf. on Electrical Contacts, 1980*, Illinois Institute of Technology, Chicago, IL, 1980, pp. 53 - 58.

10 B. Singh and R. W. Vook, Interfacial characterization of copper slip ring-wire brush contacts, *Proc. 8th Int. Vacuum Congr., Cannes*, Vol. II, *Vacuum Technology and Vacuum Metallurgy*, in *Vide, Couches Minces, Suppl., 201* (1980) 441 - 444.

11 B. Singh, B. H. Hwang and R. W. Vook, Characterization of copper slip ring-wire brush electrical contacts, *J. Vac. Technol., (1981) in the press.*

12 C. C. Chang, Analytical Auger spectrometry. In P. F. Kane and G. B. Larrabee (eds.), *Characterization of Solid Surfaces*, Plenum, New York, 1978, pp. 509 - 561.

13 R. W. Vook, B. Singh, E.-A. Knabbe, J. H. Ho and D. K. Bhavsar, Elemental surface composition of slip ring copper as a function of temperature, *Proc. Conf. on Electrical Contacts, 1979*, Illinois Institute of Technology, Chicago, IL, 1979, pp. 17 - 21.

14 B. Singh, R. W. Vook and E.-A. Knabbe, AES study of sulfur surface segregation on polycrystalline copper, *J. Vac. Sci. Technol., 17* (1) (1980) 29 - 33.

15 G. Wedler, *Chemisorption: An Experimental Approach* (Engl. transl., D. F. Klemperer), Butterworths, Boston, 1976, pp. 198 - 204.

16 R. Glang, R. A. Holmwood and J. A. Kurtz, in L. I. Maissel and R. Glang (eds.), *Handbook of Thin Film Technology*, McGraw-Hill, New York, 1970, p. 2-44.

17 H. N. Wagar, in D. Baker, W. O. Fleckenstein, D. C. Koehler, C. E. Roden and R. Sabice (eds.), *Physical Design of Electronic Systems*, Vol. III, *Integrated Device and Connection Technology*, Prentice-Hall, Princeton, NJ, 1971, p. 465.

18 I. Dietrich, Messung des Widerstandes dünner isolierender Schichten zwischen Goldkontakten im Bereich des Tunneleffektes, *Z. Phys., 132* (1952) 231 - 238.

APPENDIX II

Characterization of Copper Slip Ring-Wire Brush Electrical Contacts

by

B. Singh, B. H. Hwang, and R. W. Vook

Vacuum 32(1982)23

Vacuum/volume 32 number 1 pages 23 to 28/1982
Printed in Great Britain

0042 207X/82/010023 06$02.00 0

Characterization of copper slip ring–wire brush electrical contacts

B Singh, B H Hwang and R W Vook, *Department of Chemical Engineering and Materials Science, Syracuse University, Syracuse, NY 13210, U.S.A.*

received 30 March 1981

The chemical composition and the electrical and mechanical properties of the interface between a Cu slip ring that rotates in contact with two Cu wire brushes were investigated by Auger electron spectroscopy (AES), scanning electron microscopy (SEM), contact resistance, and frictional force measurements. The experiments were carried out in an ultra-high vacuum system and in an environment of 1×10^{-4} torr of wet CO_2. The contact resistance at both the positive and negative interfaces decreased with increasing number of slip ring revolutions while the frictional force increased. Under the wet 10^{-4} torr CO_2 environment the increase in frictional force was smaller than that in high vacuum, which suggests that wet CO_2 has a lubrication effect even at these relatively low pressures. In situ *AES measurements showed that the composition of the slip ring surface, which was initially covered by about 50 atm% of carbon, changed drastically during rotation. After many revolutions it approached that of a clean Cu surface (total impurities < 10 atm%). The decrease in contact resistance with the number of slip ring revolutions more or less paralleled the decrease in total impurities in the high vacuum experiments. This parallelism suggests that the contact resistance is caused predominantly by the surface impurities. No systematic relationship between contact resistance and brush current density was observed. SEM observations showed that the surface material was smeared out in the brush track areas and that the initial surface impurities were buried during rotation.*

I. Introduction

The current-carrying capacity and the dynamic friction and wear properties of electrical contacts are important technological considerations which are presently not very well understood. The application of some of the tools[1–5] of surface science to these problems has brought with it an increased understanding of the complexity of the situation. The present report describes the results obtained in the application of some of these techniques to an *in situ* study of the interface between a rotating slip ring in contact with two wire brushes in high vacuum (10^{-10} torr) and under an environment of 1×10^{-4} torr wet CO_2. It represents the initial stage of a broader research program in which the effects of controlled gaseous environments will be determined. Preliminary results of the high vacuum work were presented at the International Vacuum Conference[6] in Cannes in 1980.

II. Experimental arrangement and method of measurement

A stainless steel uhv system (base pressure mid 10^{-10} torr range) was used to study electrical contact phenomena associated with rotation of a copper slip ring (OFHC-99.98% Cu) in contact with two copper wire brushes (each consisting of 362, 0.005 in. dia. 99.99% Cu wires) running on separate tracks[7]. The brushes were pressed against the slip ring surface by means of an insulated steel spring. They can be removed from the surface by manipulating two linear rotary vacuum feedthroughs. The slip ring is attached to a magnetically coupled rotary vacuum feedthrough which is turned by an ac motor coupled to it by a rubber belt. The uhv system contains an Auger cylindrical mirror analyzer (CMA), a 3 keV sputter ion gun, and a 90° magnetic sector partial pressure analyzer. Schematic arrangements of the vacuum chamber, slip ring-brush assembly, CMA, sputter ion gun, mass spectrometer and linear rotary vacuum feedthroughs are shown in Figures 1 and 2.

The wet CO_2 environment was obtained by the mechanism shown in Figure 3. This arrangement allows for an initial evacuation of the stainless steel tubing via a liquid nitrogen trapped oil diffusion-rotary pump system attached to valve 3 and a final evacuation (with valve 3 closed) through the uhv leak valve into the ion pumped uhv system. In the latter case the gas manifold was baked until a pressure in the low 10^{-8} torr range was achieved in the uhv system. Gases dissolved in the water were flushed out first with helium (via valve 7) and then with CO_2 from the cylinder. The water CO_2 mixture was then doubly distilled by placing successfully liquid nitrogen baths around traps numbers 1 and 2. The water CO_2 mixture in trap 2 was then allowed to melt. Wet CO_2 was then introduced to the uhv system by running CO_2 from the cylinder through valve 4, through the doubly distilled H_2O CO_2 solutions in trap 2, and finally through the uhv leak valve.

The surfaces of the slip ring and the wire brushes were polished smooth with emery paper (grit 600-A) and then rinsed in acetone and ethanol before being put in the vacuum system. The slip ring was electrically grounded and the contact resistances between (1)

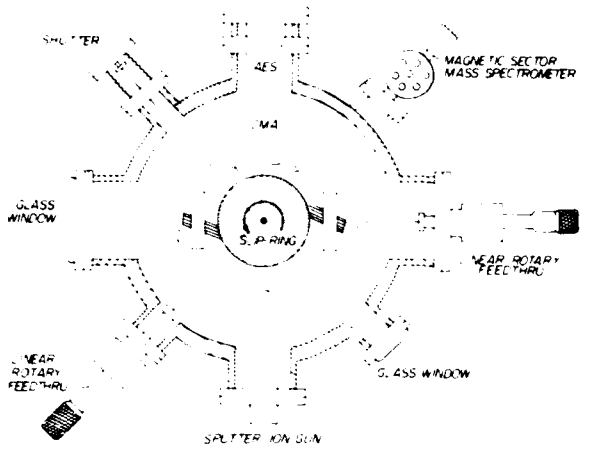

Figure 1. Top view of the uhv system and slip ring brush assembly.

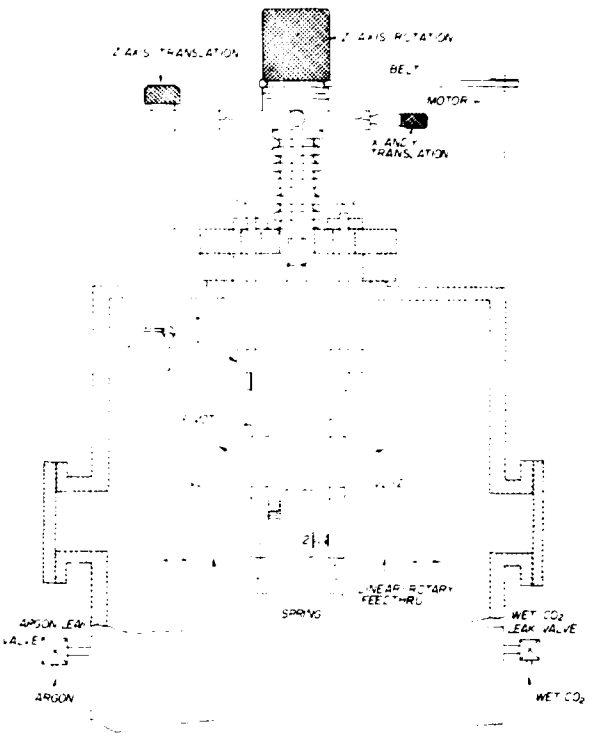

Figure 2. Schematic diagram of the slip ring-brush assembly attached to the manipulator inside the vacuum chamber.

the upper brush and slip ring and (2) the lower brush and slip ring were recorded on a dual pen recorder for brush currents of 50 mA, 5 A and 30 A in vacuum, and 50 mA and 30 A under 1×10^{-4} torr wet CO_2 environment. With brushes retracted, the slip ring rotated at a speed of about 150 rev min^{-1}, measured by an optical tachometer. The normal force on each brush was measured. The average frictional force was determined from the decrease in rotational speed of the slip ring by comparing it to a calibration involving known torques applied to the slip ring in a separate experiment in air. The Auger electron spectrometer used to determine the elemental surface composition of the slip ring surfaces was controlled by a Hewlett Packard 9825 A desktop computer using a multi-programmer. Typical Auger traces covering a 50 to 1300 eV range were directly digitized. Computerized values of peak to peak heights and concentrations of the various elements were obtained. After each experiment was over, the slip ring and brushes were removed from the chamber so that SEM pictures could be taken of both the upper (1) and lower (2) surface tracks on the slip ring and also of the brush contact surfaces.

III. Experimental results

(A) High vacuum condition

1. Contact resistance and friction. The contact resistance decreased with increasing number of revolutions. Also the rotational speed of the motor driving the slip ring decreased while the current to the motor increased, both as a result of increasing frictional force. Alternate welding and fracture at the interface resulted in an appreciable vibration culminating in permanent welding, which caused the motor to stop. The ratio of the frictional force to the measured average normal contact forces on both

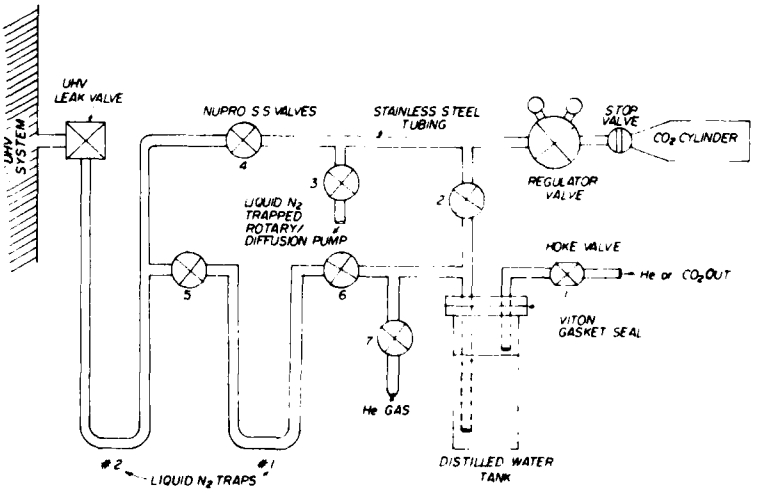

Figure 3. Mechanism for the introduction of wet CO_2.

brushes gave the average coefficient of friction μ. The contact resistances for the upper (R_1) and lower (R_2) interfaces at a 5 A dc brush current and the corrected[6] average μ are shown in Figure 4. Similar results for the contact resistance were also obtained for 50 mA and 30 A brush currents. In Figure 4 the circled points indicate the contact resistances R before the slip ring started rotating and after it stopped. It is clear that R did not depend significantly on the angular velocity of the slip ring. The lower contact resistance at the upper brush was due to the higher contact force there. It arises from the manner in which the forces on these brushes were applied[8]. In the experiment of Figure 4 the normal brush forces needed to break electrical contact with the slip ring were 260 g (upper brush) and 180 g (lower brush) respectively. No systematic relationship between contact resistance and current density was observed. Also no effect of polarity on contact resistance was detected. In any case a possibly small influence would have been difficult to observe in the presence of the dominant effect arising from the different contact forces on the brushes.

2. AES measurements. Elemental surface compositions of each of the brush tracks on the slip ring and the interface contact plus lead resistances for both brushes were reported earlier as a function of the number of revolutions n for a 50 mA brush current[6]. Figure 5 shows a similar graph except that the current was increased in 5 A steps after a certain number of revolutions.

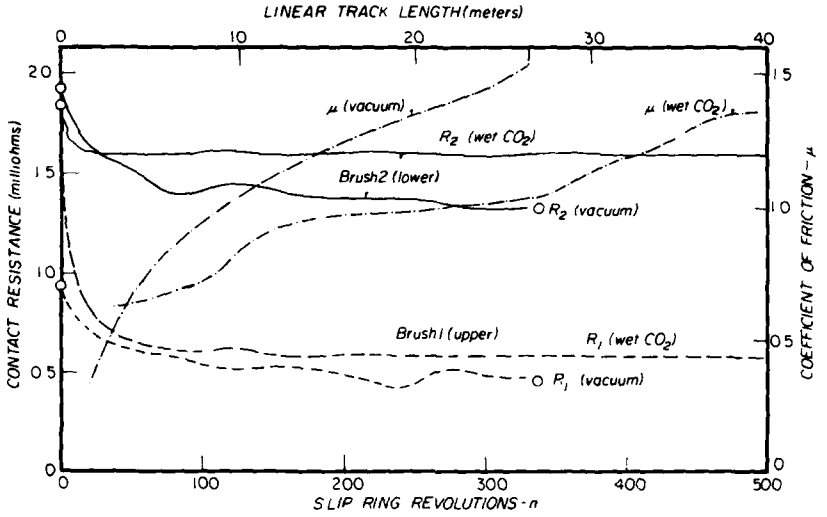

Figure 4. Contact resistance and average coefficient of friction vs slip ring revolutions. High vacuum (5 A brush current) and 1×10^{-4} torr wet CO_2 (50 mA brush current).

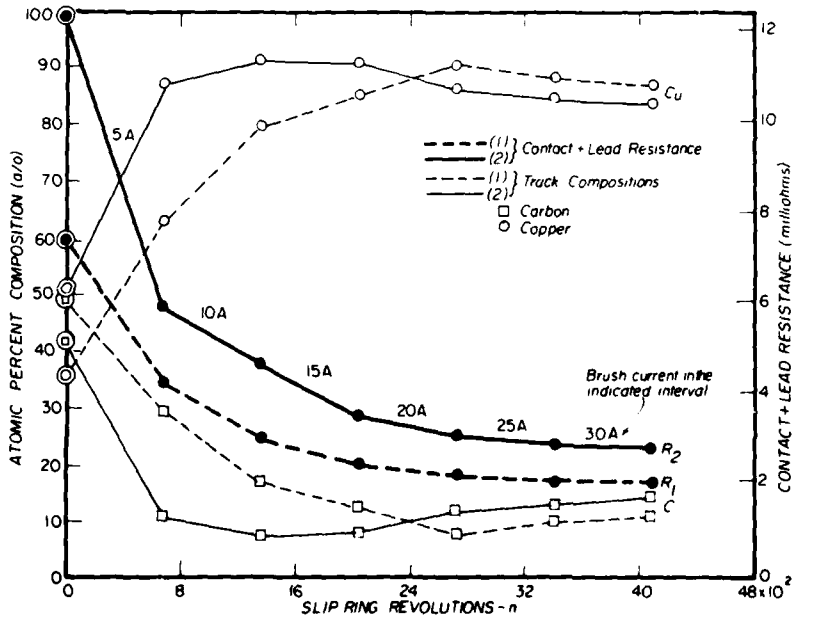

Figure 5. Contact plus lead resistance and composition of both slip ring track surfaces as a function of slip ring revolutions. (High vacuum condition.)

The circled points represent the values before the slip ring started rotating. In this set of experiments a different lead arrangement from that used for Figure 4 was employed for the contact resistance measurements. The experiments in Figure 5 included higher lead resistances. Also the normal brush contact forces were comparatively small (161–116 g), leading to an increased number of revolutions prior to permanent welding. During AES measurements the brushes were retracted and the slip ring was continuously rotated. The measurements thus gave the average surface concentrations of the whole track, with only negligible loss in resolution. Peak to peak heights of all Auger signals were normalized to fractional atomic surface concentrations without making any other corrections. Nitrogen, oxygen, chlorine and sulfur were also detected in addition to the impurities shown in Figure 5, but their concentrations decreased to less than approximately 1 atm"$_{o}$ from initial values that were less than 8 atm"$_{o}$. Figure 5 shows that the change in impurity concentration with n more or less parallels the change in contact resistance. A similar parallel was also observed in experiments in which a constant current of 50 mA was used. The results suggest that the interface impurity concentration is directly related to the contact resistance. Finally no significant electromigration effects up to current densities of 654 A in $^{-2}$ were detected.

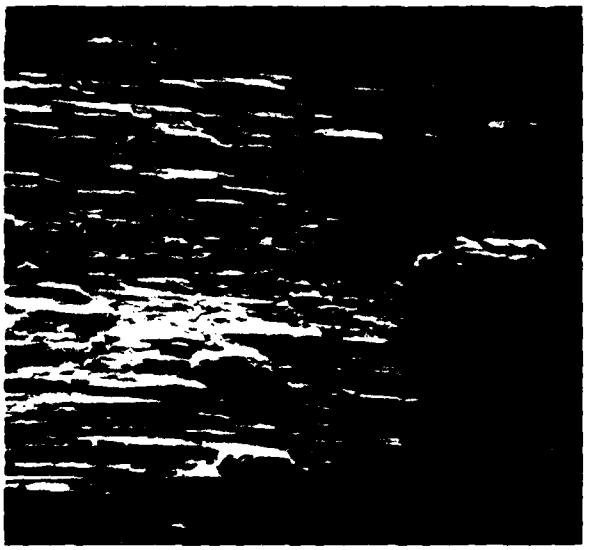

Figure 6. SEM photograph of OFHC Cu slip ring, track 2, showing broken wire pieces W and ridges. Arrow gives direction of relative brush motion. (High vacuum condition.)

3. Scanning electron microscopy. SEM pictures of the brush tracks on the slip ring showed that surface material was smeared out along the track areas. Thus the initial surface impurities appear to have been buried during rotation. Small pieces of brush wire *W* in Figure 6 were seen adhering to various places on the slip ring. The ridges shown in this micrograph lie parallel to the direction of travel. Similar ridges lying parallel to the direction of relative motion can be observed on higher magnification micrographs obtained from the brush wire ends[6]. The ridges in the contact area arise from random localized welding of a wire to the slip ring during rotation resulting in tensile plastic deformation of the region near the weld area along the direction of motion, followed by eventual fracture of the weld. Continued rotation tends to smooth these areas into ridges. The micrograph in Figure 7 shows a worn surface of the brush wire ends on the lower brush number 2. The surfaces are rough and badly deformed. Small pieces of material are also seen on their leading and trailing edges.

(B) Wet CO_2 (1×10^{-4} torr) environment. Table 1 below lists the various parameters that were measured in four experiments in a 10^{-4} torr wet CO_2 environment. After the slip ring had rotated in contact for about 5 min, the brushes were retracted and the wet CO_2 was pumped out. The AES spectra of the contact surfaces were then taken when a residual gas pressure in the 10^{-9} torr range was achieved after 15–30 min of pumping. A mass spectrum taken of this residual atmosphere (after the AES analysis was completed) showed water vapor as its major constituent. The initially dirty surfaces of the slip ring (Cu < 50 atm"$_{o}$) became much cleaner (total impurities < 10 atm"$_{o}$) after rotation. The surface impurities were buried in a manner similar to that in the vacuum experiments. The higher final resistances at the lower brush interface were due to the lower normal forces there. The contact resistances for the upper (R_1) and lower (R_2) interfaces for a 50 mA brush current and the coefficient of friction (μ) under 1×10^{-4} torr wet CO_2 environment are also shown in Figure 4 (experiment no 4 in Table 1), along with typical high vacuum

Table 1. Summary of slip ring-brush experiments in 1×10^{-4} torr wet CO_2

Exp. no	Residual pressure (10^{-9} torr)	Brush Current (A)	Brush no	Cu composition (atm"$_{o}$) Before rotation	After rotation	Contact resistance (mΩ) Before rotation	After rotation	Brush normal force (g)
1	0.8	30	1	30	95	1.0	0.6	210
			2	20	90	2.8	2.2	163
2	1.8	30	1	35	96	1.5	0.8	194
			2	31	99	1.8	1.6	153
3	1.8	0.05	1	49	91	1.8	1.4	192
			2	36	93	1.8	1.6	137
4	0.5	0.05	1	23	92	1.8	0.6	211
			2	24	95	1.8	1.6	174

Figure 7. SEM photograph of the wear surfaces on the Cu wires of brush 2. Arrow gives the direction of motion of the slip ring. (High vacuum condition.)

Figure 8. SEM photograph of OFHC Cu slip ring, track 2, showing ridged surface. Arrow gives direction of relative brush motion (1×10^{-4} torr wet CO_2.)

results. The same trends are observed for both sets of experiments except that for wet CO_2: (1) the magnitude of the increase of the coefficient of friction with the number of revolutions of the slip ring was smaller than that in vacuum, (2) the sliding contact resistances reached steady state values, (3) cold welding did not take place, and (4) the contact resistances are higher than in vacuum. All of these results imply that wet CO_2 acts as a lubricant even at the relatively low pressure of 10^{-4} torr. The higher resistance when wet CO_2 is present is most likely due to the presence of water and CO_2 molecules at the interface. Subsequent scanning electron micrographs of slip ring tracks and brushes were taken and are shown in Figures 8 and 9. Both figures show that the contact surfaces are somewhat smoother compared to the corresponding micrographs taken from the surfaces rotated in vacuum (see Figures 6 and 7). Also broken pieces of wire were much less in evidence for the surfaces rotated in wet CO_2.

Discussion

The chemical composition changes on the slip ring surface before and after rotation in contact with brushes were carefully investigated in experiments under both high vacuum and 1×10^{-4} torr wet CO_2 environments. The initial compositions depended upon the cleaning procedure and the time the slip ring was left in air before being put into the uhv chamber. In both cases the initially dirty surfaces became very much cleaner after several hundred rotations. Carbon was the major impurity observed on vacuum rotated slip ring surfaces while the concentrations of sulfur and carbon were approximately equal in the wet CO_2 case where they were the major impurities observed. The sulfur concentrations were negligible (< 1 atm"$_{\text{o}}$) in the vacuum experiments. They were about 5 atm"$_{\text{o}}$ in the wet CO_2 experiments. Preliminary results suggest that the extra sulfur in the wet CO_2 case came from an impurity in the CO_2 gas and not as a result of segregation from the slip ring bulk material[9]. In particular 5.6 atm"$_{\text{o}}$ of sulfur also appeared on sputter-cleaned flat 99.9999"$_{\text{o}}$ copper samples after exposure at 25 C to wet CO_2 atmospheric pressure.

Figure 9. SEM photograph of the wear surfaces on the Cu wires of brush 2. Arrow gives the direction of motion of the slip ring. (1×10^{-4} torr wet CO_2.)

Although the magnitude of the contact resistances differ from experiment to experiment because of inevitable differences of initial geometries, the resistance curves during slip ring rotation are much more stable in a wet CO_2 environment than in vacuum. This result is due to the lower friction and smoother rotation that resulted from the lubrication effect of wet CO_2[4,7,10,12]. The very small amounts of carbon and oxygen observed by AES on surfaces which had been rotated in wet CO_2 indicate that CO_2 was physisorbed on these surfaces, rather than chemisorbed. In the latter case high carbon and oxygen concentrations would have been expected as a result of long mean residence times of the CO_2

molecule on the surface even in vacuum. The experiments show clearly that the opposite effect was observed. Thus physically adsorbed wet CO_2 therefore appears to form a thin loosely bound lubricating layer between the brush and slip ring surface and this layer introduces a somewhat higher contact resistance.

Acknowledgements

The authors would like to thank J G Zhang and R Ziemer for technical assistance; E-A Knabbe for the computer interfacing; R A Burton, I R McNab, J L Johnson, J J Schreurs and P K Lee for helpful discussions; the Westinghouse Research and Development Center for the loan of certain equipment; and the Office of Naval Research for financial support under contract no N00014 79-0763.

References

[1] D V Keller, *J Vac Sci Technol*, **9**, 133 (1971).
[2] C A Haque, *IEEE Trans Parts, Hybrids Packaging*, **9**, 58 (1973).
[3] D H Buckley, *Wear*, **46**, 19 (1978).
[4] J Schreurs, J L Johnson and I R McNab, *Electrical Contacts 1979*, p 145. IIT, Chicago (1979), and *Electrical Contacts 1980*, p 59. IIT, Chicago (1980).
[5] R S Timsit, *Electrical Contacts 1979*, p 79. IIT, Chicago (1979).
[6] B Singh and R W Vook, Proc VIII Int Vac Congr at Cannes, France. Vol II, Vacuum Technology and Vacuum Metallurgy, p 441 (1980).
[7] P Reichner, *Electrical Contacts 1979*, p. 191. IIT, Chicago (1979) and *Electrical Contacts 1980*, p 73. IIT, Chicago (1980).
[8] B Singh and R W Vook, *Electrical Contacts 1980*, p 53. IIT, Chicago (1980).
[9] B Singh, R W Vook and E-A Knabbe, *J Vac Sci Technol*, **17**, 29 (1980).
[10] E Rabinowicz and P Chan, *Electrical Contacts 1979*, p 123. IIT, Chicago (1979).
[11] J L Johnson and O S Taylor, *Electrical Contacts 1979*, p 129. IIT, Chicago (1979).
[12] R M Slepian, *Electrical Contacts 1979*, p 137. IIT Chicago (1979).

APPENDIX III

In Situ Auger Electron Spectroscopy Characterization of Wet-CO_2-Lubricated Sliding Copper Electrical Contacts

by

B. H. Hwang, B. Singh, R. W. Vook, and J. G. Zhang

Wear 78(1982)7-16

Wear, 78 (1982) 7 - 16

IN SITU AUGER ELECTRON SPECTROSCOPY CHARACTERIZATION OF WET-CO_2-LUBRICATED SLIDING COPPER ELECTRICAL CONTACTS*

B. H. HWANG, B. SINGH, R. W. VOOK and J. G. ZHANG

Department of Chemical Engineering and Materials Science, Syracuse University, Syracuse, NY 13210 (U.S.A.)

(Received November 5, 1981)

Summary

The electrical contact resistance, elemental surface composition and friction of an OFHC copper slip ring rotating in contact with two high purity copper wire brushes on different tracks were investigated *in situ* for heavy and light normal contact forces under a wet CO_2 environment at atmospheric pressure. Scanning electron microscopy was also used to characterize the slip ring and brush surfaces. Previous work in ultrahigh vacuum showed that, as rotation proceeded, interfacial impurities were almost totally removed and the electrical contact resistance decreased until cold welding occurred. In the present work, the slip ring surface was sputter cleaned (more than 95% Cu) before contact rotation and was only slightly contaminated after rotating in wet CO_2. Both the contact resistance and the friction decreased quickly and reached steady state values almost simultaneously in the early stages of rotation. Also, cold welding phenomena did not occur. Scanning electron micrographs taken after each experiment showed that the surfaces of the slip ring tracks and the brush wire ends were much rougher when heavy normal contact forces were used than in the light normal force condition. All these results confirm that wet CO_2 is an effective lubricant for Cu–Cu electrical sliding contacts.

1. Introduction

Most previous studies of electrical contact phenomena have been carried out under normal atmospheric conditions. Recently, however, it has been found that the electrical and mechanical properties of rotating electrical contacts can be strongly influenced by the gaseous environment in which

*Paper presented at the Advanced Current Collection Conference, Chicago, IL, U.S.A., September 23 - 25, 1981.

Elsevier Sequoia/Printed in The Netherlands

they operate [1 - 3]. One particularly auspicious environment is wet CO_2 at atmospheric pressure. Not only does it give rise to low values of friction and wear but it also permits the flow of high currents across the interface [4]. In the present work, this environment was used in a study of the interface between a copper wire brush and a rotating copper slip ring across which a high current flowed. The elemental composition of the surface of the slip ring was measured *in situ* with Auger electron spectroscopy (AES) as a function of exposure and the number of rotations in contact with the brush. Similarly, measurements of electrical contact resistance and friction were made. The surfaces of both the brushes and the slip ring were examined subsequently by scanning electron microscopy (SEM). Both high and low normal contact forces were used in the experiments. The results were different from those carried out earlier under ultrahigh vacuum (UHV) conditions in several significant ways [5].

2. Experimental details

Figure 1 shows a block diagram of the complete experimental system. A stainless steel UHV system was used to investigate the electrical contact phenomena associated with the rotation of a copper slip ring in contact with two copper wire brushes running on different tracks. Residual pressures in the low (10^{-9} Torr) range were obtained in the baked system. The brushes are pressed against the slip ring by means of an electrically insulated stainless

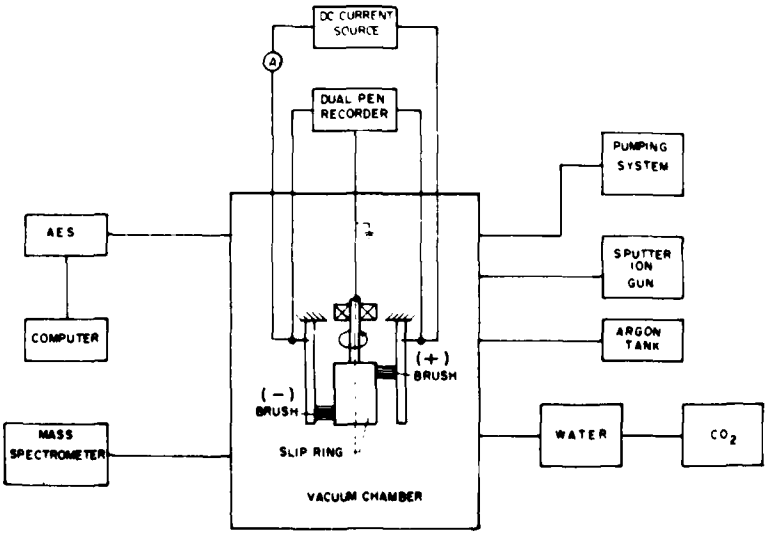

Fig. 1. Block diagram of UHV system and attachments for the electrical sliding contact experiments.

steel spring. They can be removed from contacting the slip ring surface by manipulating two linear–rotary vacuum feedthroughs. The slip ring is axially attached to a magnetically coupled rotary feedthrough which is turned by an a.c. motor coupled to it by a rubber belt. The slip ring is a cylinder (diameter, 1 in) of OFHC (99.98%) copper and the brushes each consist of 362 copper wires (wire diameter, 0.005 in; 99.999% Cu). The whole brush–slip ring assembly is mounted on a specimen manipulator capable of x,y,z displacements. The UHV system also contains an Auger cylindrical mirror analyzer, a 3 keV sputter ion gun and a 90° magnetic sector partial pressure analyzer. The details of the slip ring–brushes assembly, UHV system and AES measurements were given previously [5 - 7].

The surfaces of the slip ring and wire brushes were polished smooth with emery paper (grit 600-A), rinsed in acetone and ethanol, and then cleaned in an ultrasonic bath for 30 min before being put in the vacuum system. After the system was baked and pumped to a 5×10^{-9} Torr pressure, Auger spectra were taken from the contaminated slip ring surface (less than 50% Cu). Argon was then introduced into the vacuum chamber through the leak valve to a pressure of $(1 - 2) \times 10^{-5}$ Torr and the slip ring surface was sputter cleaned for 2.5 h with a primary electron beam setting of 3000 V and 30 mA. Subsequent AES measurements showed that the slip ring surface was almost completely cleaned (more than 99% Cu in the center region of the bombarding ion beam).

Wet CO_2 at atmospheric pressure was obtained by allowing the gas to flow through a distilled-water trap and then into the vacuum chamber via a vacuum leak valve. The detailed procedures will be reported elsewhere [8]. The rotating electrical contact experiment was then performed with a current of 30 A running through the contact interfaces. An angular velocity of about 150 rev min^{-1} was used. During the experiment, the slip ring was electrically grounded by means of thick copper wires sliding on the stainless steel axis, the neutral contact. The contact resistances between (1) the lower brush and slip ring and (2) the upper brush and slip ring were recorded on a dual-pen recorder. The rotational speed of the slip ring was measured with an optical tachometer together with the input power to the motor. The frictional force was determined from the calibrated decrease in rotational speed of the slip ring [9]. Then the ratio of the frictional force to the sum of the measured normal contact forces on both brushes gave the friction coefficient μ.

After 10 min of rotation, the brushes were retracted and the wet CO_2 was pumped out. AES spectra of the contact surfaces were taken when a residual gas pressure in the 10^{-8} Torr range was achieved after at least 30 h of pumping. Subsequent sputtering was carried out and AES spectra were taken alternately at regular intervals to obtain the concentration depth profiles of the elements on the slip ring surface. After the experiment was over, the slip ring and brushes were removed from the vacuum chamber. SEM pictures were taken of both the lower and the upper surface tracks and also of the brush contact surfaces.

3. Results

3.1. Contact resistance and friction measurements

The coefficients of friction and the electrical contact resistances of both the lower and the upper interfaces for two different experiments are shown in Fig. 2. Both experiments were carried out under similar conditions except for different contact forces. During rotation, a direct current of 30 A (approximately 4200 A in^{-2}) ran through the contacts. The subscripts s, w, u, l in Fig. 2 denote strong spring, weak spring, upper interface and lower interface respectively, *e.g.* R_{wl}(27 gf) denotes the electrical resistance of the lower interface in the weak spring experiment. 27 gf is the corresponding normal contact force. Contrary to the corresponding experiments carried out in UHV [9], the coefficients of friction in the present experiments decreased with increasing number of slip ring revolutions until steady state values were obtained. Although the electrical contact resistances of the lower and upper interfaces in the present experiments decreased with increasing number of slip ring revolutions, as in the UHV experiments, they reached their steady state values more rapidly and remained stable without adhesion in the former case. This stability and lack of cold welding demonstrated the lubricating function of wet CO_2. In addition, the resistance curves were more or less parallel to each other,

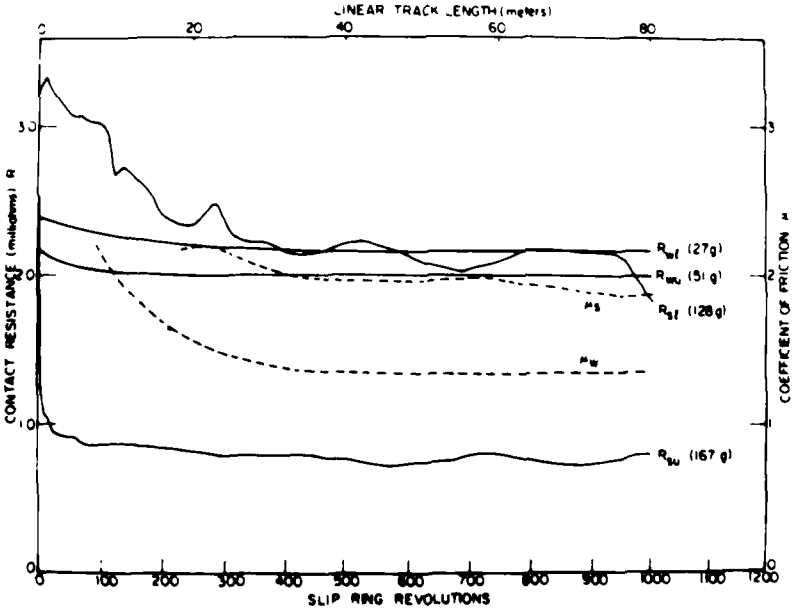

Fig. 2. Electrical contact resistances and coefficients of friction *vs.* number of slip ring revolutions under 1 atm of wet CO_2 and a 30 A brush current (4.2 kA in^{-2} (654 A cm^{-2})): the notation is discussed in the text.

indicating that the initial conditions determined whether a curve was "low" or "high". These initial conditions include such variables as brush orientation, stiffness and contact force. In the latter case a higher contact force always resulted in a lower contact resistance, as expected.

3.2. Auger electron spectroscopy

The elemental compositions of the lower track (track 1), upper track (track 2) and neutral track (track 0, which is between tracks 1 and 2) of the slip ring surface before sputtering, after sputtering and after running in wet CO_2 for the strong and weak spring experiments are listed in Table 1. The elemental balances in Table 1 mainly consisted of chlorine and nitrogen. The slip ring surfaces for both experiments were initially largely covered by impurities. With the ion sputter gun aimed at the neutral track region, *i.e.* between tracks 1 and 2, very clean surfaces were obtained for all three tracks in the weak spring experiment. In the strong spring experiment similar cleaning effects were observed after sputtering, but somewhat more impurities remained on track 1 and the neutral track regions because the ion gun had been aimed at track 2 instead.

After running in wet CO_2, the slip ring surfaces became contaminated only slightly (Table 1). The major contaminants were carbon and sulfur. It should be noted also that the contamination in the near-surface region is less serious in the strong than in the weak spring experiment. Figures 3 and 4 show the elemental depth profiles of sulfur and carbon on the slip ring after running in 1 atm of wet CO_2. The order of taking AES spectra was track 2, neutral and track 1. The impurities on the neutral track generally were more easily sputtered away because they were only adsorbed on the surface of the slip ring. The impurities on tracks 1 and 2, however, took a longer time to be sputtered away because they were buried in the near-surface region of the copper substrate by the mechanical mixing action of the brushes. For example, in Fig. 4, it took four times as long for the carbon concentration to reach the initial (or "background") level for track 2 than for the neutral track. It should be noted also from Table 1 and Figs. 3 and 4 that the mechanical mixing of impurities in the near-surface region by the brushes is more significant when there are *light* loads on the brushes.

A separate experiment was carried out to examine the high concentration of sulfur on the slip ring surface after rotating in wet CO_2. A very pure flat copper specimen (99.9999% Cu) was cleaned and mounted on the manipulator in the UHV chamber. The system was evacuated and the copper specimen was cleaned by sputter ion etching. It was then exposed to 1 atm of wet CO_2, which was then pumped out. Although all measurements and experimental processes took place at room temperature without any mechanical disturbance of the surface, the sulfur concentration on the flat specimen surface was found to be about the same (about 5 at.%) as that of the slip ring surface after rotating in contact with two brushes in 1 atm of wet CO_2 (Table 1). Clearly, the extra amount of sulfur on the surfaces of both the flat specimen and the slip ring came from an impurity in the

TABLE 1

Elemental compositions of slip ring tracks before sputtering, after sputtering and after rotating in wet CO_2 (and 30 h of pumping) for the strong and weak spring experiments

	Track	*Concentration on slip ring*[a] (at.%)					
		Strong spring			*Weak spring*		
		Before sputtering	*After sputtering*	*After rotating in wet CO_2*	*Before sputtering*	*After sputtering*	*After rotating in wet CO_2*
Cu	1	48.4	83.6	93.3	39.9	99.4	88.0
	0	29.8	95.8	91.8	45.7	99.1	89.3
	2	16.9	99.0	93.3	49.8	99.7	88.8
S	1	0.0	0.1	4.5	0.0	0.0	4.7
	0	0.0	0.1	3.2	0.0	0.2	5.0
	2	0.0	0.1	4.8	0.0	0.0	5.2
C	1	35.3	12.9	2.2	40.9	0.6	7.3
	0	59.7	3.6	4.7	39.3	0.5	5.5
	2	68.9	0.6	1.6	35.1	0.2	5.6
O	1	15.6	3.3	0.0	14.2	0.0	0.0
	0	10.4	0.3	0.2	12.9	0.0	0.1
	2	14.2	0.2	0.1	11.4	0.1	0.2
Balance	1	0.7	0.1	0.0	5.0	0.0	0.0
	0	0.1	0.2	0.1	2.1	0.2	0.1
	2	0.0	0.1	0.2	3.7	0.0	0.2

[a]Accuracy, ± 0.1 at.%.

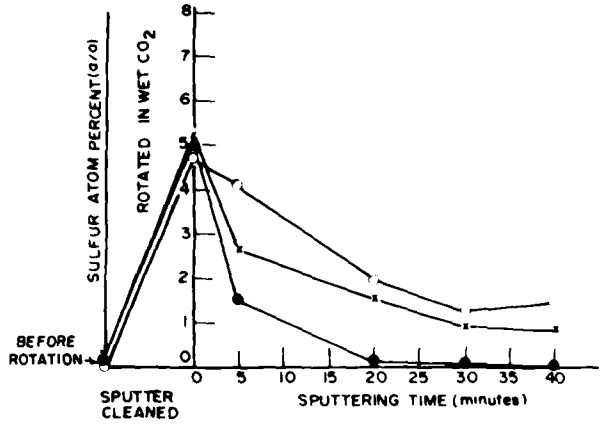

Fig. 3. Sulfur concentration depth profile on slip ring surface after rotating in wet CO_2 (weak spring condition): ○, track 1; ×, track 2; ●, neutral.

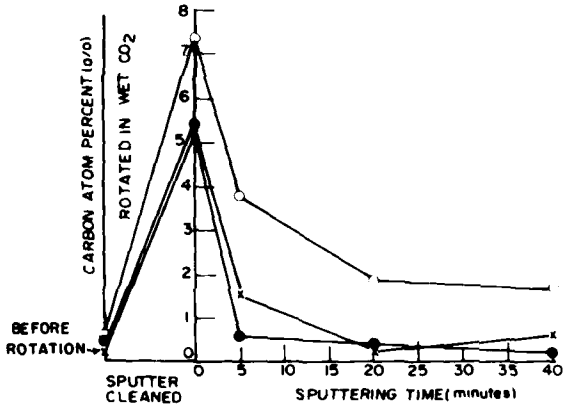

Fig. 4. Carbon concentration depth profile on slip ring surface after rotating in wet CO_2 (weak spring condition): ○, track 1; ×, track 2; ●, neutral.

CO_2 gas and not as a result of segregation from the bulk of the copper sample [7].

3.3. Scanning electron microscopy

SEM pictures of slip ring tracks and brush wire ends for both the strong and the weak spring experiments were taken after the experiments were over and the manipulator was taken out of the vacuum chamber. Figures 5 and 6 show the brush wire ends after each experiment. Clearly, the contact surface of the brush wire end in the weak spring experiment is much smoother than that in the strong spring experiment. The rough region of the brush wire in Fig. 6 was produced by the initial emery paper polishing

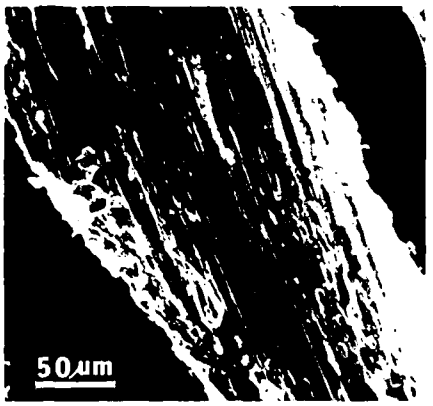

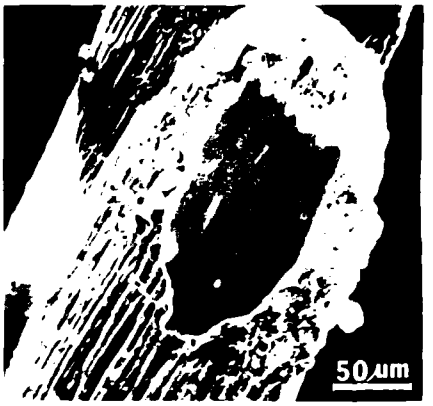

Fig. 5. SEM micrograph of a single brush wire end after sliding contact in wet CO_2 (strong spring condition; lower brush negative).

Fig. 6. SEM micrograph of a single brush wire end after sliding contact in wet CO_2 (weak spring condition; upper brush positive).

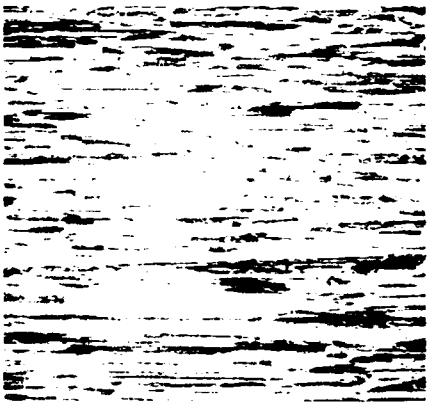

Fig. 7. SEM micrograph of a slip ring track after sliding contact in wet CO_2 (strong spring condition; lower track).

Fig. 8. SEM micrograph of a slip ring track after sliding contact in wet CO_2 (weak spring condition; lower track).

before insertion in the UHV chamber. It apparently did not touch the slip ring during rotation. In contrast, the brush wire end in Fig. 5 shows a smoother surface and longer ridges compared with the rough region in Fig. 6. This surface resulted from frictional contact during rotation. Figures 7 and 8 show SEM pictures of slip ring tracks after the strong and weak spring experiments respectively. Obviously the size of the ridges in the surface of the slip ring track is much smaller in the weak than in the strong spring experiment.

These results dramatically show that the normal contact force plays an important role in determining the properties of a rotating electrical contact: the smaller the normal contact force, the lower the contact frictional force and consequently the smoother the contact interface.

4. Discussion

In these experiments an initially clean copper slip ring rotated in electrical and mechanical contact with two copper wire brushes through which a current of approximately 4200 A in ^{2} flowed. Rotations were made in a UHV system that had been back filled with wet CO_2 at a 1 atm pressure. Both strong and weak normal forces were applied to the brushes in successive experiments. The results show that, except for a slight contamination with sulfur, rotation in wet CO_2 does not contaminate the surface of the slip ring. Since the surface remained essentially clean, the lubricity of the thin film at the interface must be due only to the H_2O and CO_2 molecules that are present.

In previous experiments carried out in UHV [5, 7], it was shown that the interface became much cleaner as the copper brush rotated over the copper slip ring. The present results in wet CO_2 are consistent with the earlier result. In addition, it was found that weak contact forces resulted in greater near-surface–bulk mixing of surface contaminants than stronger springs. This interpretation follows from the Auger depth profile studies. We can conclude that the greater penetration of the brush asperities into the bulk of the slip ring in the case of a stronger normal force is less effective in distributing the contaminants in the near-surface region.

It was also found that during rotation the adsorbates were pumped off in less than 30 h. This result means that they were not very tightly bound to the copper surfaces. We could not examine the surfaces by AES in a much shorter time because of the high residual gas pressure in the vacuum system. These results are consistent with the known desorption energies of water on metal surfaces, which range from 22 to 24 kcal mol ^{1} [10]. Since the adsorption energy of CO_2 is much less than that of H_2O, it is expected that the H_2O molecule aids the adsorption of CO_2 during rotation.

The decreases in electrical contact resistance and friction during rotation presumably arise from an increase in the contact area as the asperities on the contacting faces are smoothened. This effect is most noticeable in the weak spring case where the normal forces were in the neighborhood of 30 - 50 gf. Because cold welding did not occur in the wet CO_2 case, as observed in UHV, the H_2O–CO_2 molecules must form a more or less continuous layer at the slip ring–brush interface. If this layer were broken, localized cold welding would occur. Presumably, the higher friction in the case of higher normal forces arises from the partial fracture of this H_2O–CO_2 layer. It is also expected that, on the basis of this model, the thickness of the H_2O–CO_2 interfacial layer would depend on the contact pressure. The electrical con-

tact resistance measurements support this view. In all cases the higher normal force has the lower contact resistance. It is expected that the interfacial resistance arises from a combination of quantum mechanical tunneling through the CO_2–H_2O layer as well as occasional erratic direct brush–slip ring cold welding, resulting in the fracture of surface regions from the bulk and concomitant wear. It is therefore clear from these studies that the film resistance at a Cu–Cu interface is not due to contamination by carbon, organic impurities etc. but rather arises from the presence of this thin H_2O–CO_2 layer at the interface.

Acknowledgments

The authors would like to express their appreciation to I. R. McNab, J. L. Johnson, P. Reichner, J. J. Schreurs, P. K. Lee and E. Rabinowicz for helpful discussions, the Westinghouse Research and Development Center for the loan of certain equipment, and the Office of Naval Research for financial support under Contract N00014-79-0763.

References

1 J. L. Johnson and O. S. Taylor, High current brushes. Part IV: machine environment tests, in *Proc. Conf. on Electrical Contacts, 1979*, Illinois Institute of Technology, Chicago, IL, 1979, pp. 129 - 135.
2 P. Reichner, Metallic brushes for extreme high current applications, in *Proc. Conf. on Electrical Contacts, 1979*, Illinois Institute of Technology, Chicago, IL, 1979, pp. 191 - 197.
3 I. R. McNab and W. R. Gass, High current density carbon fiber brush experiments in humidified air and helium, in *Proc. Conf. on Electrical Contacts, 1979*, Illinois Institute of Technology, Chicago, IL, 1979, pp. 159 - 163.
4 J. Schreurs, J. L. Johnson and I. R. McNab, High current brushes. Part VI: evaluation of slip ring surface films, in *Proc. Conf. on Electrical Contacts, 1979*, Illinois Institute of Technology, Chicago, IL, 1979, pp. 145 - 151.
5 B. Singh and R. W. Vook, *In situ* AES characterization of rotating electrical contacts, in *Proc. Conf. on Electrical Contacts, 1980*, Illinois Institute of Technology, Chicago, IL, 1980, pp. 53 - 58.
6 R. W. Vook, B. Singh, E.-A. Knabbe, J. H. Ho and D. K. Bhavsar, in *Proc. Conf. on Electrical Contacts, 1979*, Illinois Institute of Technology, Chicago, IL, 1979, pp. 17 - 21.
7 B. Singh, R. W. Vook and E.-A. Knabbe, AES study of sulfur surface segregation on polycrystalline copper, *J. Vac. Sci. Technol., 17* (1) (1980) 29 - 33.
8 B. Singh, B. H. Hwang and R. W. Vook, Characterization of copper slip ring wire brush electrical contacts, *J. Vac. Technol.*, (1981) in the press.
9 B. Singh and R. W. Vook, Interfacial characterization of copper slip ring wire brush contacts, in *Proc. 8th Int. Vacuum Congr.*, Vol. II, *Vacuum Technology and Vacuum Metallurgy*, in *Vide, Couches Minces, Suppl., 201* (1980) 441.
10 R. Glang, R. A. Holmwood and J. A. Kurtz, in L. I. Maissel and R. Glang (eds.), *Handbook of Thin Film Technology*, McGraw-Hill, New York, 1970, p. 2-44.

APPENDIX IV

Characterization of Ag Wire Brush-Cu Slip Ring Electrical Contacts Rotating in Wet CO_2

by

R. W. Vook, J. G. Zhang, A. Banerjee, M. Garshasb, and L. R. Zhang

1. Electrical Contacts - 1982 (I.I.T. Chicago), Proc. 28th Annual Holm Conference, p. 193-199.
2. To be published in IEEE Transactions on Components, Hybrids, and Manufacturing Technology.

ELECTRICAL CONTACTS - 1982

Proceedings

of the

Twenty-Eighth Annual Meeting

of the

Holm Conference on Electrical Contacts

The purpose of the Conference is to provide a forum for the presentation and discussion of practical information on the latest developments in the field of electrical contacts. The technical papers cover a broad span of interests ranging from practical application of contacts to contact theory. The technical content of the Conference is focused on six major application areas:

Low Current Connections
Medium Current Switching
High Current Arcs
Aluminum Connections
Sliding Contacts
Contact Materials and Design

and with a special panel discussion on:

Cost Effective Manufacturing Technologies Employed in Making Electrical Contacts

Price: Forty Dollars

September 13-15, 1982

Illinois Institute of Technology
Electrical Engineering Department
Chicago, Illinois 60616

CHARACTERIZATION OF Ag WIRE BRUSH-Cu SLIP RING ELECTRICAL CONTACTS ROTATING IN WET CO_2

R. W. Vook, J. G. Zhang, A. Banerjee, M. Garshasb, and L. R. Zhang

Department of Chemical Engineering and Materials Science
Syracuse University, Syracuse, New York 13210

ABSTRACT

Current-carrying silver wire brushes were run on the same track against a rotating copper slip ring in a conventional stainless steel ultra high vacuum system. The experiments were performed after sputter cleaning of the slip ring in a H_2O-CO_2 ambient held at one atmosphere of pressure. The electrical contact resistance and the frictional coefficient were measured in-situ. Subsequently, scanning electron microscopy, electron probe microanalysis and elemental mapping studies were carried out ex-situ on the slip ring, brush end, and wear particle surfaces. Both low (50mA) and high (40A) currents were used for comparison. Interestingly, it was found that not only was silver transferred to the copper slip ring, but copper was also transferred to the wire brush ends. Moreover, the wear particles were mainly of two types, one being rich in silver and the other rich in copper, the relative concentrations depending on the current flowing through the contacts. These results demonstrate clearly that mechanical mixing of brush and slip ring material and the incorporation of both materials in wear particles play important roles in rotating current carrying electrical contact phenomena.

INTRODUCTION

The last two decades have witnessed a considerable research interest in the field of sliding and rotating contacts in terms of friction and interfacial electrical resistance. As a result novel materials holding great promise, including some exotic binary and ternary alloys (1,2) have been developed. Different sliding environments (3,4) have been investigated to improve lubrication between the moving parts and consequently reduce wear and tear. In fact, the problem of electrical contacts can be subdivided into the three following constituents: (1) providing a large number of electrical contact spots at the interface, (2) reducing the friction by using suitable lubricating ambients, and (3) microstructural characterization and chemical composition analysis of the interface. The importance of the last aspect is increasingly being realized since it furnishes fundamental information regarding the physical events occurring at the interface as well as necessary feedback for further improvement in contact phenomena.

With the above as background we have undertaken a study of the electrical, tribological and microstructural properties of a system consisting of a rotating Cu slip ring in contact with a pair of static Ag wire brushes. The work is an extension of our previous work (5-7) on a Cu slip ring-Cu brush assembly. The present heterogeneous system has been motivated by our interest in determining the nature and direction of metal transfer between the brush and the slip ring and the chemical composition of the wear particles collected for different current load conditions. This type of work was, of course, not possible with the previous Cu-Cu system. The choice of Ag was governed by the consideration that both the brush and the slip ring should possess similar properties in terms of electrical resistivity, melting point, tensile strength, hardness, and thermal conductivity. Out of the few elemental possibilities, Ag seemed to be the most suitable.

In the present work we report some of the results of our ongoing program using Ag brush riders on a rotating Cu slip ring. The experiments were performed in one atmosphere of humidified CO_2, which is known in some cases (7-9) to be a good lubricant. Scanning electron microscopy (SEM), electron probe microanalysis (EPM), x-ray elemental mapping and Auger electron spectroscopy (AES) were the main techniques used for characterizing the slip ring, brushes and resultant debris particles. While the 50mA brush current case will be emphasized in this report, the results will be compared with those obtained in the 40A case. Finally, a model is proposed to explain the bidirectional metal transfer observed in both current domains.

EXPERIMENTAL DETAILS

The experimental set up used was essentially similar to the one reported earlier (7,9) for Cu-Cu contacts. Briefly, a stainless steel UHV chamber evacuated in the present case by a diffusion pump backed by a rotary pump was used to house the slip ring-brush assembly. The OFHC Cu slip ring consisted of a 1" diameter cylinder. It was rotated about a vertical axis at an angular velocity of $\sim$ 150 per minute by means of an indirectly coupled a.c. motor situated outside the vacuum chamber. The two essentially identical brushes consisted of 342 Ag wires of diameter 0.005" and 99.9% purity. They were pressed against the slip

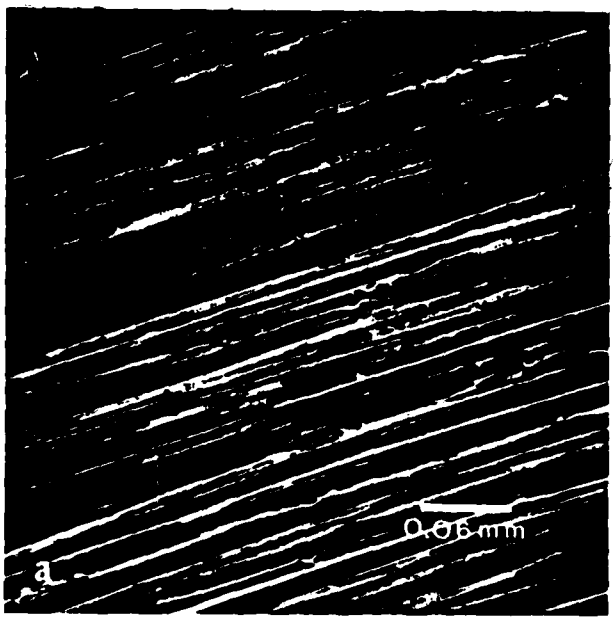

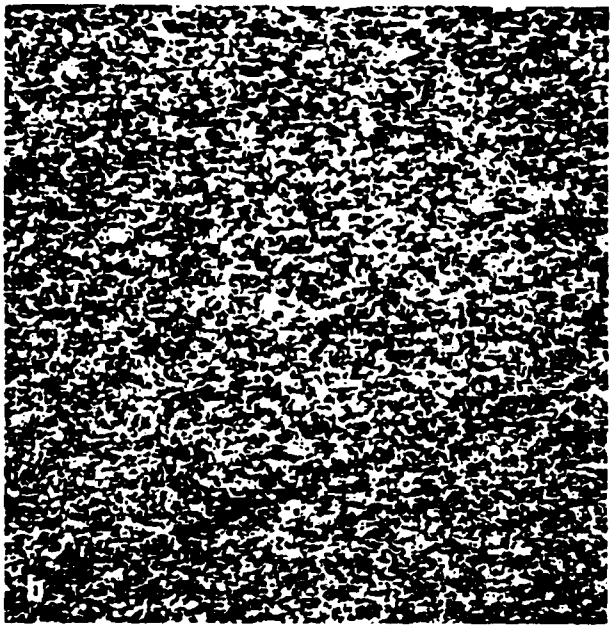

Fig. 1 (a) Secondary electron image of the Cu slip ring for a brush current of 50mA. The grooves and ridges are due to prior emery paper polishing.
(b) Cu elemental map of same region.
(c) Complementary Ag element map of same region. The white dots show the distribution of Ag on the slip ring surface.

ring from opposite sides with the help of an electrically insulated spring of known force constant. The contact force was approximately 40g. The brushes were aligned to the same horizontal level so as to run on the same track on the Cu ring. The entire slip ring-brush assembly was mounted on a specimen manipulator with the facility for X, Y, Z displacements. A 3kV Ar ion gun and an Auger electron spectrometer on this UHV system were used for in-situ sputter cleaning and elemental analysis.

The surfaces of the slip ring and brushes were polished using emery paper (grit 600-A). The brushes were polished till the brush heads attained the curvature of the slip ring. The assembly was cleaned ultrasonically with conventional organic solvents before mounting in the UHV chamber. The system was baked and evacuated to a base pressure of 5×10^{-9} Torr. Sputter cleaning of the slip ring was done at 25mA emission current for two hours at a dynamic Ar pressure of $3 - 5 \times 10^{-5}$ Torr with the baffle valve of the diffusion pump open. The dynamic flow of Ar ensured a clean Ar gas environment. Subsequently, UHV was obtained again and Auger analysis showed a clean Cu surface.

CO_2 gas, bubbled through a distilled water trap, was introduced into the vacuum chamber through a variable leak valve. A vacuum pressure gauge fixed to the CO_2 gas tank was used to measure pressures inside the system in the range of -30" Hg to above atmosphere.

The slip ring was rotated with a fixed motor voltage of 115 V and the current through the motor was measured to get the friction force between the rider and the ring. Initially, the brushes were in the retracted position with the slip ring rotating freely for a few hours in order to attain a steady state motor current value. The brushes were then released into their normal position and a direct current of 50mA was passed between the brushes through the slip ring. The two interfacial contact voltages were measured using an x-t dual pen recorder. The incremental increase in the motor current caused by the loading of the brush contacts was used to read the

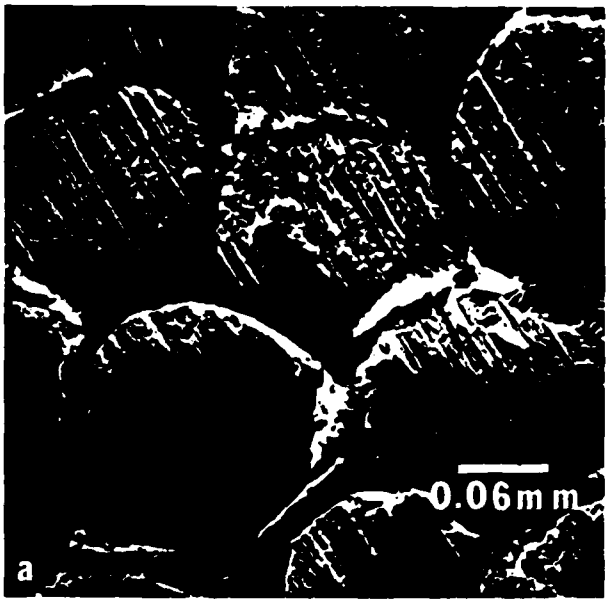

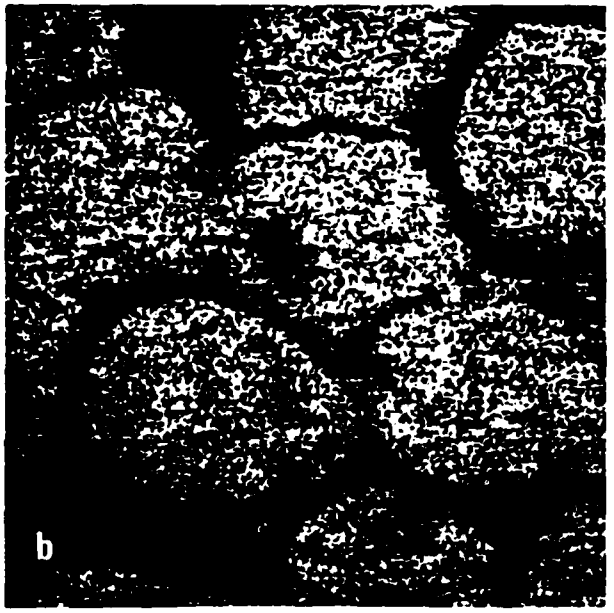

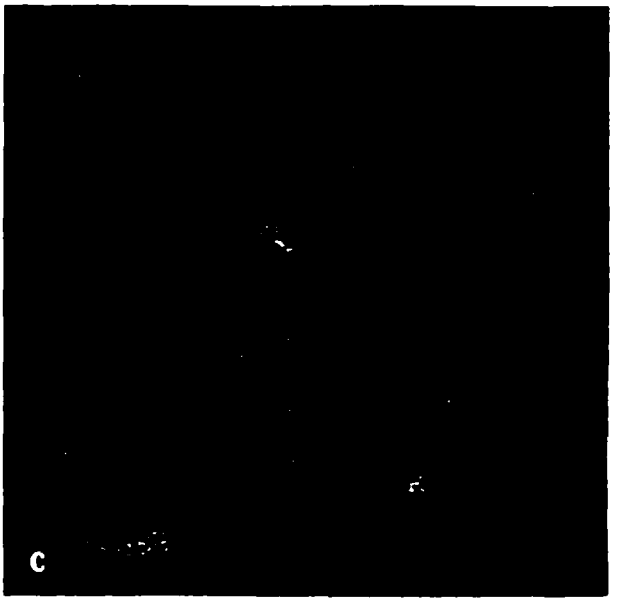

Fig. 2 (a) Typical secondary electron picture of Ag brush wire ends for the 50mA case. The ruts are the effect of emery paper polishing. The dark region shown by the arrow is due to Cu.
(b) Ag elemental map of the same region.
(c) Cu elemental map of the same region.

corresponding friction force from a predetermined calibration curve of friction force versus motor current. The ratio of this friction force to the normal force of the spring yielded the friction coefficient. In all experiments rotation was carried out for times $\sim$ 40 minutes. Brush currents of 50mA and 40 Amperes were used.

The ring, the brushes, and the wear debris collected in a tray placed under the slip ring during the experiment were examined using SEM, EPM and elemental mapping techniques. The x-ray emission spectra were analysed using an energy dispersive spectrometer with a Si(Li) detector.

RESULTS

A. Contact Resistance and Friction Measurements

Initial investigations reveal that the contact resistance at both interfaces are similar and are $\sim$ 0.15 to 0.20 mΩ. These values are significantly lower than those obtained (7,9) for the Cu-Cu interfaces. This result is attributed entirely to an improved contact between the brush and the ring along with better measurement techniques. Moreover, the contact resistance was independent of the magnitude and direction of the current flowing through a particular contact. The measured coefficient of friction for the 50mA current case is about 0.25. It is independent of the polarity. Wet CO_2 is therefore a good lubricant for both the Ag/Cu and Cu/Cu systems. A detailed in-depth study is presently under way to determine the dependence of both these quantities on a host of parameters which include brush current, spring force, and ambient wet CO_2 pressure.

B. SEM, EPM and Elemental Mapping

Fig. 1(a) shows a secondary electron micrograph of the surface of the slip ring after it had rotated at about 150 rpm for $\sim$ 40 minutes in contact with the brushes at a current of 50 mA. The surface morphology is essentially similar to the one obtained earlier (7,9) for the Cu/Cu system. The long diagonal ruts are the emery paper scratches left on the ring. The elemental x-ray maps of Cu and Ag on the same area are shown in

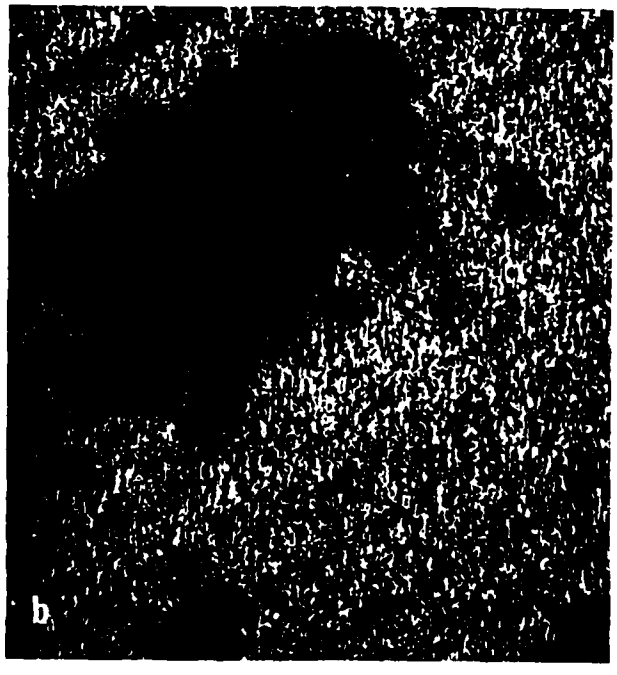

Figs. 1(b) and 1(c), respectively. The white dots in Fig. 1(c) imply that Ag has been transferred from the brush to the slip ring during the course of the experiment. Ag is reasonably evenly distributed over the surface of the ring but some regions do have higher concentrations than others. The actual amount of Ag transferred is small. Typically the ratio of the Ag to Cu x-ray intensities is 1:99. This ratio and the subsequent ones quoted below have not been corrected for factors such as backscattering, fluorescence, etc.

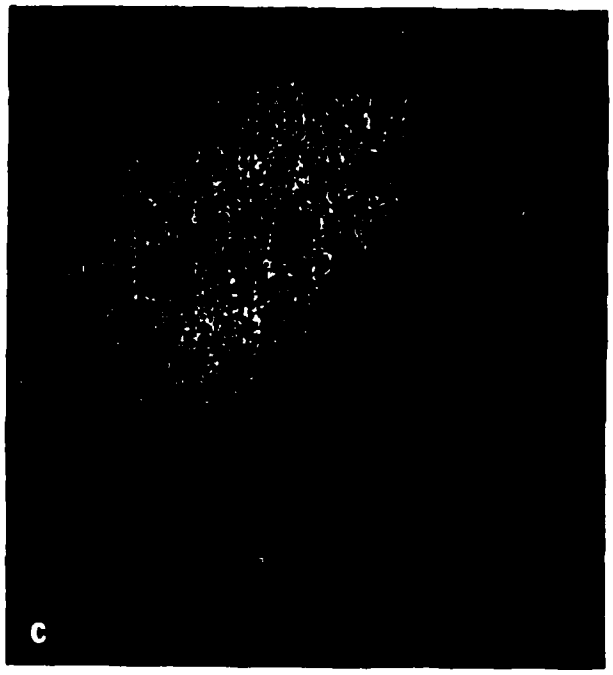

Fig. 3 (a) An enlarged secondary electron image of the dark patch indicated by the arrow in Fig. 2(a).
(b) Ag elemental map of the same region.
(c) Complementary Cu elemental map of the same region.

Figure 2(a) is the secondary electron picture of a typical region of brush ends, which was in contact with the slip ring. The diagonal ruts are attributed to scratches from the emery paper. The corresponding elemental maps for Ag and Cu are shown in Figs. 2(b) and 2(c), respectively. The dark regions on the wire brush ends in Fig. 2(b) are complementary to the bright regions in Fig. 2(c). Clearly some Cu has been transferred from the slip ring to the brush. This result is indeed suprising since Cu is the stronger material. The Ag to Cu ratio in this region is $\sim$ 96:4. To elucidate this unexpected transfer, one of the brush wire ends was magnified further and the dark region marked with an arrow in Fig. 2(a) is shown in Fig. 3(a). The secondary electron mode also creates an atomic number contrast with the Cu region looking darker on a bright Ag background. The fact that the dark region is indeed Cu is well illustrated by the elemental maps shown in Figs. 3(b) and 3(c), which are due to Ag and Cu, respectively.

An extensive study of 18 wear particles was carried out in order to make some sort of a reasonable statistical distribution. Two kinds of particles were observed: Cu-rich and Ag-rich. The secondary electron image of one of the most common kinds (Cu-rich) is shown in Fig. 4(a). As witnessed in the Cu/Cu case (7), the particles were rolled up in layers. The x-ray maps of this particle are shown in Figs. 4(b) and 4(c). Clearly both Cu and Ag are present with Cu as the

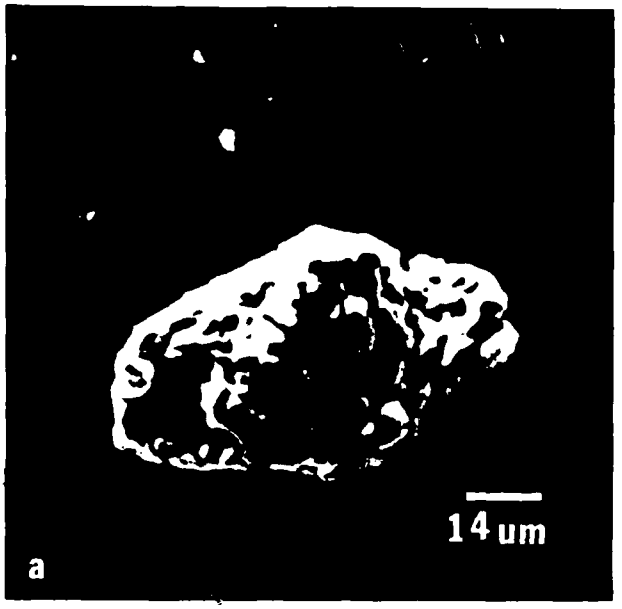

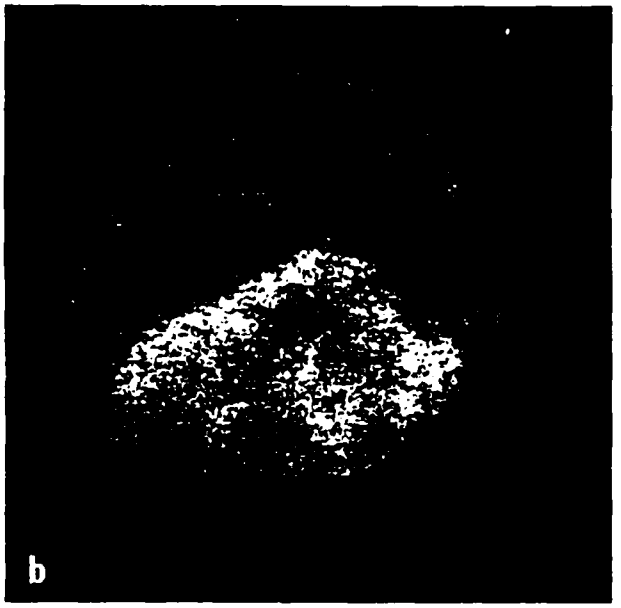

Fig. 4 (a) Secondary electron micrograph typical of a Cu-rich wear particle encountered in the 50 mA brush current experiments.
(b) Cu elemental map.
(c) Complementary Ag elemental map of the same particle.

major constituent. This result is true for the majority of particles observed. In this particular wear particle the Ag to Cu ratio is 10:90. Out of the eighteen particles surveyed, only two were found to be Ag-rich. They possessed peculiar morphologies and were different from each other, as seen in Figs. 5(a) and 5(b). The one in Fig. 5(a) had a Ag:Cu ratio of 60:40 and the one in Fig. 5(b), 96:4. The foregoing observations on the wear particles thus show that $\sim$ 90% are Cu rich and only $\sim$ 10% Ag rich. This result is indeed noteworthy since Cu, being the stronger of the two materials, was not expected to contribute to the wear debris.

A statistical distribution of the particle sizes revealed that the larger dimension varied from less than 30 μm to more than 100 μm.

DISCUSSION

The detailed microstructural and chemical analysis of the heterogeneous rotating Cu slip ring-Ag brush system has gone a long way in enhancing our knowledge of the physical events occurring at the interface. The use of UHV conditions and sputter cleaned slip ring surfaces avoided several ambiguities which could arise from contamination and has led to results which are reproducible from run to run. The wet CO_2 layer in between the sliding contacts appears to be a good lubricant. The low values of the electrical contact resistance and the coefficient of friction indicate a good electrical, mechanical, and wear resistant contact.

The most significant outcome of this work is that the constituent with higher strength and melting point can be worn away by the softer constituent with lower melting point. This observation is contrary to popular belief amongst tribologists that only the softer material is susceptible to wear and tear (10,11). Table I (12, 13) lists some relevant properties of Ag and Cu. It is known (14) that in an inhomogenous system like Ag/Cu, the isotherm of the highest temperature attained during the course of the experiment is located inside the material having lower thermal conductivity or higher resistivity, and near to the actual geometrical interface. Thus for Ag/Cu, the highest temperature should occur in the Cu slip ring.

In the actual experiment, because of the few electrical contact spots available between slip

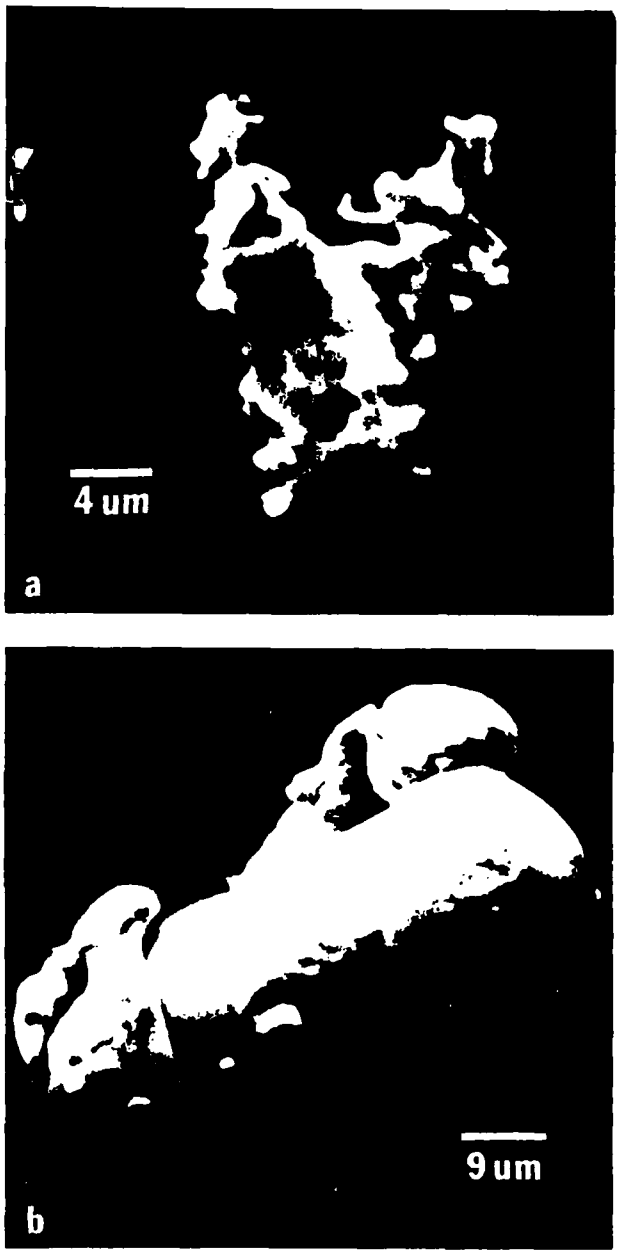

Fig. 5 (a) Secondary electron image of one of the two Ag-rich wear particles obtained for a 50mA brush.current experiment. Note the peculiar shape.
(b) Secondary electron micrograph of the other Ag-rich wear particle showing a completely different morphology.

ring and brushes, a very high current density flows and is accompanied by a corresponding I^2R drop in the interfacial regions. The tremendous heating caused thereby is localized to the few contact spots. As explained above, the associated highest temperature spot regions exist inside the Cu ring, located slightly away from the surface. As the slip ring rotates, the loci of these spots circumscribe round circular tracks.

Table I: Some Properties of Ag and Cu

	Ag	Cu	Ref.
Hardness (N/m^2)	2.5	3-9	(13)
Tensile strength (10^3 lbs/in^2)	42	60-70	(12)
Electrical Resistivity at 20°C (10^{-9} ohm-m)	15.9	16.8	(13)
Thermal conductivity (W/mdeg.)	418	380	(13)
Melting point (°C)	960	1083	(13)

In the case of the 50mA experiments, at any instant of time there are a number of weak molten spots near the ring surface. The pressure applied by the individual brush wires to the thin surface regions 'floating' on the underlying weak spots suffices to scrape it off. The presence of Cu on the Ag brushes and the predominantly Cu wear particles strongly suggest this type of mechanism. Of course, the reverse metal transfer, which is a fundamental process, is not ruled out. Thus, a small amount of the softer (Ag) material is transferred to the slip ring as well as to the debris. But our experiments show that this latter phenomenon is less significant then the preponderant harder material (Cu) removal effect.

An essentially similar picture exists for the 40A experiment. Both metal transfer mechanisms are expected to be prevalent. We do find both Cu and Ag transferred to the mating component in the slip ring-brush interface as well as to the debris. However, with the current being much higher, the voltage drop and the heating at the interface increases considerably. This result leads to a hike in the value of the highest temperature in the Cu ring and is accompanied by a concommitant increase in the temperature existing at the interface as well as inside the Ag brush. In effect, the temperature distribution curve (14) at the interface moves higher on the temperature scale. Ag being the low melting point constituent may now also melt in the near interface regions. Thus, the brushes are also exposed to severe wear. This result is clearly reflected in the composition of the wear particles, about half of which are Ag rich, as well as in the surface of the slip ring which contains a large amount (Ag:Cu::40:60) of Ag. Also, smooth and fibrous wear particles were observed in the high current case. They indicate the presence of melting and near melting conditions supporting our model. Thus in the high current regime, bidirectional transfer of metal attains essentially equal probability.

ACKNOWLEDGMENTS

The authors are grateful to the Office of Naval Research for financial support on Contract No. N00014-79-C-0763.

REFERENCES

1. J. L. Johnson and O. S. Taylor, "High Current Brushes, Part IV: Machine Environment Tests," Electrical Contacts 1979 (I.I.T. Chicago), pp. 129-135, 1979.
2. R. M. Slepian, "High Current Brushes V-Subdivided Monolithic Brushes at Very High Current Levels," Electrical Contacts 1979 (I.I.T. Chicago), pp. 137-144, 1979.
3. I. R. McNab and G. A. Wilkins, "Life Tests with Carbon Fiber Brushes," Sixth Conference on Electrical Contact Phenomena, Chicago, 1972.
4. I. R. McNab and W. R. Gass, "High Current Density Carbon Fiber Brush Experiments in Humidified Air and Helium," Electrical Contacts 1979 (I.I.T. Chicago), pp. 159-163, 1979.
5. B. Singh and R. W. Vook, "In Situ AES Characterization of Rotating Electrical Contacts," IEEE Transactions on Components, Hybrids, and Manufacturing Technology, 4, 36-40, 1981.
6. B. Singh, B. H. Hwang and R. W. Vook, "Characterization of Copper Slip Ring-Wire Brush Electrical Contacts," Journal of Vacuum Technology Applications and Ion Physics, 1981.
7. B. Singh, J. G. Zhang, B. H. Hwang and R. W. Vook, "Microstructural Characterization of Rotating Cu-Cu Electrical Contacts in Vacuum and Wet CO_2 Environments," Electrical Contacts 1981 (I.I.T. Chicago), pp. 279-285, 1981.
8. J. L. Johnson and L. E. Moberly, "High Current Brushes I. Effect of Brush and Ring Materials," Proc. 23rd Holm Conference on Electric Contacts, Chicago, 1977.
9. B. H. Hwang, B. Singh, R. W. Vook and J. G. Zhang, "In Situ AES Characterization of Wet CO_2 Lubricated Sliding Copper Electrical Contacts," Electrical Contacts 1981 (I.I.T. Chicago), pp. 273-278, 1981.
10. D. H. Buckley, Surface Effects in Adhesion, Friction, Wear, and Lubrication, Elsevier, 1981, Chapter 5.
11. M. Antler, "Sliding Wear of Metallic Contacts," Electrical Contacts 1980 (I.I.T. Chicago), pp. 3-24, 1980.
12. H. N. Wagar, Physical Design of Electronic Systems Vol. III (Ed. D. Baker, W. O. Fleckenstein, D. C. Koehler, C. E. Roden, and R. Sabia) Prentice Hall, New Jersey, 1971, Chapter 8.
13. C. D. Hodgman ed., Handbook of Chemistry and Physics, 36th edition, Chemical Rubber Publishing Co., Cleveland, Ohio (1954).
14. Ragnar Holm, Electric Contacts Theory and Application, Springer-Verlag, N.Y., 1967, pp. 78-86.

APPENDIX V

Wear Debris Analysis in Rotating Ag-Cu Electrical Contacts

by

A. Banerjee, J. G. Zhang, M. Garshasb, L. R. Zhang, and R. W. Vook

Accepted for publication in Wear

WEAR DEBRIS ANALYSIS IN ROTATING Ag-Cu ELECTRICAL CONTACTS

A. Banerjee, J. G. Zhang, M. Garshasb, L. R. Zhang, and R. W. Vook

Department of Chemical Engineering and Materials Science
Syracuse University, Syracuse, New York 13210

ABSTRACT

A Cu slip ring was rotated in contact with two current carrying Ag wire brushes in an ultra high vacuum system. The Cu ring was initially sputter cleaned and the experiments were performed in humidified CO_2 at atmospheric pressure. The wear particles produced at the two contacts were collected for subsequent investigations by scanning electron microscopy and electron probe microanalysis. Currents ranging from 0 to 40 A were used and the slip ring was rotated at 150 rpm. In one zero current experiment a speed of 15 rpm was used for comparison. The wear particles consisted of pure Ag, pure Cu and mixed particles with the relative amounts depending upon the current through the contact. Some of the characteristic features of the most frequently occurring wear particles are explained and the mechanisms for the generation of the particles discussed.

INTRODUCTION

In the recent past some attention has been focussed towards understanding the origin of wear particles [1-4] resulting from two sliding constituents. It is generally recognized that in any application in tribology, wear and tear should be reduced to a minimum. The reduction is usually realized by the use of solid, liquid or gaseous lubricants. However, in spite of all improvements, a finite amount of wear remains which leads to physical removal of material from the interface in the form of small particles. An analysis of these wear particles in terms of their size, shape and chemical composition can go a long way towards understanding the wear phenomena at the interface. It should be pointed out that the problem is extremely complex since various types of wear mechanisms [1,2] are possible and, more often than not, all of them are present simultaneously. The determination of the individual contributions of each of these mechanisms is difficult and necessitates study of a host of parameters, e.g., the mechanical contact force, sliding velocity, real area of contact, environmental conditions, interfacial contaminant or lubricant layers, nature of the materials, temperature at the interface, coefficient of friction and contact resistance. Clearly, a strict control over all these parameters is a difficult task and frequently exotic wear particles are produced defying explanation. Therefore, effort should be directed towards collecting and analyzing as many wear particles as possible so that conclusions based on a statistical distribution can be reached. Obviously, the experiments tend to become tedious.

In the present case of rotating electrical contacts [4-7], the generation of wear particles involves an added complexity arising from the electric current which passes through the sliding contact. Thus, a new domain in tribology is

involved, one in which the effects of a direct current flowing from one sliding constituent to the other are superimposed on those due to conventional sliding. A detailed literature survey indicates that little knowledge exists in this field. In the present work, we report on a series of careful studies that involve a Cu slip ring rotating in contact with two fixed Ag wire brushes. A current was passed through the two contacts and the resulting wear debris was analyzed. The results of our initial investigations on the shapes, sizes and compositions of the debris particles as a function of different currents passing through the system are reported.

EXPERIMENTAL DETAILS

Figure 1 shows the geometrical configuration of the OFHC Cu slip ring-Ag(99.9%) brush assembly. The Cu ring was basically a solid cylinder rotating about a vertical axis. The two similar Ag brushes were made from 342 Ag wires of diameter 0.005". The spring shown in the figure held the two brushes in firm contact with the Cu ring and with a known force. The slip ring could be aligned with respect to the brushes about the X, Y and Z directions using a specimen manipulator. This entire assembly was mounted in an ultra high vacuum (UHV) system capable of achieving a vacuum $< 10^{-9}$ Torr. The slip ring was rotated from outside using a magnetic rotary feedthrough which was coupled to an interchangeable motor that was used for imparting different angular velocities to the slip ring.

The exact experimental procedure consisted of first mechanically polishing and chemically cleaning the individual brushes and slip ring in order to obtain conventionally clean surfaces for sliding. The brush ends were shaped to obtain the curvature of the ring to ensure as good an electrical and mechanical contact as possible by running them on an emery paper sleeve fitted on the slip ring.

The assembly was subsequently mounted on the UHV chamber for evacuation and baking, thereby achieving pressures in the low 10^{-9} Torr range. The surface oxide and other contaminant layers of the slip ring were sputter cleaned using an Ar sputter ion gun. The cleanliness of the slip ring surface was checked in-situ using Auger electron spectroscopy. Next, the chamber was backfilled to one atmosphere pressure of humidified CO_2. (Humidified CO_2 is known [4,6,8] to be a good gaseous lubricant). This gaseous atmosphere was achieved by bubbling CO_2 through a triply distilled water trap.

The actual experiment was carried out by rotating the slip ring with a fixed motor voltage in the humidified CO_2 atmosphere and with the two brushes in contact as shown in Fig. 1. In all cases except one, the angular velocity of the slip ring was 150 rpm, as recorded by an optical tachometer. In the exceptional case it was 15 rpm. All the experiments were carried out for a fixed number of revolutions, namely 6000, irrespective of the slip ring velocity. Some of the wear particles which were generated at the two contact interfaces were collected below on a Mo tray. The effect of current on the wear particles was investigated by passing a direct current of 0, 0.05, 1.0 and 40 A from one brush to another through the slip ring in four different experiments. Whereas the fast motor (150 rpm) was used for studying the four above cases, the slow motor (15 rpm) was used with zero current for comparison with the zero current-fast motor case.

After each experiment, the wear particles were observed in a scanning electron microscope (SEM) for their shapes and sizes. The chemical composition and elemental distributions in each particle were determined using an electron probe microanalyzer (EPM) fitted with an x-ray energy dispersive spectrometer. More than twenty particles were investigated in each case.

RESULTS AND DISCUSSION

The sizes of all the particles investigated by SEM were recorded. Because of the peculiar shapes, only the longest dimension was used to determine the size distributions, which varied from a few micrometers to a fraction of a millimeter. It should be pointed out that the smaller size particles were difficult to collect because of the mechanical nature of transfer from the tray to the SEM specimen holder. No clear systematic variation of the size distribution was observed as a function of current or motor speed. The sizes of the particles and their distributions are expected to depend on a host of parameters, e.g., motor speed, nature of brush and slip ring, force of the spring, interfacial layers, interface geometrical roughness, and current. It is very difficult to keep a strict control over all the parameters and, therefore, some variation of the size distribution was found to occur from one experiment to another under essentially similar conditions.

It is generally believed that when a hard material slides across a softer material, the soft material is worn away, leading to its predominance among the wear particles. In the present case at zero brush current, the majority of particles were pure Cu or Cu-rich. However, the hardness at room temperature in N per m^2 of Cu is 3.9×10^8 [9] and is higher than that of Ag, 2.5×10^8 [9]. This result can be understood if the various wear mechanisms are considered. Because of the experimental conditions one can eliminate corrosion, erosion, fatigue, fretting, and cavitation as possible wear mechanisms [1,2]. Adhesive wear alone will result in the preponderance of the softer material (Ag) in the wear debris. The dominance of Cu in the wear particles for zero current and 15 rpm rotational speed (where we expect negligible frictional heating at the interface) can thus be attributed only to abrasive wear. In this mode, a Cu

wear particle initially gets embedded in a Ag brush wire end and subsequently becomes work hardened with successive revolutions of the slip ring. The work hardened particle then functions as a cutting tool, removing material from the Cu slip ring. The presence of Cu particles on the surface of the brushes has been confirmed experimentally by EPM analysis after completion of the experiment. This phenomenon of a softer material wearing away a harder material has been reported earlier [10] for the Al-teflon system. The adhesive wear mechanism has been evidenced, in addition to the abrasive wear, in all the current rating experiments. Experimental corroboration has been obtained by in-situ Auger analysis and ex-situ EPM analysis of the Cu slip ring surface which showed the presence of Ag.

Apart from these two relatively better known modes of wear, a third wear mechanism, namely, interfacial melting was also observed to occur in the present Ag-Cu system. When current flows across the interface, the electrical power dissipation may lead to melting conditions at small localized spots, that is the electrical contact spots, at any instant of time. When melting occurs, one can expect Ag and Cu to be mixed in the resulting melted region. This process thereby accounts for the higher concentration of mixed Ag-Cu wear particles in the high current regime. The melting phenomenon is clear in the 40 A case and will be illustrated later in the SEM pictures taken of the wear particles.

In all the experiments the wear particles possessed various shapes and sizes. Typical micrographs of the most commonly found particles will be presented in order to determine the major causes of friction and wear. A sequence of photographs is presented according to the various proposed wear models. Basically, four major modes of wear have been identified, namely, those due to adhesion, abrasion (the chisel effect), polishing, and melting. The features of the majority of wear particles can be explained on the basis of these four effects and combinations thereof.

The Chisel Effect

It has already been mentioned that Cu particles embedded in Ag brush wire ends act as a cutting 'tool tip' or 'chisel' for Cu. It is noteworthy that $\lesssim$ 10% of all the brush wires were in actual contact with the slip ring after 6000 rotations of the ring. This conclusion was based on SEM observations of the wire ends after the completion of each experiment. During the initial part of the experiment, even a lesser number of wires was in contact since with successive revolutions both the slip ring and wire ends become polished, thereby increasing the true contact area. Further, only a certain fraction of the total cross sectional area of each individual contacting wire was in actual contact. This result was evidenced by SEM observations which showed only partial polishing of the wire ends. One can conclude from the foregoing discussion that the cutting tips for wear particle formation can be situated only in these areas of contact. The shapes, sizes and lengths of the wear particles depend on a host of parameters which include the geometrical configuration of the tool tip, its hardness relative to the material being cut, possibly the speed of the motor, and interactions among the various wear particles.

For elucidation of the chiselling action, a pictorial representation in chronological sequence of the formation of a wear particle is shown in Fig. 2. The picture is highly simplified assuming no interference from one brush to another, no mixing of wear particles and that no other wear mechanisms are present. The work hardened wear particle embedded in the Ag brush wire ploughs out material as the Cu slip ring rotates anticlockwise as shown in Fig. 2(a). A thin layer of Cu is chiselled out which then curls up as shown in Fig. 2(b) and (c) to form the rolled up wear particle shown in Fig. 2(d).

In the actual experiments, the presence of the chiselling phenomenon is strongly supported by wear particles of the type shown in Fig. 3(a) which was created in the zero current, 15 rpm case. The particle consists mainly of Cu, though a small amount of Ag was also detected by the multichannel analyzer of the EPM. The presence of Ag can be attributed to small Ag particles trapped inside the curled up layer, which presumably existed at the interface prior to the chiselling event. Their origin lies in the adhesion wear phenomenon.

The above example of the chiselling effect is almost an ideal one and frequently other non-ideal events occur which modify the shape of the curled up layer. For example, the curling up process can be abruptly interrupted by the particle being chipped away before it can curl up completely. Figures 3(b) and (c) are two examples of non ideal but common variations of the chiselling effect. The pure Cu particle in Fig. 3(b), produced in the zero current, 15 rpm experiment, has the characteristics of a partly rolled up layer with sharp folds resembling long ruts parallel to each other. This morphology can be understood on the basis of the uneven surface of the slip ring which gives rise to a wear particle which is thin in some regions and thick in others. The weaker regions collapse giving rise to the corrugated finish of the particle in Fig. 3(b). Also noteworthy is the smooth appearance of the particle on the left hand side. Apparently this region of the particle was joined to the Cu ring surface while the entire chip was being formed. It would thus have been twisted somewhat before it broke off. The wear particle in Fig. 3(c) is a pure Cu one and was produced in the 1.0A current, 150 rpm case. This particle is yet another example of a variation of the sequence shown in Fig. 2. The folding of the Cu layer can be attributed to a finite ($\lesssim$ 1 mm) vibration

in the vertical plane of the rotating slip ring during the course of the experiment. As a result the contact force and hence the ploughing force changes periodically leading to the folded up particle in Fig. 3(c).

All the particles shown hitherto were either pure Cu or Cu rich. A similar phenomenon of chiselling is also possible for producing pure Ag or Ag-rich particles. The only difference lies in the nature of the cutting tool. Ag particles produced by this process can arise because of two types of cutting edges. One is the Cu slip ring surface itself in which some regions are jagged and act as chisels. The second consists of Cu wear particles trapped at the interface. Figure 4 is an example of a Ag rich particle produced in the 40 A, 150 rpm experiment. The particle is a completely rolled up Ag layer and the presence of a Cu signal in addition implies the presence of Cu particles trapped inside in analogy to Fig. 3(a).

The chiselling phenomenon can also lead to wear particles which appear like rolled up wires. Two such examples are shown in Figs. 5(a) and (b). These wire-like shapes of the wear particles can be explained on the basis of a cutting tip which is very small in diameter. Both particles were produced in the same zero current, 150 rpm motor experiment. However, the one in Fig. 5(a) is a pure Cu one whereas Fig. 5(b) shows a Ag rich particle.

The Polishing Effect

Wear particles produced by those brush wires which are not situated at the circumscribing edges of the brush but somewhere centrally get trapped in between the brush and slip ring where they spend some time while the slip ring rotates before being released from the interface. During this time, the particles may undergo several modifications in terms of their shapes, sizes, and chemical

compositions. The particle shown in Fig. 6 is a typical example of such a situation. The particle is the result of a zero current, 15 rpm experiment. It appears that at least three particles have coalesced, and the smooth surface indicates polishing of the particle by the motion of the slip ring. As expected in such a case, the particle is a mixture of both Ag and Cu with Ag as the major constituent.

Another example of the polishing phenomena is shown in Fig. 7. Figure 7(a) illustrates a Ag rich wear particle in the form of a layer obtained in the 50 mA, 150 rpm experiment. A glance at Fig. 7(b) which is the SEM micrograph of one brush wire taken after the experiment, shows the great similarity between the encircled loose region and the wear particle in Fig. 7(a). Clearly, rotation of the slip ring has resulted in a thinning and polishing action which resulted in the thin, flat layer shown in Fig. 7(b) and still attached to the wire end. Continued rotation would result in breaking off this heavily cold worked layer to form a particle such as the one shown in Fig. 7(a).

The Melting Effect

Because of friction between the slip ring and brush ends in addition to I^2R heating at the interface, where I is the current flowing and R is the constriction resistance, an intense amount of heat is generated locally. Temperatures of the order of many hundreds of degrees Celsius are generated instantaneously at the interfacial contact spots. The dissipation of heat from the few high temperature contact spots occurs by conduction through the bulk Ag brushes and slip ring and convection and radiation to the ambient humidified CO_2. However, the temperatures attained at the interface are sufficient to melt both Ag and Cu so that many particles carry a history of being associated

with melting phenomena. Our experimental evidence shows that even at zero current 150 rpm, some wear particles are produced by the melting phenomenon, though no melting effect has been observed for the zero current 15 rpm case. It should be noted that the temperature increase at the interface is not an average one but localized to the available electrical and mechanical contact spots at the interface. In the present work, the melting effects are the greatest at 40 A, the highest current used. It is therefore expected that particles which are mixed in nature should be more prevalent. Experimental investigations do reveal that the fraction of mixed particles is the highest for the 40 A case.

Melting conditions lead to the creation of wear particles whose shapes are different from the ones described earlier. One particular example is shown in Fig. 8(a) which has been produced by the zero current 150 rpm experiment. The dark hollow spots are attributed to shrinkage voids produced in this pure Cu particle on solidification.

Melting can also produce particles which resemble straight or intertwined strings as shown by the examples of Fig. 8(b) and (c). One can explain this morpholc by using the simplified model shown in Fig. 9. Figure 9(a) shows one brush wire in contact with the slip ring at only one point for the sake of simplicity. Because of a combination of friction and I^2R heating at this interface, a small amount of material adjacent to the interface either in Ag or Cu or both will melt. It is known [11] that the highest temperature is attained not at the geometrical interface but slightly away from it in the material with the lower thermal conductivity at that temperature. Let us assume that in Fig. 9(a), a small Cu region melts. A magnified picture of the contact region is shown in

Fig. 9(b). As the slip ring rotates, a small string of Cu is pulled out, as displayed in Fig. 9(c), which finally breaks off from the Ag wire. Before the end of this string that is held by the parent Cu ring can solidify, it would be expected to develop a spherically shaped head because of surface tension effects. This state is shown in Fig. 9(d). After solidification occurs, the protruding string would be knocked off by another wire end, giving rise to the wear particle of the type shown in Fig. 9(e).

A good example of the string type particle is shown in Fig. 8(b) which was produced in a zero current, 150 rpm experiment. The particle is pure Cu in nature. That this particle resulted from a melting phenomenon is supported by the expectation that tensile deformation and fracture after cold welding should have resulted in a particle that was Ag or Ag rich. Moreover it is difficult to envision the formation of the spherical shape at the end of the string by some means other then melting and solidification.

The above model is a simplified version and more than one molten contact spot (from the same brush wire or different wires) is possible whereby several strings could be created. Figures 9(b), (f), (g) and (h) can be invoked to predict the morphology of the wear particle in such a case. Figure 9(b) is a contact area which when magnified shows several smaller contact spots and strings as shown in Fig. 9(f). The strings shown in Fig. 9(f) could consist of both Ag or Cu because of the high temperature condition. As the slip ring rotates, the strings get intertwined as shown in Fig. 9(g). The final wear particle in Fig. 9(h) is, therefore, a jumbled series of strings consisting of a mixture of both Ag and Cu. A practical demonstration of this type of wear particle is

shown in Fig. 8(c), which was formed in a 40 A, 150 rpm experiment. The particle is clearly a mixture of both Cu and Ag as witnessed by the corresponding elemental maps shown in Figs. 8(d) and (e), respectively. This morphology is characteristic of the high current cases and was not observed with zero current. It should be noted that the chisel and polishing effects are also present in the high current experiments as confirmed by other wear particles.

Another example of a particle formed by melting is shown in Fig. 8(f). This Cu particle exhibits layered structure and is the result of the 40 A, 150 rpm experiment. The layered structure can be explained if repeated melting-solidification conditions at the interface region are invoked. If the area of contact is small, the I^2R heating may lead to melting in the interface. Because of the mechanical contact force between the brush and the slip ring, the molten region may be flattened out to a layer. In the dynamic situation, as the slip ring rotates the molten layer adhering to the surface solidifies as it moves away from the region of electrical contact. In the next contact position between this layer and the slip ring and if the contact area is again small, another flattened molten region may be created. Again the loss of electrical contact during progressive rotation would result in solidification. Thus layer upon layer of solidified formerly molten regions could be produced resulting in the wear particle shown in Fig. 8(f).

SUMMARY

It has been shown conclusively that friction between a soft (Ag) and hard (Cu) material can lead to the wear and tear of predominantly the harder species. The wear debris consists of pure Cu, pure Ag, and mixed Cu-Ag particles. The relative quantities of the pure and mixed particles produced have been shown to be dependent on the current flowing through the contacting materials. A

study of the shape and the characteristic features of various wear particles has revealed four major modes of particle formation: abrasion, adhesion, polishing and melting. The models proposed explain the shapes and chemical compositions of most of the particles observed.

ACKNOWLEDGMENT

The authors are grateful to the Office of Naval Research for financial support on Contract No. N00014-79-C-0763.

REFERENCES

1. Donald H. Buckley, Surface Effects in Adhesion, Friction, Wear, and Lubrication, Tribology Series 5, Elsevier, 1981, p. 429-509.

2. A. D. Sarkar, Friction and Wear, Academic, 1980, p. 33-191.

3. A. D. Sarkar, Wear of Metals,Pergamon, 1976, p. 42-159.

4. B. Singh, J. G. Zhang, B. H. Hwang and R. W. Vook, Wear, 78 (1982) 17.

5. B. Singh, B. H. Hwang and R. W. Vook, Vacuum, 32 (1982) 23.

6. B. H. Hwang, B. Singh, R. W. Vook and J. G. Zhang, Wear, 78 (1982) 7.

7. B. Singh and R. W. Vook, IEEE Transac. on Components, Hybrids and Manufacturing Technol. 4 (1978) 36.

8. J. L. Johnson and L. E. Moberly, IEEE Transac. on Components, Hybrids and Manufacturing Technol., 4 (1981) 36.

9. H. N. Wagar, Physical Design of Electronic Systems, Vol. III, Bell Telephone Laboratories, Prentice-Hall, 1971, p. 450.

10. Donald H. Buckley, Surface Effects in Adhesion, Friction, Wear, and Lubrication, Tribology Series 5, Elsevier, 1981, p. 483-485.

11. Ragnar Holm, Electric Contacts Theory and Application, Springer Verlag, 1967, p. 78-86.

FIGURE CAPTIONS

1. Experimental configuration of Cu slip ring and two Ag brushes.
2. Schematic diagram of the formation of wear particles by the chisel effect.
3. Pure Cu and Cu rich particles produced by the chisel effect: (a) Cu rich, formed in zero current, 15 rpm experiment, (b) pure Cu formed in zero current, 15 rpm experiment, and (c) pure Cu formed in 1.0 A, 150 rpm experiment.
4. Ag rich particle formed by chisel effect: experimental conditions: 40 A, 150 rpm.
5. Wire shaped particles produced by narrow chisel. Experimental conditions for (a) and (b) are zero current, 150 rpm. (a) Pure Cu and (b) Ag rich.
6. Wear particle formed by polishing effect. Experimental conditions: zero current, 15 rpm.

7(a). Layer like Ag rich wear particle formed by the polishing effect. Experimental conditions: 50 mA, 150 rpm.

(b). SEM view of a partly polished Ag brush wire end. Encircled region shows a loose layer which would give rise to a wear particle of the type shown in Fig. 7(a).

8. Wear particles formed by the melting effect: (a) pure Cu showing shrinkage voids in zero current, 150 rpm experiment, (b) pure Cu fiber formed under zero current, 150 rpm condition, (c) Cu rich intertwined fibers formed in 40 A, 150 rpm experiment, (d) and (e) Cu and Ag x-ray elemental maps, respectively, of particle (c), and (f) Cu particle exhibiting layered structure and formed in the 40 A, 150 rpm experiment.
9. Schematic diagram of the formation of wear particles involving melting effects.

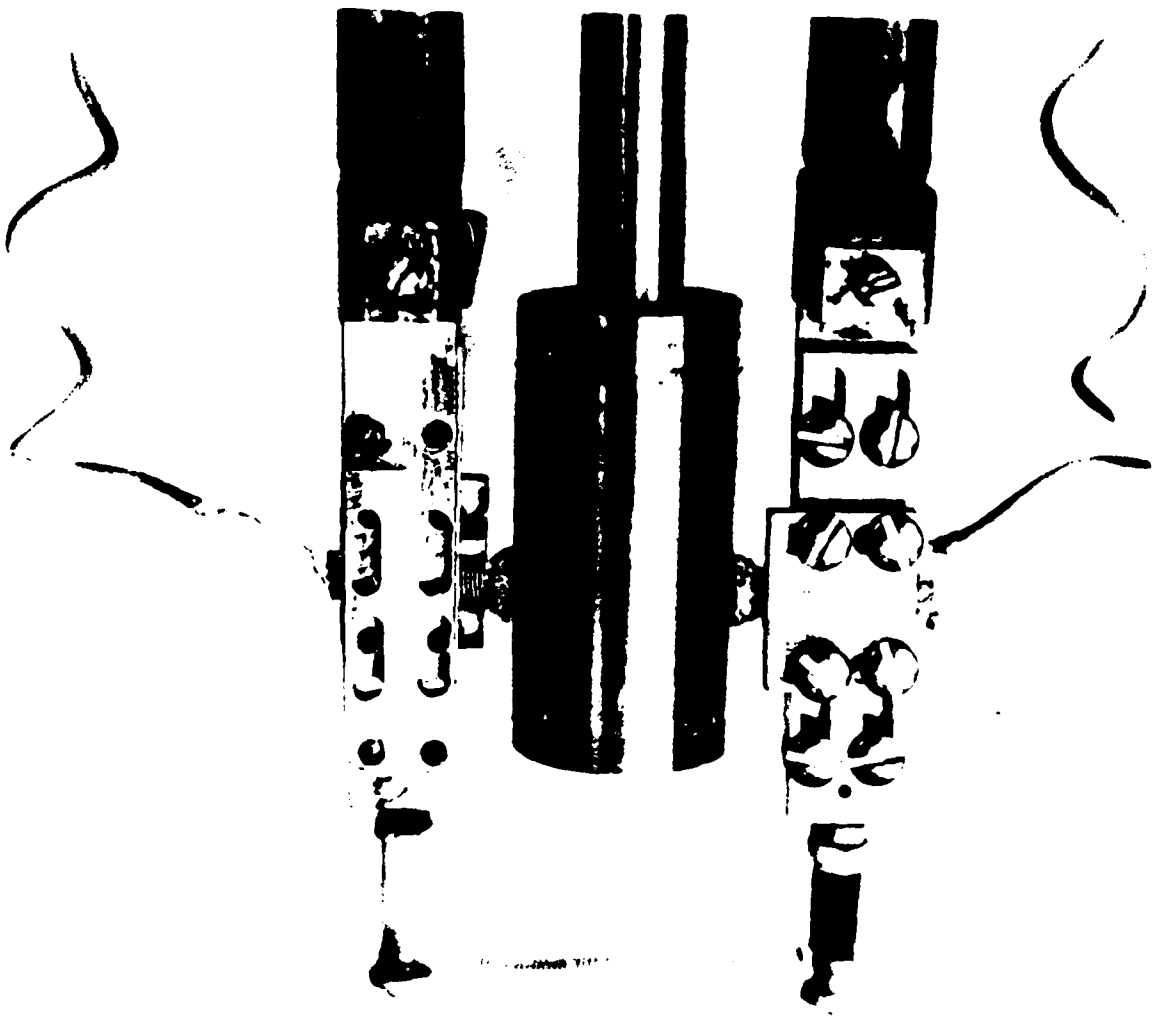

EXPERIMENTAL CONFIGURATION OF CU SLIP RING AND TWO AG BRUSHES.

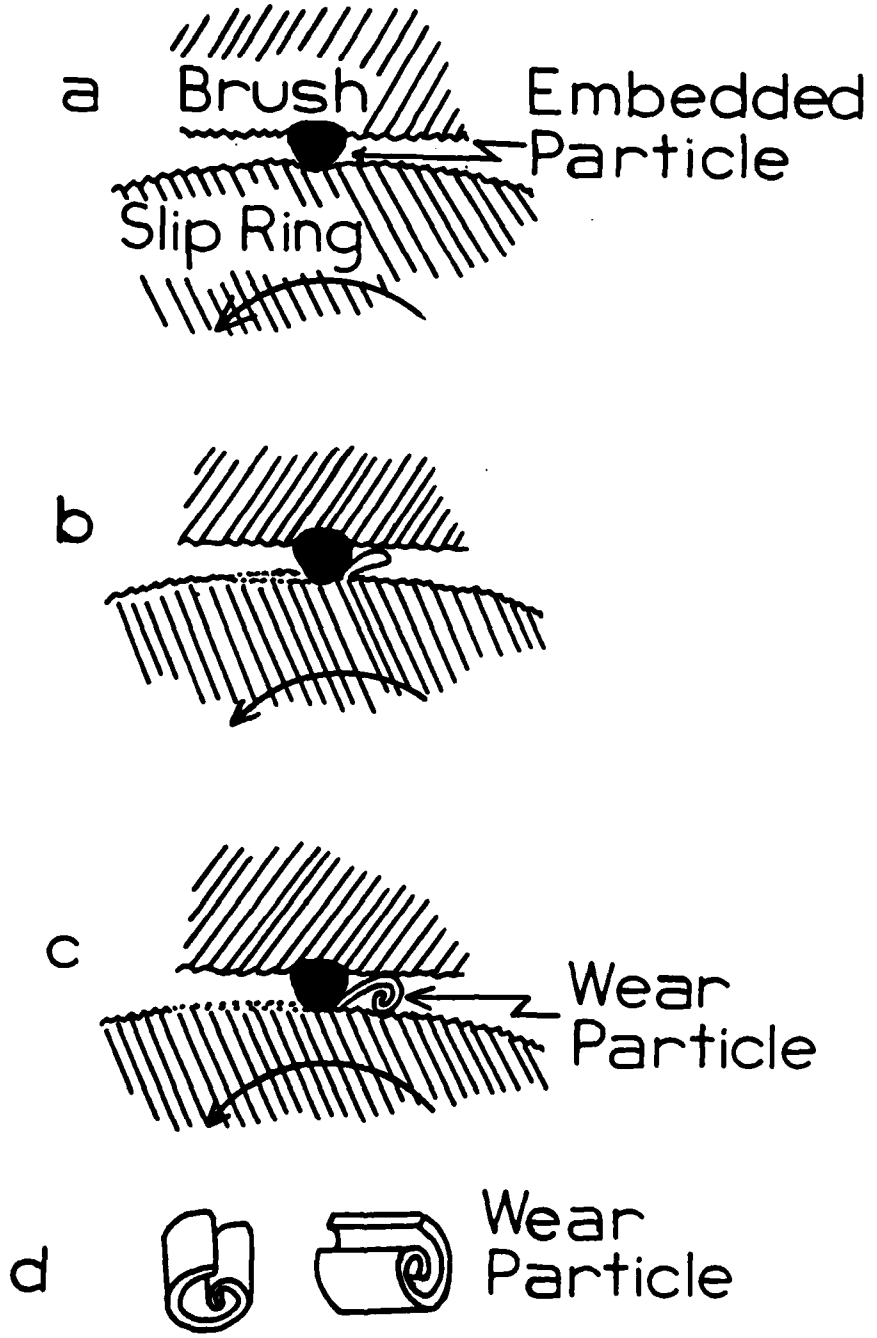
a
Brush
Embedded
Particle
Slip Ring
b
c
Wear
Particle
d
Wear
Particle

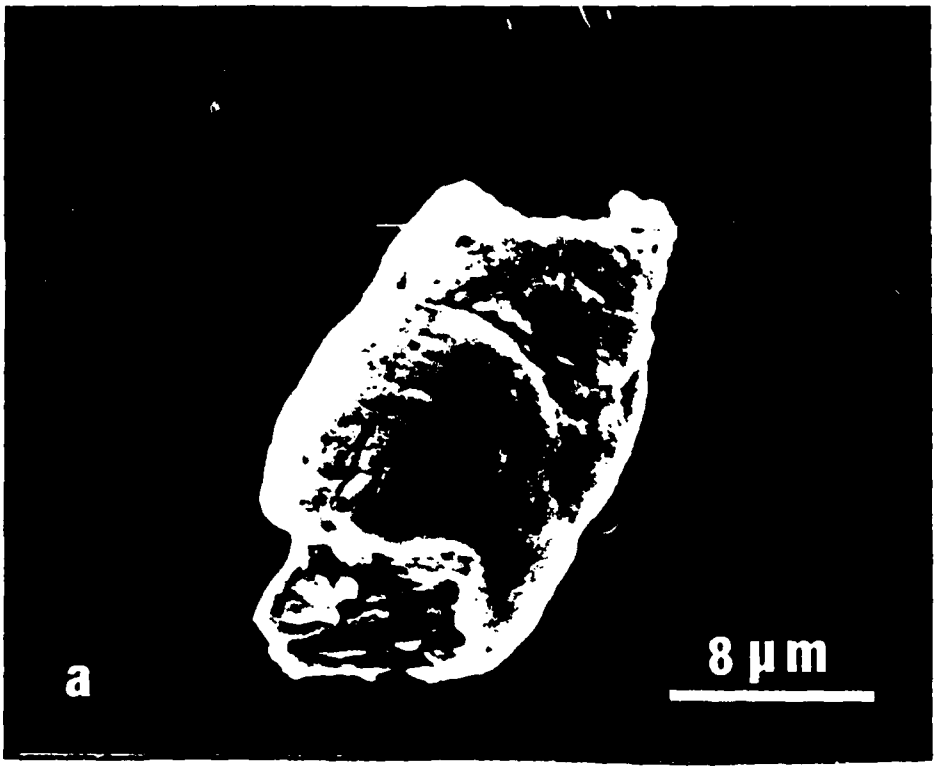

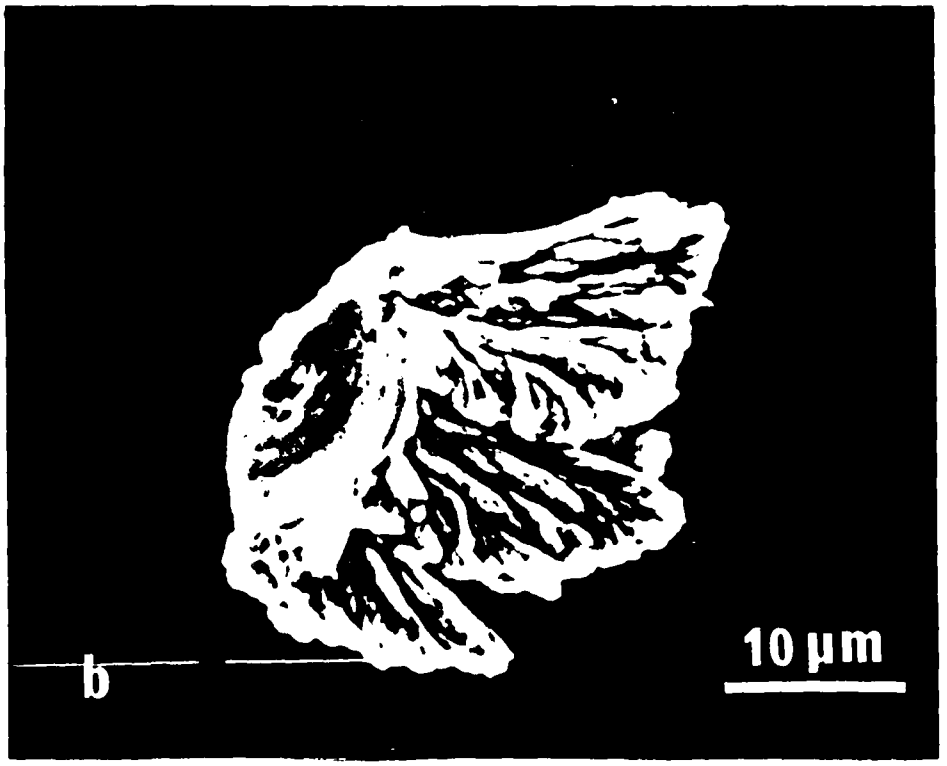

Fig 3a + b

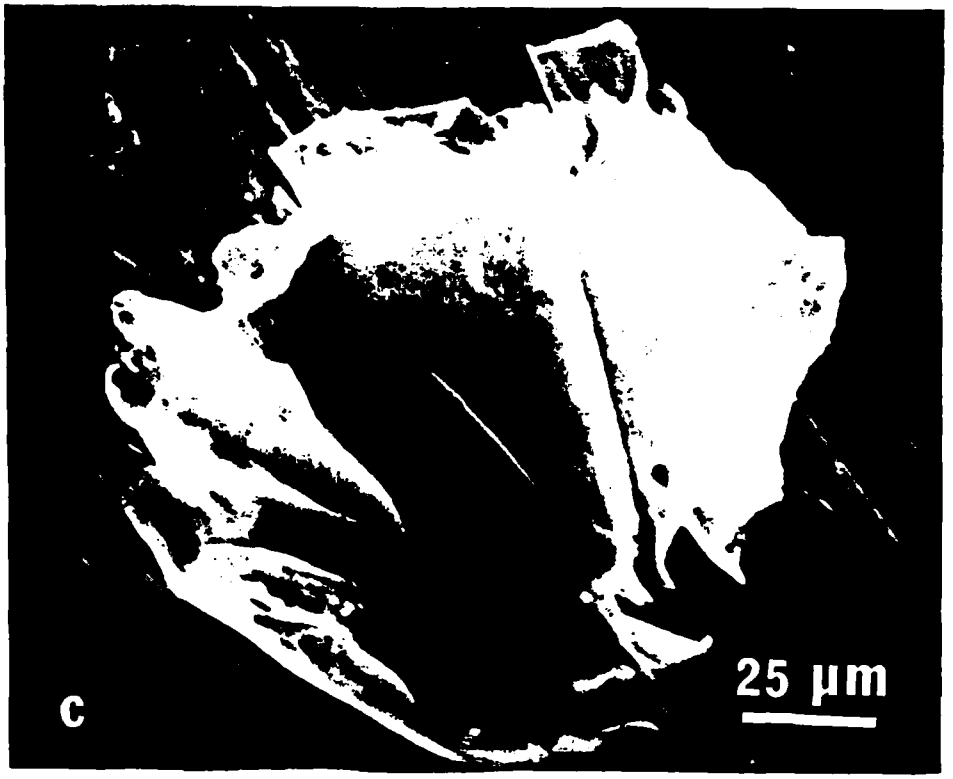

Fig 3c

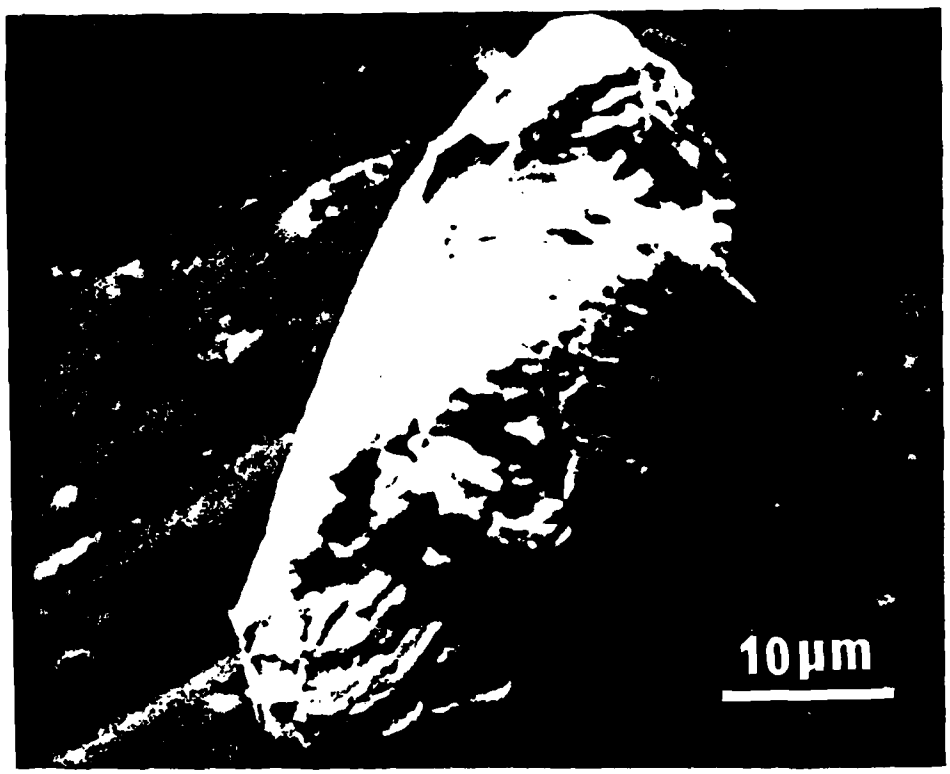

Fig 4

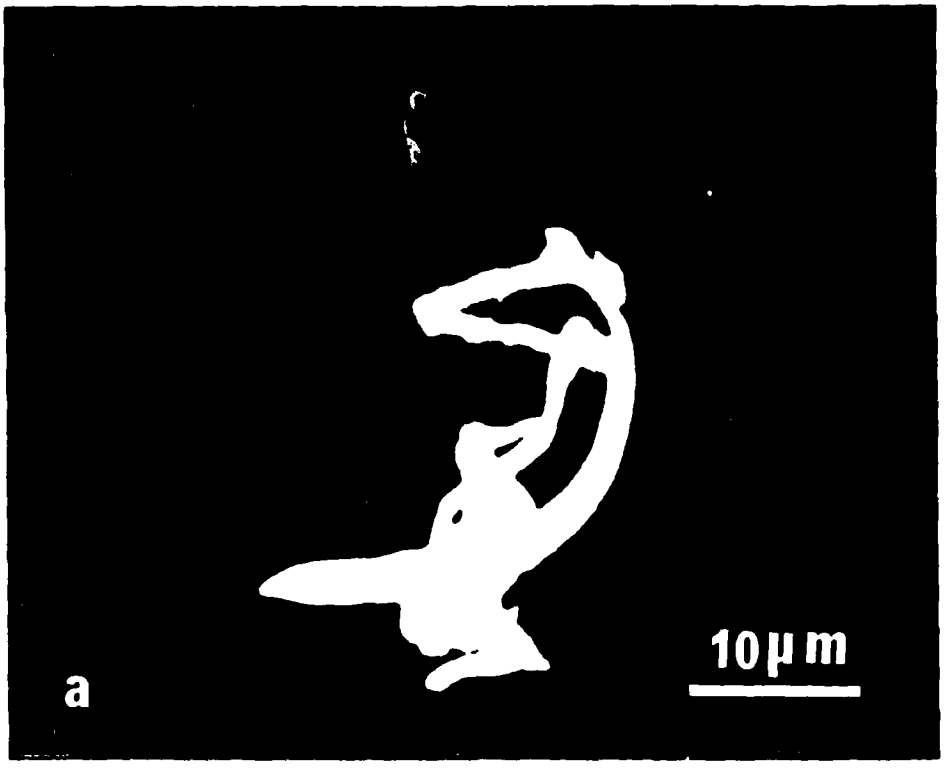

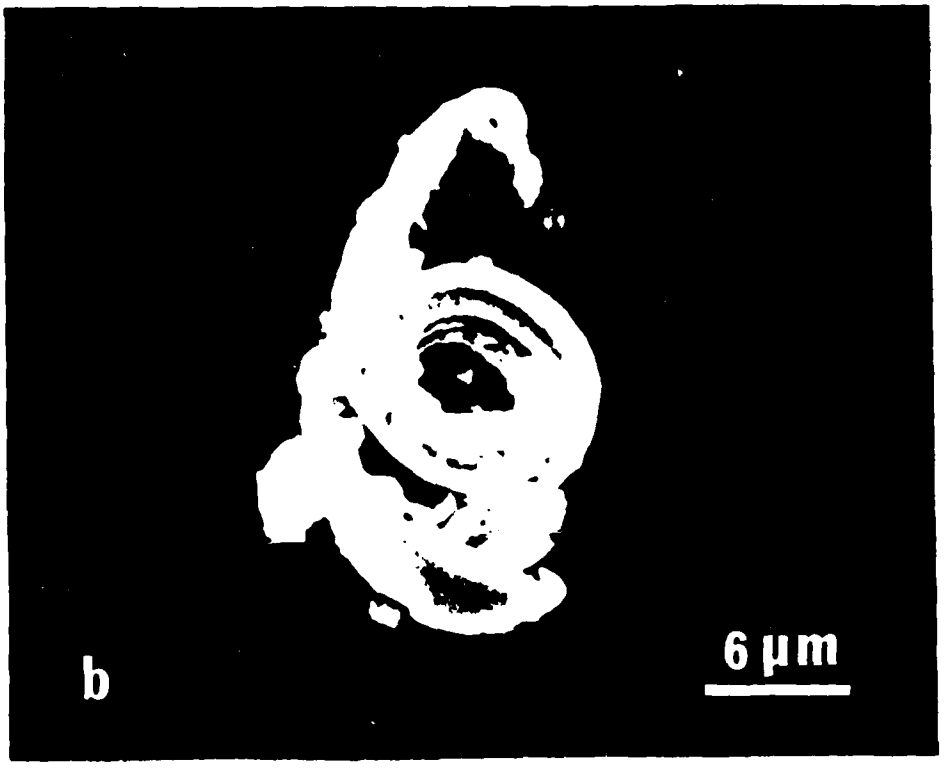

Fig 5a,b

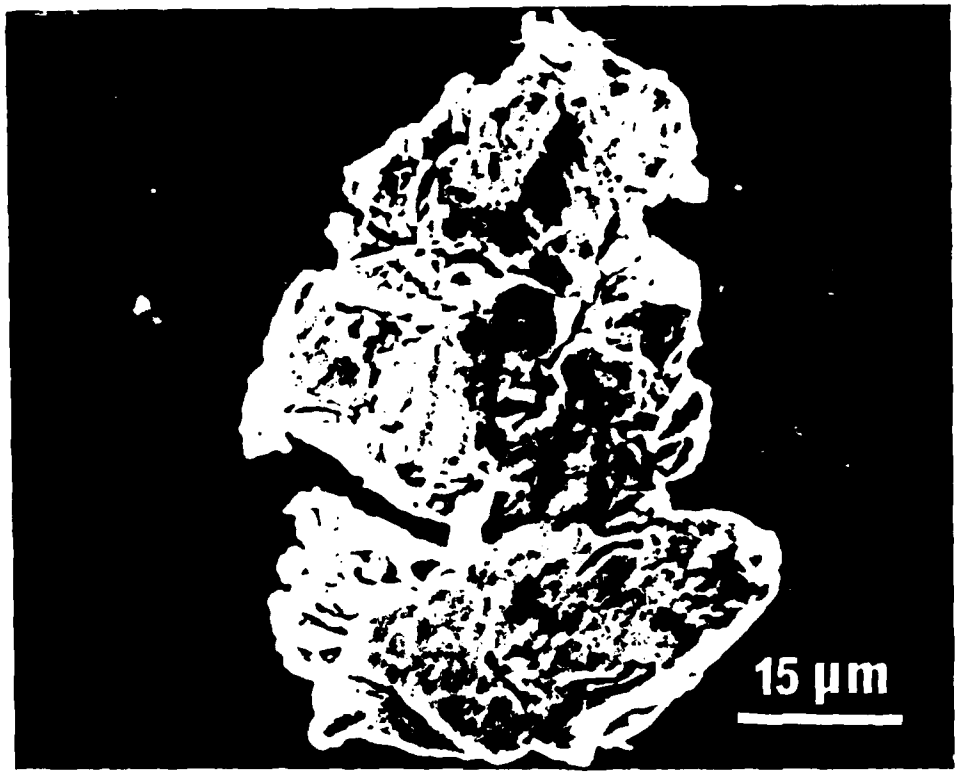

Fig 6

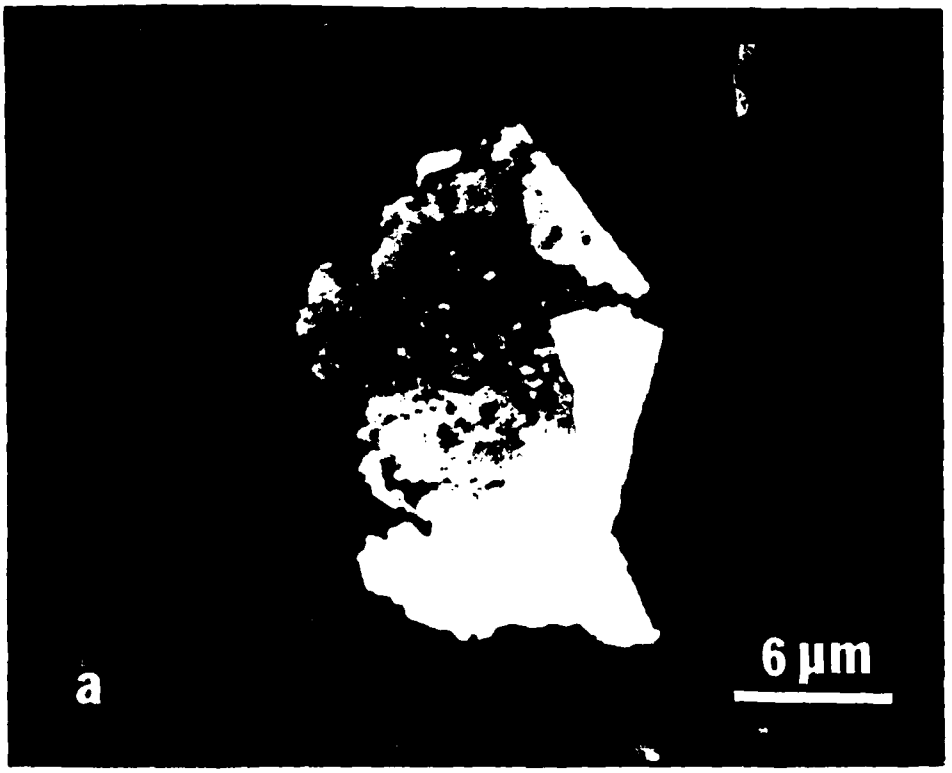

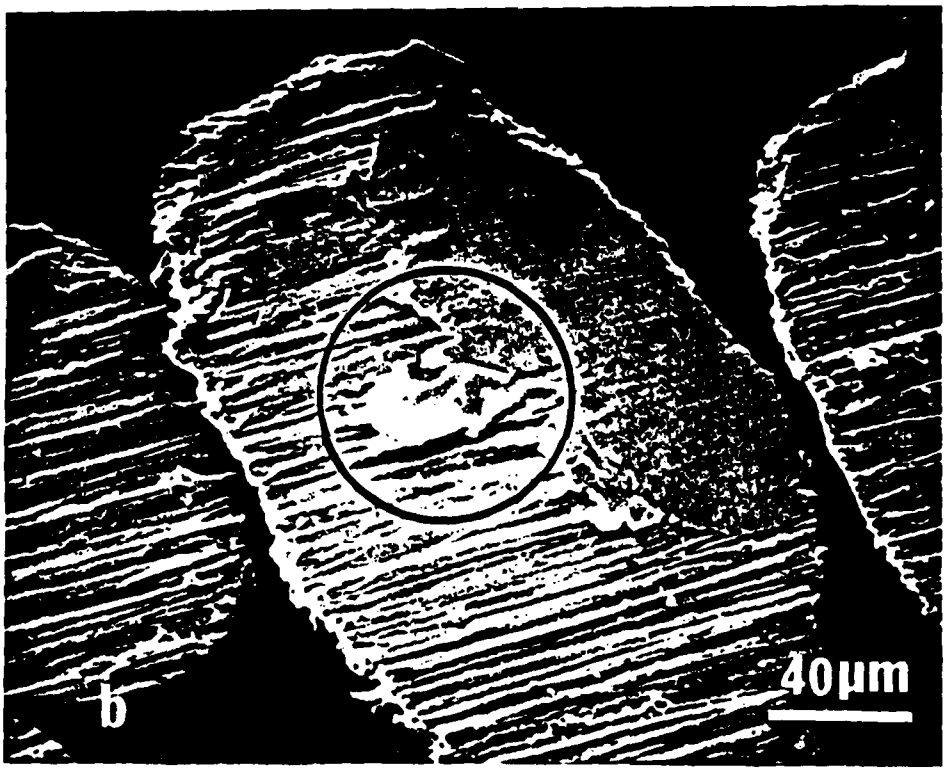

Fig 7a,b

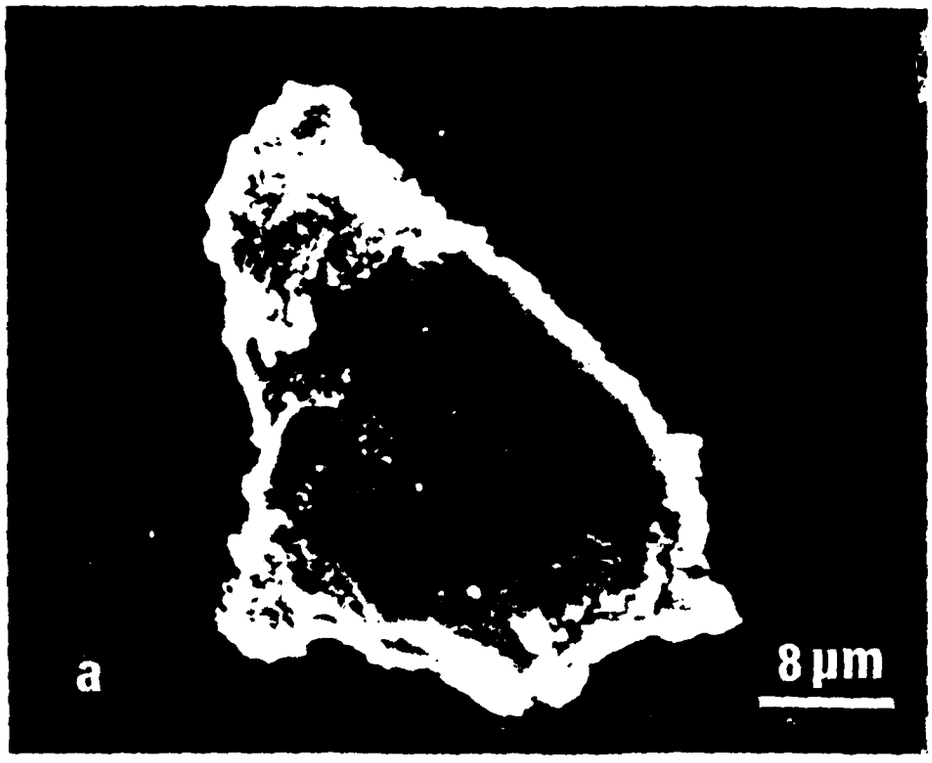

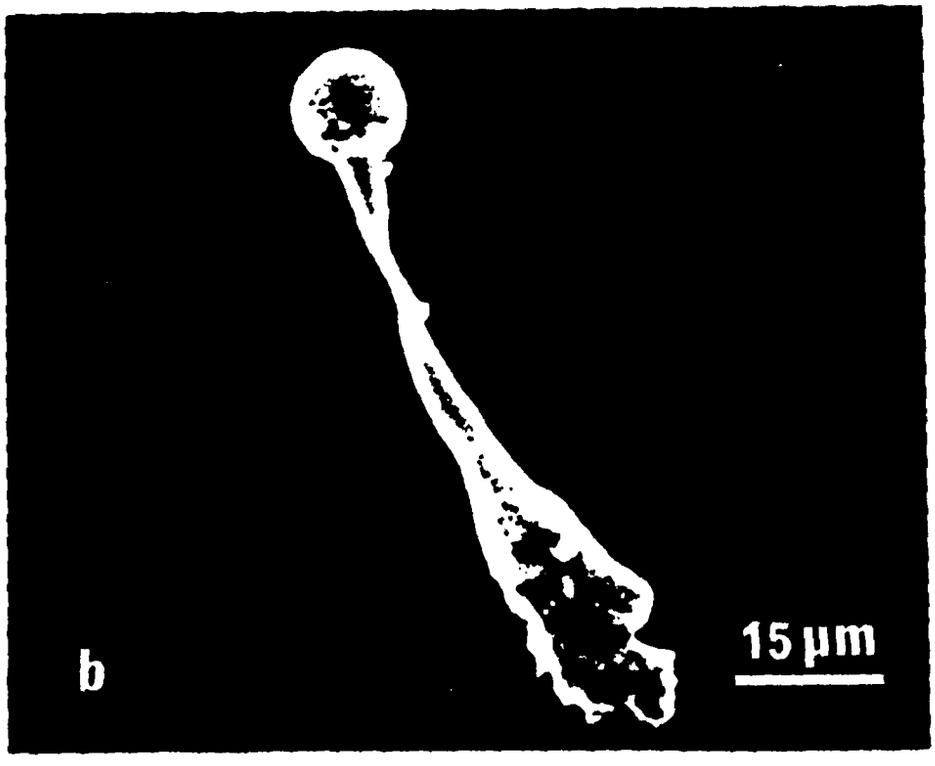

Fig. 8a b

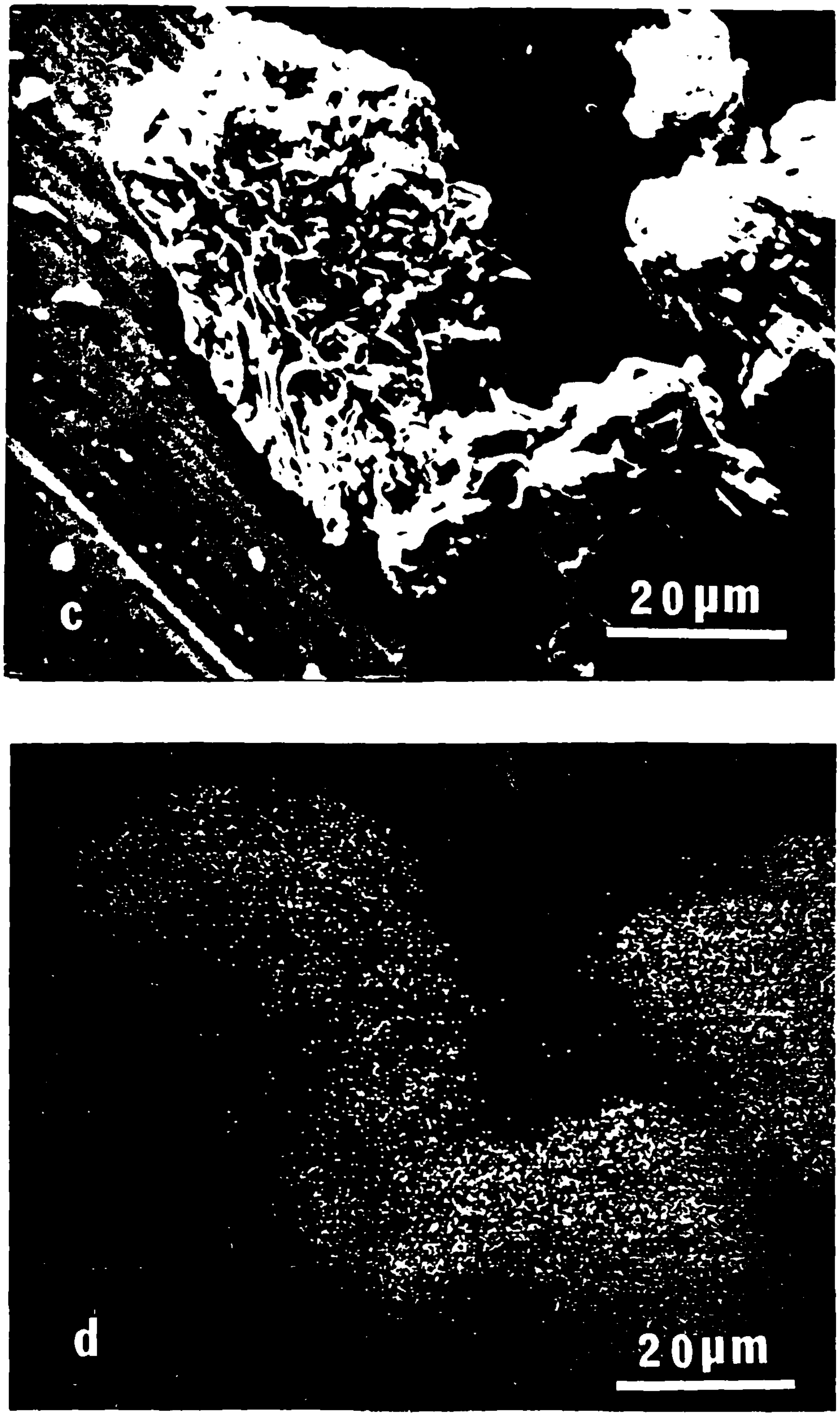

Fig 8c,d

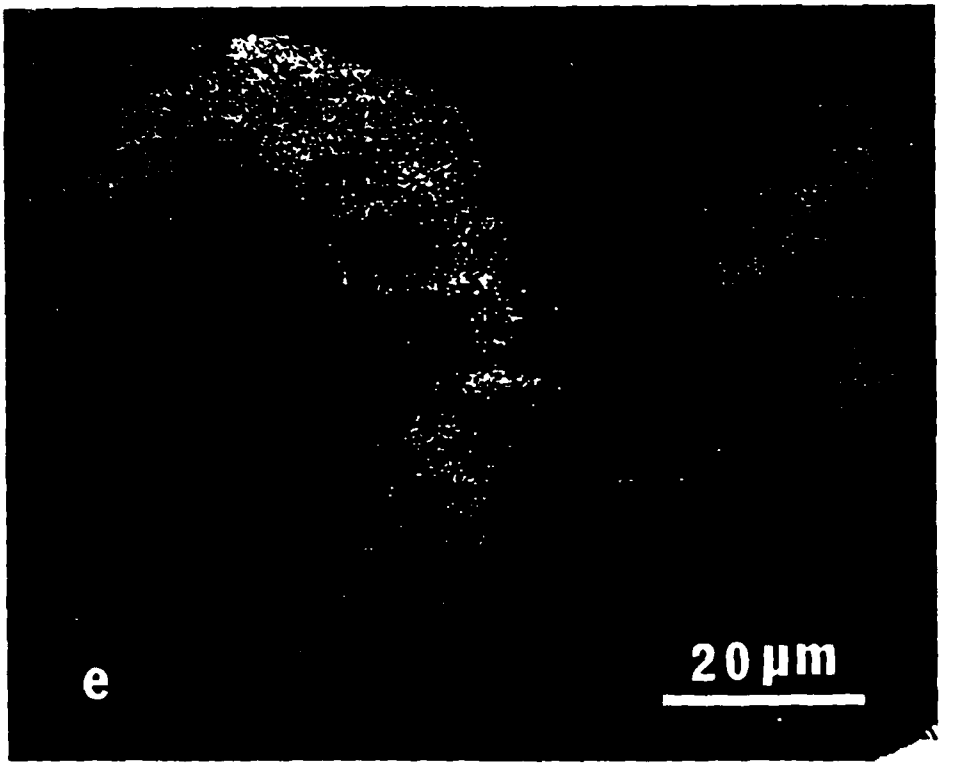

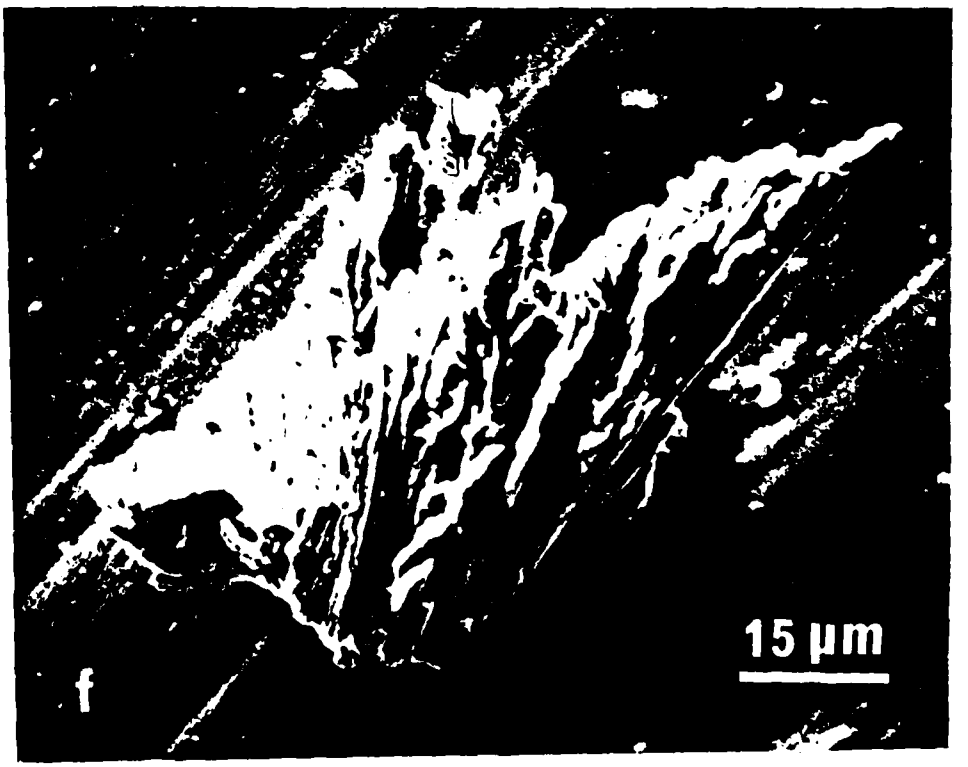

Fig 3f

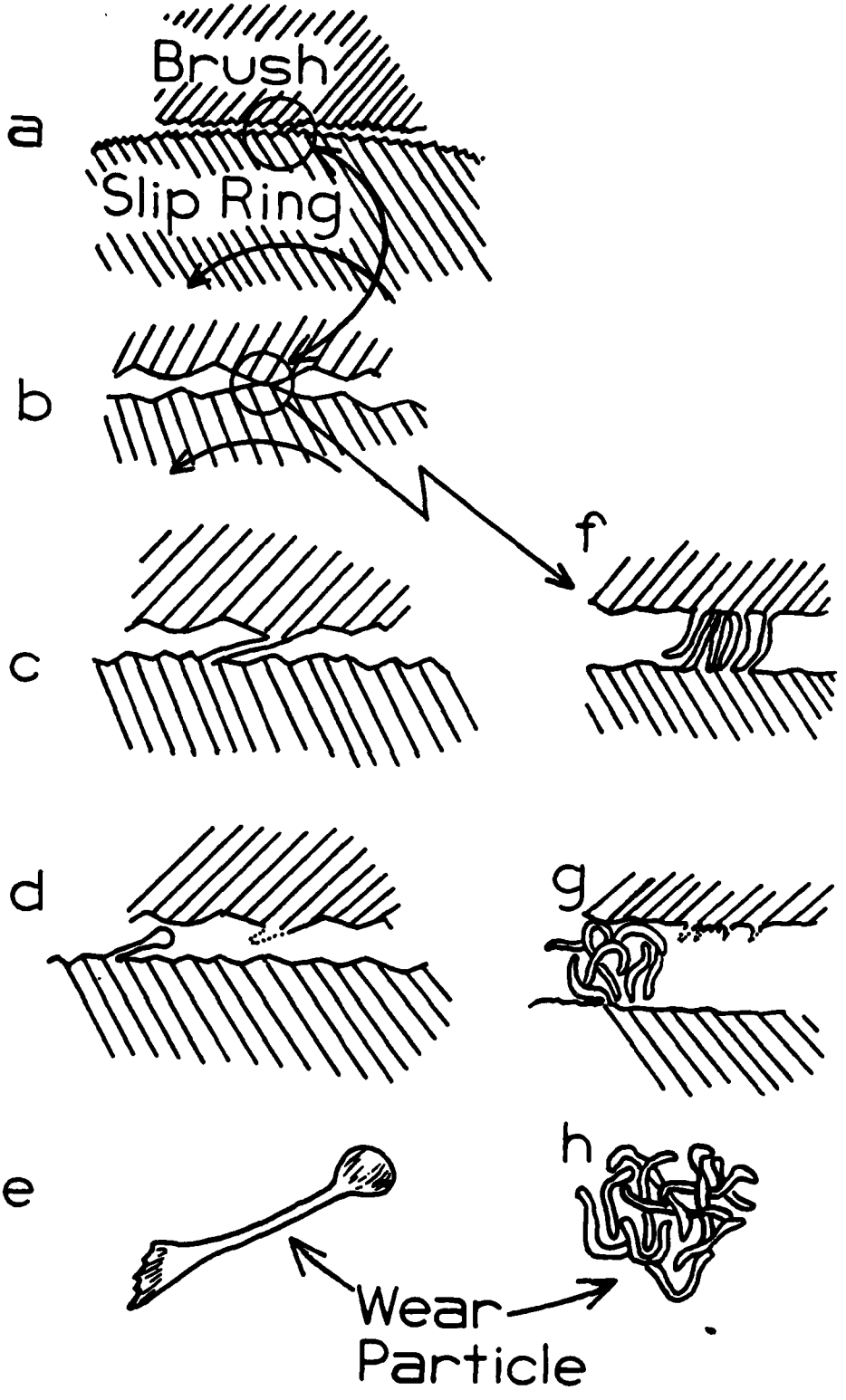
Brush
a
Slip Ring
b
f
c
d
g
e
h
Wear
Particle

APPENDIX VI

Electric Current Effects in Wear Phenomena at A Rotating Cu-Ag Interface

by

A. Banerjee, M. Garshasb, L. R. Zhang, J. G. Zhang, and R. W. Vook

Submitted to Wear

ELECTRIC CURRENT EFFECTS IN WEAR PHENOMENA AT A ROTATING Cu-Ag INTERFACE

A. Banerjee, M. Garshasb, L. R. Zhang, J. G. Zhang, and R. W. Vook

Department of Chemical Engineering and Materials Science
Syracuse University, Syracuse, New York 13210

ABSTRACT

Two Ag wire brushes were held in contact with a rotating Cu slip ring in an ultra high vacuum system. After initial sputter cleaning of the Cu slip ring, the vacuum system was backfilled with one atmosphere of humidified CO_2. A d.c. electric current was passed across the Ag brush-Cu slip ring-Ag brush assembly and the resulting wear particles were analyzed using scanning electron microscopy and electron probe microanalysis. The slip ring surface was analyzed using Auger electron spectroscopy to determine the amount of Ag transferred. Currents ranging from 0 to 50 A were used. In each case, the numbers of pure Cu, pure Ag, Cu rich, and Ag rich particles were recorded as a function of current. The Auger signal from the slip ring and the concentrations of the elements in the wear debris were plotted versus current to determine the role of current in the present Cu-Ag system.

INTRODUCTION

Study of sliding electric contact between two metals encompasses two major parameters. The first is the conventional tribological problem of wear and lubrication at the interface. The second is the effect of electric current flowing across the junction. The former problem has been studied [1,2] earlier in some detail. However, very little knowledge [3-5] exists in wear and tear behavior when current crosses the interface.

It is well known that when two constituents are sliding against each other, material is worn away from the interface region resulting in wear particles. Various wear mechanisms [1,2] are known to exist which can be used to explain the creation of the particles. It is generally believed that the harder sliding constituent removes material from the softer member though some [5-8] exceptions to this rule have been identified. However, in all cases, the wear particles could either escape from the interface or become incorporated on the surfaces of the sliding members at the interface region. Further, the chemical nature of the wear species could vary from pure elements corresponding to one of the parent members to a mixture of both. The wear and tear process could be drastically reduced by the incorporation of suitable lubricants. The lubricant material may belong to the solid, liquid or gaseous state. For example, humidified CO_2 gas is known [3,9] to be a good lubricant for many applications. Electric current flow across the interface is yet another important parameter which is expected to alter the wear mechanisms. This case is typically the one that exists in the operation of a motor in which the current carrying brushes are constantly rubbing against the slip ring. One well known effect due to the additional current parameter is the famous polarity effect [10]

observed by Ragnar Holm. Another obvious ramification of current flow is the localized heating at the relatively few [11] electrical contact spots between the two current carrying members. We have established [5] earlier that the generation of some of the wear particles can be attributed directly to melting conditions existing at the interface because of current heating effects.

In this paper we have extended our previous work [4,5] to investigate the chemical composition of the metal transfer in the rotating Cu slip ring-Ag brush electric contact system. Ultra high vacuum and sputter cleaning techniques were used to eliminate many of the possible wear mechanisms so that the number of variable parameters was reduced to a minimum. The effect of current was established by passing different currents through the Cu-Ag assembly. Based on our observations a model has been proposed to explain the role of current.

EXPERIMENTAL DETAILS

The details of the experimental techniques have been published earlier [4,5]. Briefly a high purity Cu cylinder (diameter $\sim$ 1"), constituting the slip ring, was rotated in an ultra high vacuum (UHV) system. Two current carrying pure Ag wire brushes,each consisting of 342 individual Ag wires of diameter 0.005", were held in contact with the Cu ring. The slip ring and the brushes were initially polished and cleaned before mounting onto the UHV system. The slip ring was later cleaned in the system using an Ar sputter ion gun to get rid of surface contaminant layers. In-situ Auger electron spectroscopy (AES) was used to analyze the chemical composition of the slip ring surface. CO_2 was then bubbled through a triply distilled water trap into the vacuum system till a pressure of one atmosphere was attained.

The slip ring was next rotated at a fixed rpm of $\sim$ 150 with the two brushes held in contact. The number of rotations in each experimen was 6000, except for the 50 A experiment in which it was only 750 because of intense arcing. The different current values investigated were 0, 0.05, 1.0 1.8, 5, 15, 30, 40, and 50 A. In one exceptional experiment an rpm of 15 with zero current was used, but the total number of rotations was the same, namely 6000. After the experiments, the system was pumped down to a pressure of $\sim$ 1 x 10^{-6} Torr within $\sim$ 1-2 hours and AES was done on the slip ring surface. The AES spectrum was taken with the slip ring rotating so that an average signal coming from the entire track on the slip ring which was in contact with the Ag brush was recorded. During this time, the brushes were withdrawn from the slip ring with the help of controls from outside, so that no further wear took place.

The wear particles collected during each experiment were analyzed according to their shapes, sizes, and chemical composition using scanning electron microscopy and electron probe microanalysis (EPM). In each case, about twenty five particles or more were selected at random so that a conclusion based on a statistical distribution could be reached.

RESULTS AND DISCUSSION

Probably the most typical wear particles out of the large variety of particles formed in all the experiments is shown in Fig. 1(a), which was obtained in the zero current, 150 rpm experiments. The shapes of such particles resemble a completely or partially rolled up layer. The particle shown is pure Cu and the origin of these particles has been treated at length earlier [5]. Briefly, heavily cold worked Cu particles get embedded in the relatively softer Ag brush

wire ends and subsequently dig out more Cu wear particles as the slip ring rotates in contact with the Ag brushes. This phenomenon also explains the preponderance of Cu amongst the wear particles in the low current regime where current heating effects are negligible.

However, the 'chiselling' phenomenon [5] mentioned above does not explain the initial formation of the Cu particles since Cu is known [12] to be a harder material than Ag. Therefore, one has to invoke the concept of prow or wedge formation [7,8,13] by which a softer material in rider form (Ag brush) could remove a harder material in flat form (Cu ring). A picture of a prow which was later knocked off to form a wear particle is shown in Fig. 1(b). The particle is mixed in nature with Cu as the major constituent and is the result of a 40 A, 150 rpm experiment. The layered structure and the wedge shape of the particle are characteristic of a prow. Later on in this paper it will be shown that the prow formation mechanism, though present, is not the dominant wear mechanism, as is evident from the experimental results.

Each wear particle analyzed in all the current experiments was placed in four different categories depending on its chemical composition as determined by EPM. The first consisted of those particles which were pure Cu, the second pure Ag, the third mixed particles with Cu as the major constituent (Cu rich), and the fourth mixed particles with Ag as the major constituent (Ag rich). To further clarify the definition of mixed particles, a Cu rich particle is one in which the Cu intensity is greater than 50% and there is a finite Ag signal as well. The definition of Ag rich particles is similar. The number of particles in each of these categories for each current was normalized according to the percentage of the category in the whole. Thus, at any

particular current, the sum of all the categories adds up to 100. Plots of some of these categories and combinations thereof as a function of current are shown in Fig. 2. The large error bars are due to the variation in data from run to run for any specific current experiment.

The 50 A current experiment was a failure from the point of view of adding another data point in Figs 2 and 3 since it could not be run to completion. Within five minutes of rotation at 50 A, considerable arcing developed between the Ag brushes and the slip ring and could be seen visibly. Large numbers of wear particles were generated within this short period of time (corresponding to 750 rotations) compared to 40 minutes in the other experiments. Clearly, the new phenomenon of arcing cannot be considered to be an extension of the other lower current experiments. The experimental condition for the generation of the wear debris as well as the physical material removal mechanisms are expectedly different. Hence, no experimental point corresponding to the 50 A case has been included in Figs. 2 and 3. Nevertheless, the results obtained are important and therefore briefly dwelt upon towards the end of the paper.

In Fig. 2, the zero current experiments have two data points on the curve corresponding to the 150 rpm and 15 rpm cases. The fraction of pure Cu particles is approximately constant in the 0 to $\sim$ 100 mA current range and the value is $\sim$ 72%. At currents exceeding $\sim$ 100 mA, the fraction of pure Cu particles increases to a maximum of $\sim$ 96% in the current interval $\sim$ 1.5 to $\sim$ 5.0 A. In the high current regime $\gtrsim$ 10 A, the pure Cu fraction falls drastically to attain a value of $\sim$ 32% at 40 A. The curve for the sum of pure Cu and Cu rich particles increases monotonically with current in the range, $\sim$1.5 - 5.0 A,

where it shows a maximum value of $\sim$ 96% before plummeting down to a value of $\sim$ 51% corresponding to a current of 40 A.

The pure Ag + Ag rich curve shows an exact complementary behavior (as expected) to the pure Cu + Cu rich curve since at any current the sum of the two should be 100. In Fig. 2, the fourth curve is for the Cu rich + Ag rich particles. It shows a dip in the current range $\sim$ 1.5 to $\sim$ 5.0 A. On the high current side, the curve shows a steep increase to $\sim$59% at a current of 40 A. The curve for pure Ag particles has not been shown since the fraction is small $\sim$ 0 to $\sim$ 10% and no systematic behavior with current has been observed.

There are three important features corresponding to three different current regimes in Fig. 2 which deserve closer consideration. The first is the low current range from 0 to $\sim$ 100 mA where a high concentration of Cu particles is observed, the second is the intermediate current range of $\sim$ 1.5 to $\sim$ 5.0 A where the pure Cu concentration increases to a maximum along with a concomittant decrease in the mixed particle concentration to a minimum. The third is the high current regime of $\gtrsim$ 10 A, where the concentration of pure Cu and pure Cu + Cu rich particles shows a phenomenal decrease. The concentration of mixed and pure Ag + Ag rich particles exhibits a corresponding increase. In the low current range, the high concentration of Cu and Cu rich particles, as compared to that for Ag (despite the fact that Cu is harder than Ag [12]), has been explained earlier [5] on the basis of work hardened Cu particles embedded in the Ag brush wire ends which act as cutting tips for Cu from the slip ring.

To explain the increase in Cu particles in the intermediate current range, one has to invoke the concept of additional heating caused by the I^2R

drop at the interface. Here I is the current flowing through the system and R is the junction resistance. The first and foremeost consequence of this heating is the desorption of the lubricating humidified CO_2 layer from the surfaces of the Cu ring and the Ag brush wire ends. The removal of the lubricant will enhance the cutting ability of the Cu 'chisels' embedded in the Ag brush ends. Thus, the fraction of Cu particles is expected to go up. The curve for pure Cu + Cu rich particles is greatly influenced by the pure Cu curve since most of the particles are pure Cu, $\sim$ 96%. Once the fraction of pure Cu particles goes up, the remaining fraction of mixed particles (Ag rich and Cu rich) expectedly goes down. Therefore, in this intermediate current regime, Cu removal by the 'chisel' effect is the strongest and the effect overshadows other wear mechanisms.

In the high current regime, there is a reversal in the trend that was prevalent at intermediate currents. This result is attributed to increased heating at the interface due to the higher I^2R power loss which leads to localized softening and partial melting at the electrical contact spots. The immediate ramification is the mixing up of both Ag and Cu to form mixed wear particles. The melting points of Ag and Cu are 960°C and 1083°C, respectively. That is, they are reasonably close to each other and, therefore, melting and near-melting conditions would generally lead to wear particles of the mixed variety. The accompanying decrease in thepure Cu concentration as a function of current can also be explained by the higher heating at the interface. The heating tends to melt or soften the work hardened Cu 'chisels', thereby decreasing their cutting power. Because of the dominance of the pure Cu curve, the pure Cu + Cu rich value also falls in a concomittant manner. The curve for pure Ag + Ag rich increases mainly because of an increase in the concentration of Ag rich particles.

Another noteworthy feature of Fig. 2 is the Y coordinate value at the intersection points of the upper and lower series of curves. The crossover occurs at about 25 to 40 A and the fraction of particles for all the curves shown is $\sim$ 50% in this region. In other words, the number of Ag + Ag rich particles is equal to the number of Cu + Cu rich particles at high currents ($\sim$ 40 A) or equivalently high interfacial temperatures. This phenomenon is indeed expected since softening and melting will tend to mix up Ag and Cu more or less equally (both have melting points close to each other), thus giving rise to equal concentrations of the two species of particles. The tendency for Cu and Ag to become mixed up in the wear particles will affect all wear mechanisms. This result is born out by the fact that the mixed particle concentration increases in the high current regime albeit the number of wear particles formed exclusively by the 'melting' phenomenon [5] is quite low.

The crossover for the curves (b) and (c) in Fig. 2 occurs at $\sim$ 25 to 30 A. The intersection of the curves at the 50% particle concentration value implies firstly that the number of pure metal particles (which is approximately equal to the number of pure Cu particles) is the same as the number of mixed particles at this current value. Further, it also implies that the chiselling phenomenon, which is the major wear mechanism mode for Cu, and the high current heating effects attain equal importance at the crossover current value. At still higher currents, one would expect the melting effects to overshadow other wear mechanisms.

The transfer of Ag from the brush ends to the wear particles can be explained on the basis of adhesive wear [1,2] since Ag is the softer of the two materials. A behavior similar to the Ag + Ag rich curve in Fig. 2 is exhibited

by the Ag Auger signal on the Cu slip ring taken after each of the above experiments was performed, see Fig. 3. The plot gives the peak to peak height ratio of the Ag to the Cu (60 eV) Auger signals on a dN/dE spectrum as a function of current. The 60 eV line of Cu has been intentionally selected for giving the ratio since the actual surface composition is of interest and the 60 eV line is more surface sensitive than the 920 eV line [14]. The Ag to Cu ratio plotted on the Y axis is a measure of the amount of Ag coverage on the slip ring surface after each experiment. It should be noted that the peak heights have been directly used for the ratio calculations and no sensitivity factor corrections have been made since only the qualitative behavior is of interest. The units on the Y axis are, therefore, arbitrary. As seen in Fig. 3, the Ag coverage is, or equivalently the Ag transferred to the slip ring, is almost independent of current in the 0-5 A range, suggesting that adhesive wear remains constant. The small amount of Ag transferred to the slip ring shows that the brushes are experiencing very low wear rates. At currents greater than 5 A, the Ag coverage increases rapidly, a result which can be explained as per the earlier argument that complex softening and/or melting effects start dominating and interfering with other wear modes, thereby resulting in Ag transfer from brush end to not only the wear particles but also to the Cu slip ring surface. In addition it could be argued that interfacial melting would cause both surfaces to become coated with Ag because the surface energy of Ag is less than that of Cu. Also, if Ag becomes sufficiently softer than Cu at higher temperatures, one would expect Ag to become smeared out over the contacting surfaces. Both arguments could be used to interpret the increasing Ag transfer to the slip ring with increasing current. Thus, the results of Fig. 3 are consistent with those of Fig. 2.

It is quite clear that in the present experimental setup, prow formation is not a major wear mechanism. There is only indirect evidence of its existence as seen by the layered structure of some of the wear particles (for example Fig. 1(b))which adequately explains the initial generation of the Cu particles. Apart from this, other characteristics of prow or wedge formation are not observed. Firstly, SEM investigations do not reveal any prow-like Cu particles stuck to the slip ring surface. Even if they are formed to some extent initially, they are just knocked off by the many brush wires to add to the wear debris. Secondly, the brush ends also do not reveal any Cu prows. On the other hand, small Cu particles have been detected embedded in a smooth polished Ag matrix. Prow formation necessarily requires contact only between prow and flat so that the Ag brush would not get polished. Thirdly, even after 6000 rotations of the slip ring, there is not sufficient evidence of rider wear since the majority of the wear particles in the low and intermediate currents range are pure Cu (pure Cu concentration is $\sim$ 96% at intermediate currents). The probable reason for the weak prow effect is that it requires severe sliding conditions. In the present experiment a load of only $\sim$ 40 gm is used in a lubricating atmosphere of wet CO_2. Therefore, the 'chisel' effect is the more powerful wear mechanism compared to prow formation.

It can be extrapolated from the foregoing discussion that results of higher (> 40 A) current experiments would strengthen our present understanding of the Cu-Ag system and also confirm the proposed models on the role of current. Unfortunately 40 A appears to be the upper limit for the present configuration since an attempted experiment at 50 A, 150 rpm led to severe arcing between the brushes and the slip ring after $\sim$ 5 minutes of rotation. However, the results are interesting and a brief discussion of them is given below.

The first and foremost consequence of the arcing was the creation of a groove in the initially well polished slip ring along the Ag brush track. An SEM picture of the track is shown in Fig. 4(a). Apart from the groove, round pitted regions on both sides of the track are observed. An enlarged view of one of these pits is shown in Fig. 4(b). The morphology in Fig. 4(b) strongly suggests a history of melting in the region. EPM analysis showed that the region consists of both Cu and Ag. Apparently, these pits were sites of arcing and consequent melting, in addition to the central continuous groove where the arcing was most severe. Arcing between the brushes and the slip ring can take place if and only if at any instant of time the electrical contact between the slip ring and one of the brushes is broken. The genesis of such a situation lies in the complex phenomenon of interfacial melting due to I^2R heating accompanied by the rapid rotation of the slip ring which changes the contact spots continuously. In the absence of any direct experimental evidence it could be conjectured that the interfacial molten regions smear out because of the motion of the slip ring. Subsequently, these smeared layers solidify(due to increased cooling rates caused by the enhanced contact surface area) resulting in the welding of the slip ring to the Ag brush wires. However, the slip ring, powered by the electric motor from outside, is able to break away from the welded regions. Consequently, the brush jumps off the slip ring, leading to a momentary electrical discontinuity between the slip ring and the brush. Because of the proximity of the two voltage carrying constituents, electric arcing occurs. Arcing is necessarily accompanied by intense localized heating which leads to the removal of material from both the arcing constituents. With subsequent arcing events, more and more material

would be removed in a haphazard manner resulting in rough and poorly contacting surfaces. Consequently more frequent arcing occurs. Experimentally too, the number of arcs increased with time. The groove and the bordering pits observed on the slip ring (Fig. 4(a) and 4(b)) can, therefore, be explained as a consequence of the arcing events. The light observed during such arcs is the result of ionization/deionization processes of the gaseous ambient and/or the arcing members.

Regarding the effect of arcing on the brushes, it was experimentally observed that most of the arcs were generated between one particular brush and the slip ring. The result was probably due to a poorer contact between the arcing brush and the slip ring as compared to the other one. An SEM picture of the heavily arced brush is shown in Fig. 5(a). In the top part of the picture, the different wire ends constituting the contacting brush surface can be easily differentiated. However, the lower half shows one continuous region - the result of melting and subsequent fusion of the wire ends. A number of such sites was detected and the fused regions have been found to be peculiar to only the 50 A, 150 rpm experiment. Therefore, these regions can be attributed to arcing effects; since in the other experiments,no arcs were observed. A magnified view of the fused region in Figure 5(a) is shown in Fig. 5(b). Both Cu and Ag signals were detected in an EPM trace of the regions proving thereby that both elements became intermixed during the arcing process.

In addition to the different types of wear particles observed in the lower current experiments, a new type of particle was detected in the 50 A, 150 rpm experiment. A typical SEM photograph of this type is shown in

Fig. 6(a). These particles are spherical in shape and possess a reasonably smooth surface. Consequently very little topographical contrast existed in the secondary electron picture. The specific particle shown is a mixed one, as confirmed by the EPM graph in Fig. 6(b). The lines at 2.96 keV and 8.04 keV correspond to the LαAg and KαCu excitations, repectively. The strong lines on the lower energy side of the figure are from the base Al specimen holder. However, other spherically shaped particles have been detected which belong to the pure Cu species. Such spherically shaped particles can be attributed to the arcing process. The spherical shape is the result of molten droplets which emerge from the arc and subsequently solidify into round particles because of surface tension effects.

It is almost definite that a 50 A current leads to interfacial melting, thereby causing arcing between brush and slip ring. However, if one uses the Kohlrausch relation [15] one would calculate too low an interfacial temperature. The junction resistance in all the experiments is $\sim$ 0.1 to 0.3 mΩ. With a current of 50 A, the voltage developed will be less than $\sim$ 15 mV, which is too low to cause melting. Of course, the Kohlrausch relation does not take into account frictional heating. Recently Williamson and Allen [16] have considered thermal instabilities existing at a slip ring-brush interface whereby they have shown that small current surges can raise the junction temperature from a few hundred degrees Centigrade to a few thousand degrees Centigrade. In the present experimental setup, a quantitative calculation of the temperature attained is difficult since a large number of Ag brush wires is involved, out of which only a certain number is in actual contact. However, the results especially at 50 A clearly point towards melting temperatures. Further, the

AD-A121 111 SURFACE PHYSICS AND CHEMISTRY OF ELECTRICAL CONTACT PHENOMENA(U) SYRACUSE UNIV N Y DEPT OF CHEMICAL ENGINEERING AND MATERIALS SCIENCE R W VOOK 24 SEP 82

2/2

UNCLASSIFIED 1982-1-ONR N00014-79-C-0763 F/G 20/3 NL

END

FILMED

DTIC

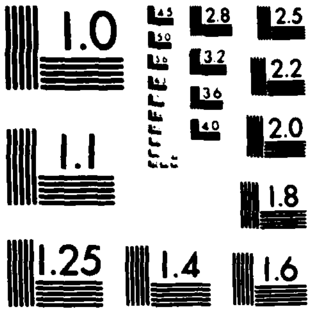

MICROCOPY RESOLUTION TEST CHART
NATIONAL BUREAU OF STANDARDS-1963-A

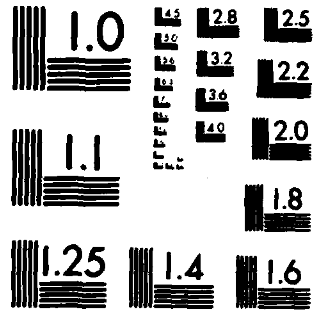

MICROCOPY RESOLUTION TEST CHART
NATIONAL BUREAU OF STANDARDS-1963-A

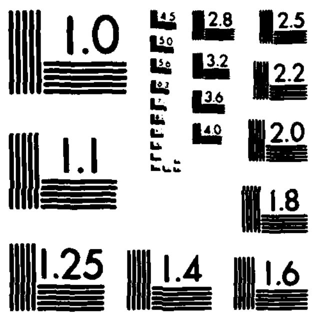

MICROCOPY RESOLUTION TEST CHART
NATIONAL BUREAU OF STANDARDS-1963-A

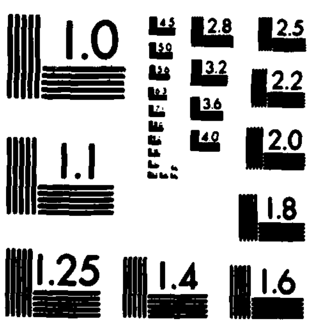

MICROCOPY RESOLUTION TEST CHART
NATIONAL BUREAU OF STANDARDS-1963-A

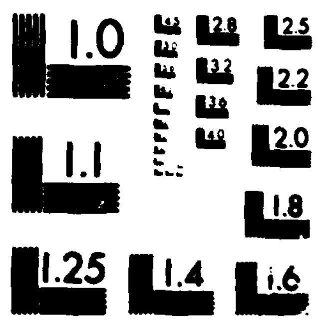

MICROCOPY RESOLUTION TEST CHART
NATIONAL BUREAU OF STANDARDS-1963-A

results in Fig. 2, even at currents greater than 10 A, strongly suggest considerable heating at the interface which leads to softening and/or partial melting conditions. Such a situation clearly explains the mixing up of Cu and Ag amongst the wear particles. It is not evident whether the brush or the slip ring surface softens more. If Ag softens at a faster rate than Cu as a function of temperature, then obviously more Ag will be transferred by adhesive wear to both the slip ring surface and the wear particles.

SUMMARY

An understanding of the role of current in wear phenomena in the rotating Cu slip ring-Ag wire brush system has been obtained. At low currents (< 100 mA), the chiselling effect is dominant and accounts for the very high Cu particle concentration in the wear debris. The wet CO_2 layer at the sliding interface acts as a lubricant, thereby reducing the fraction of Cu and Cu rich particles. In the intermediate current range (1.5 A to 5.0 A), the I^2R heating effect causes the desorption of the lubricating layer, thereby increasing the relative concentration of Cu wear particles. At high currents (> 10 A), high interfacial temperatures lead to softening and partial melting conditions. With increasing current, softening and melting effects tend to overshadow the other wear mechanisms, resulting in equal concentrations of Cu + Cu rich and Ag + Ag rich particles. Also, the transfer of Ag from the brush to the slip ring increases rapidly. At currents exceeding 40 A,melting is definite and arcing occurs between the slip ring and brushes, accompanied by rapid wear.

ACKNOWLEDGMENT

The authors are grateful to the Office of Naval Research for financial support on Contract No. N00014-79-C-0763 and to Professor D. Kuhlmann-Wilsdorf for helpful discussions.

REFERENCES

1. A. D. Sarkar, Friction and Wear, Academic, 1980, p. 33-191.
2. Donald H. Buckley, Surface Effects in Adhesion, Friction, Wear, and Lubrication, Tribology Series 5, Elsevier, 1981, p. 429-509.
3. B. Singh, J. G. Zhang, B. H. Hwang, and R. W. Vook, Wear, 78 (1982) 17.
4. R. W. Vook, J. G. Zhang, A. Banerjee, M. Garshasb, and L. R. Zhang, Proc. Holm Conf. on Electrical Contacts, I.I.T., Chicago, 1982, p. 193-199.
5. A. Banerjee, J. G. Zhang, M. Garshasb, L. R. Zhang, and R. W. Vook, Wear (in press).
6. Donald H. Buckley, Surface Effects in Adhesion, Friction, Wear, and Lubrication, Triboloby Series 5, Elsevier, 1981, p. 483-485.
7. M. Antler, Proc. Holm Conf. on Electrical Contacts, I.I.T., Chicago, 1980, p. 3-24.
8. M. Antler, Wear 7 (1964) 181.
9. J. L. Johnson and L. E. Moberly, IEEE Transac. on Components, Hybrids and Manufacturing Technol., 4 (1981) 36.
10. Ragnar Holm, Electric Contacts Theory and Application, Springer-Verlag, 1967, p. 245-248.
11. J.B.P. Williamson, Proc. Holm Conf. on Electrical Contacts, I.I.T., Chicago, 1981, p. 1-10.
12. H. N. Wagar, Physical Design of Electronic Systems, Vol. III, Bell Telephone Labs., Prentice-Hall, 1971, p. 450.
13. M. Cocks, J. Appl. Phys., 33 (1962) 2152.
14. M. P. Seah and W. A. Dench, N.P.L. Specification Chem. 1, 1978.
15. F. Kohlrausch, Ann. Phys. (Leipzig), 1 (1900) 132.
16. J. B. P. Williamson and N. Allen, Wear 78 (1982) 39.

FIGURE CAPTIONS

1. Wear particles formed in the (a) Ocurrent, 150 rpm and (b) 40 A current, 150 rpm experiments. (a) shows the chiselling and (b) the prow formation phenomena.
2. Fraction of wear particles as a function of contact current: (a) Pure Cu + Cu rich, (b) Pure Cu, (c) Mixed (Cu rich + Ag rich), and (d) Pure Ag + Ag rich.
3. Ag/Cu (60 eV) Auger peak to peak height ratio of the Cu slip ring as a function of contact current.
4. (a) SEM picture of the slip ring after the 50 A, 150 rpm experiment, and (b) magnified view of one of the molten pits of (a).
5. (a) Brush end view of the 50 A, 150 rpm experiment and (b) magnified picture of the fused region of (a).
6. (a) Wear particle formed in the 50 A, 150 rpm experiment and (b) EPM trace of the particle showing presence of both Ag and Cu.

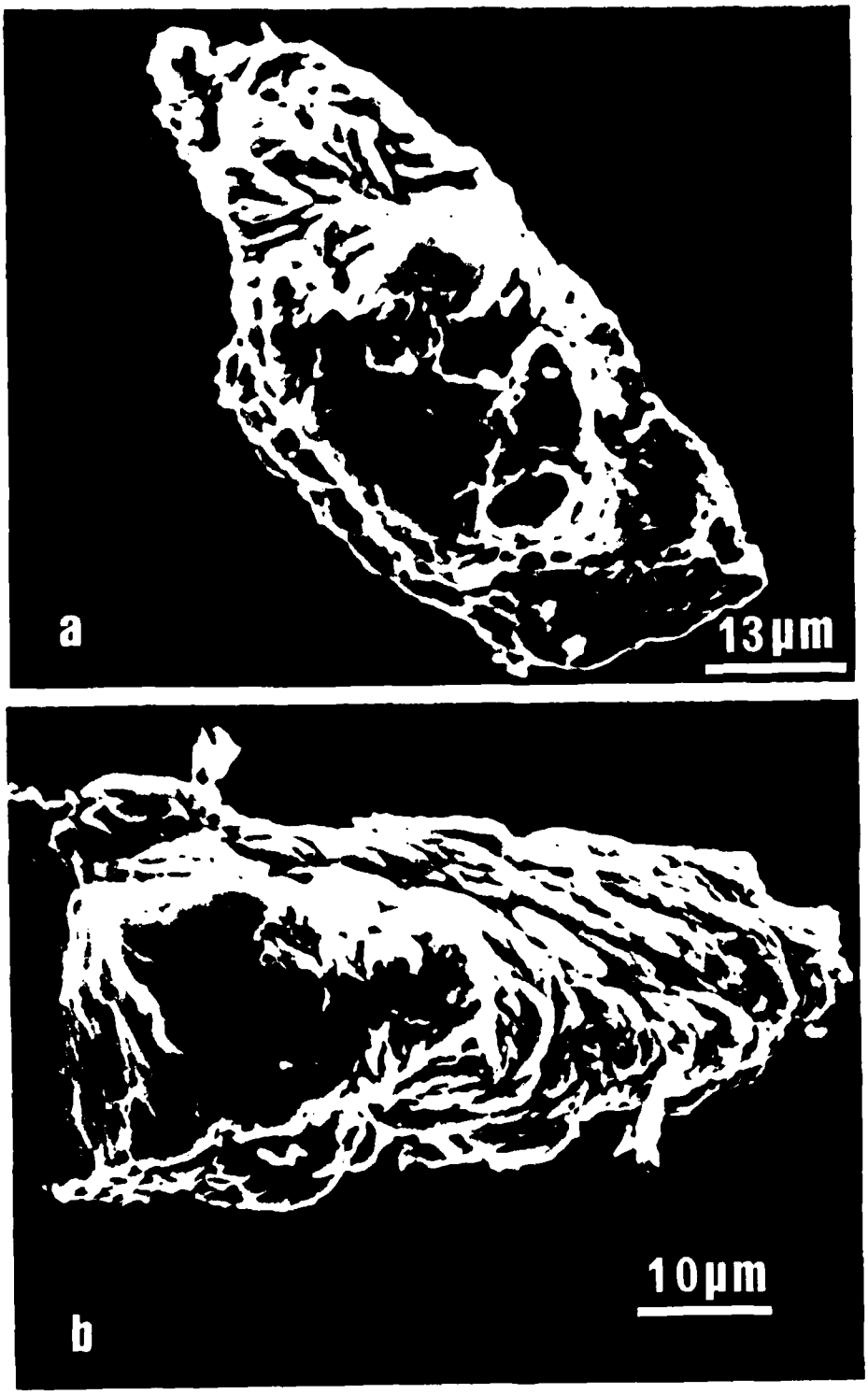

WEAR PARTICLES FORMED IN THE (a) 0 CURRENT, 150 RPM AND (b) 40 A CURRENT, 150 RPM EXPERIMENTS.

Fig. 1 of 6
A Bowman et al

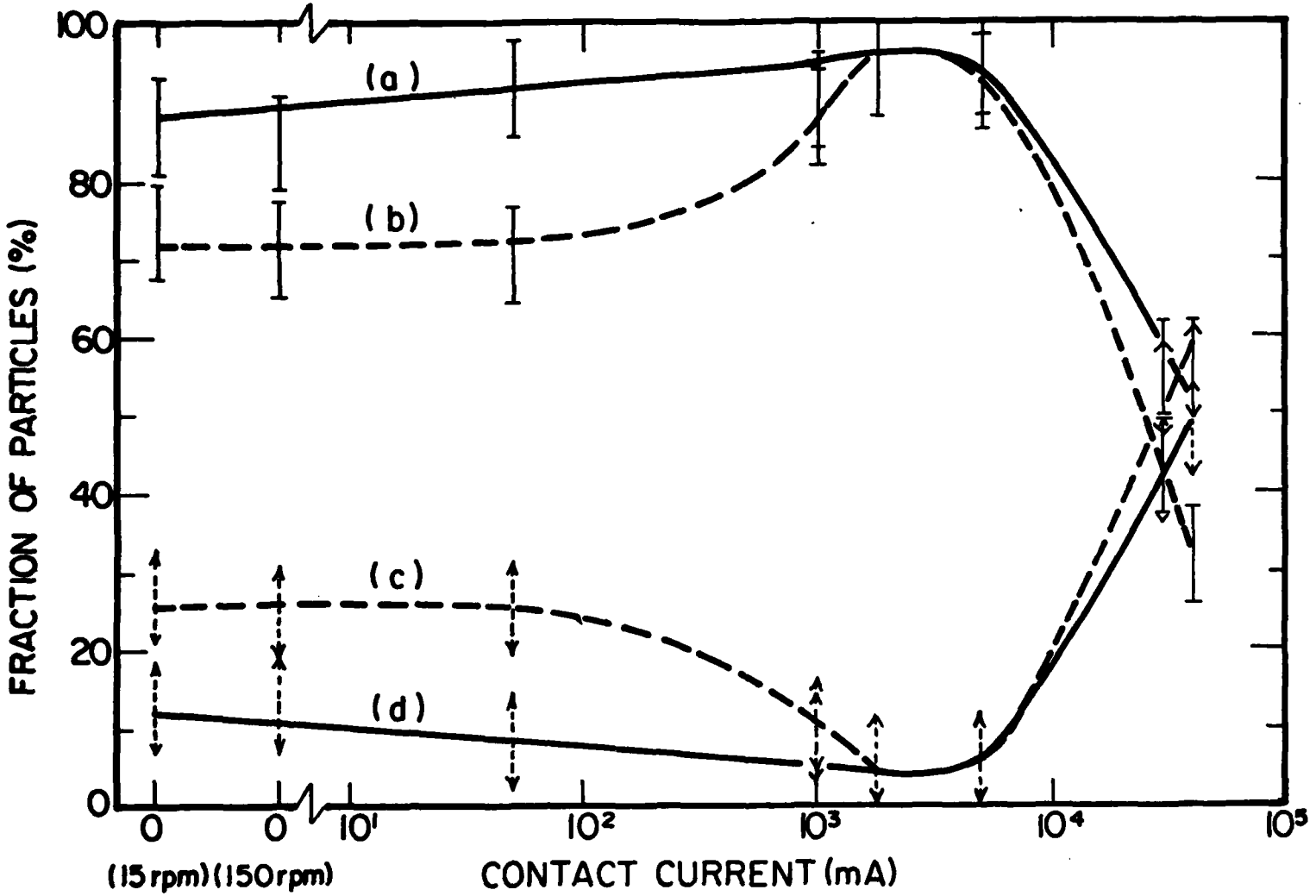

Fig 2 of 6
A Ruehijee et al

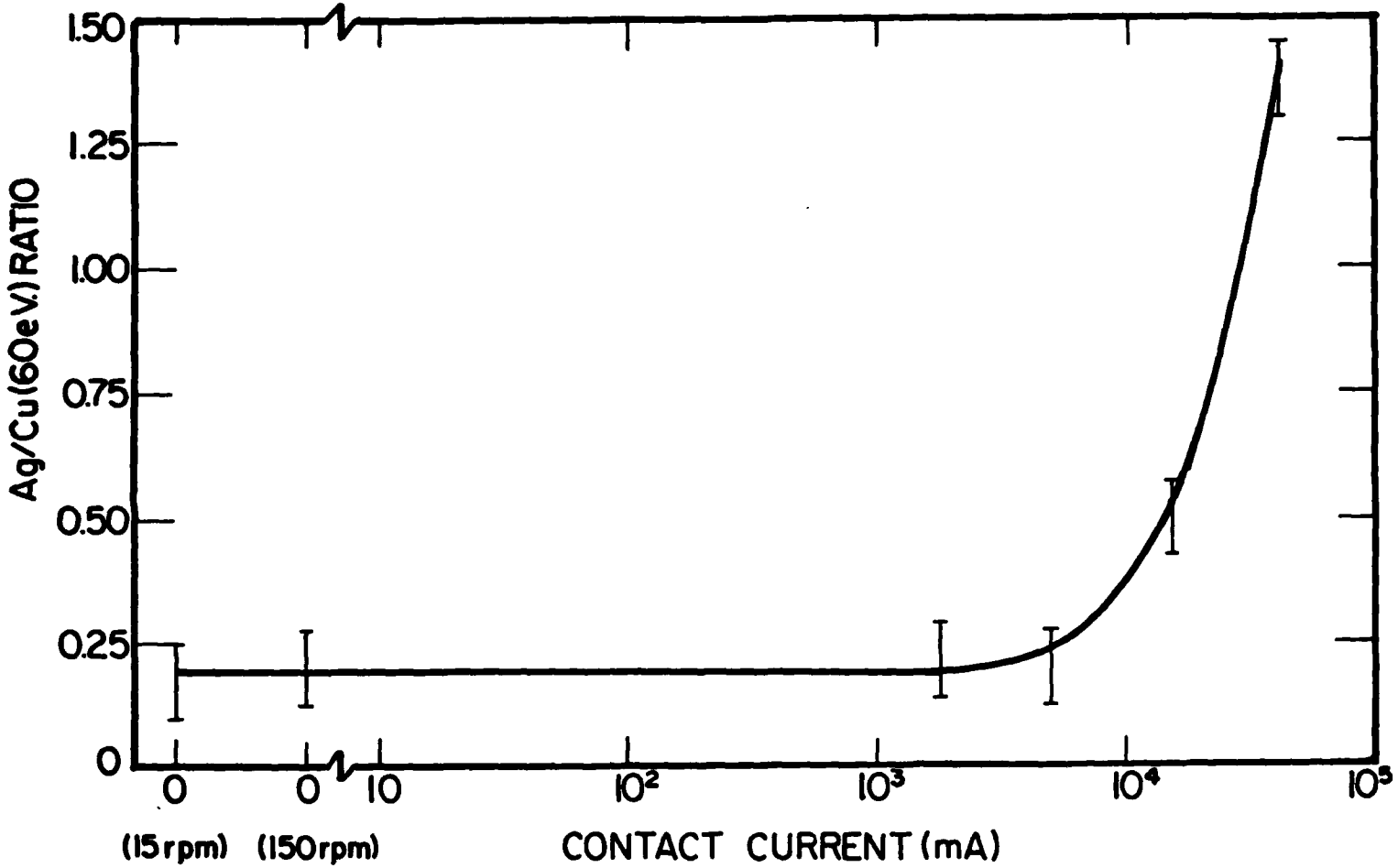

Fig 3 of 6
N. Bansal et al.

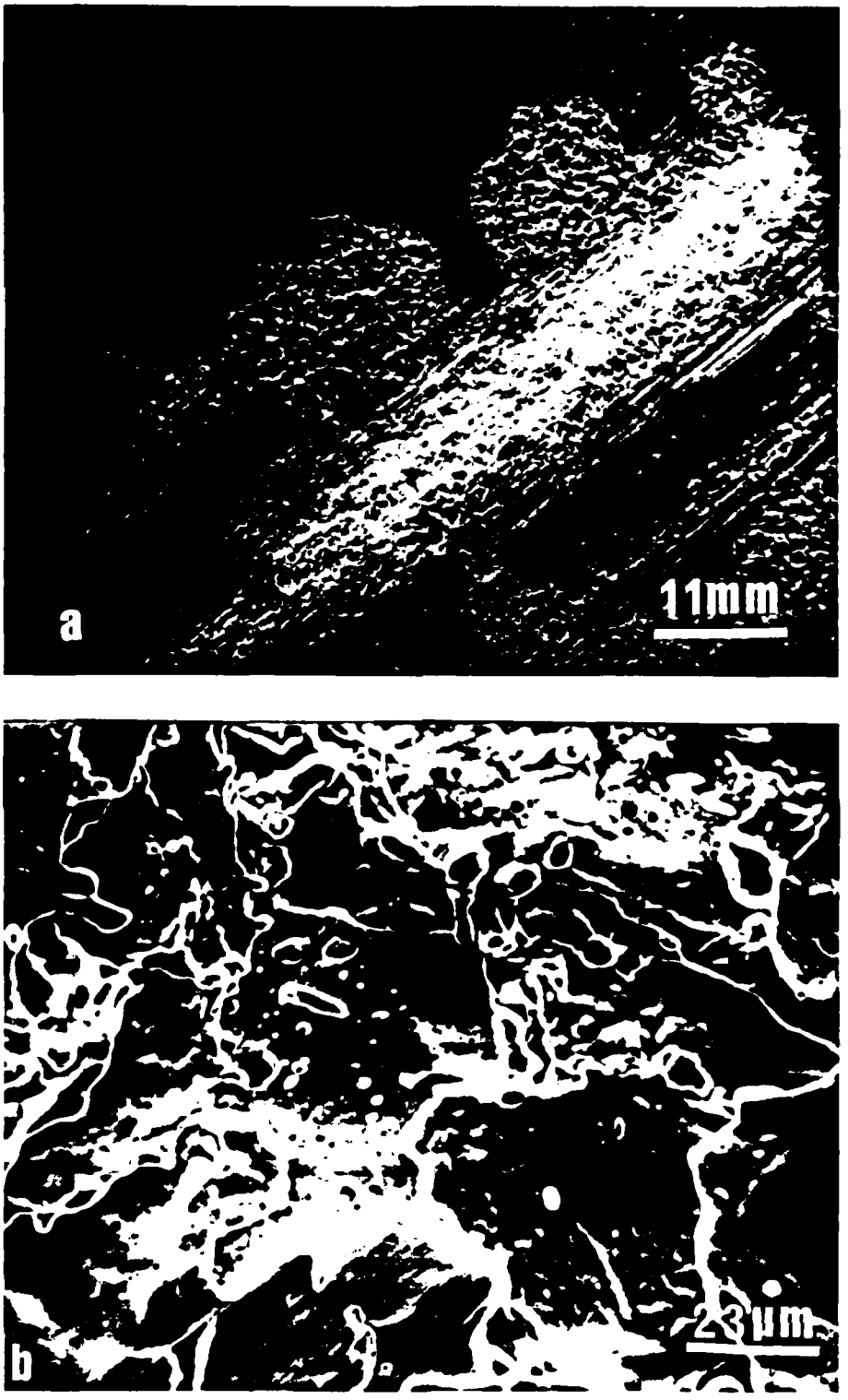

(a) SEM PICTURE OF THE SLIP RING AFTER THE 50 A, 150 RPM EXPERIMENT AND (b) MAGNIFIED VIEW OF ONE OF THE MOLTEN POINTS OF (a).

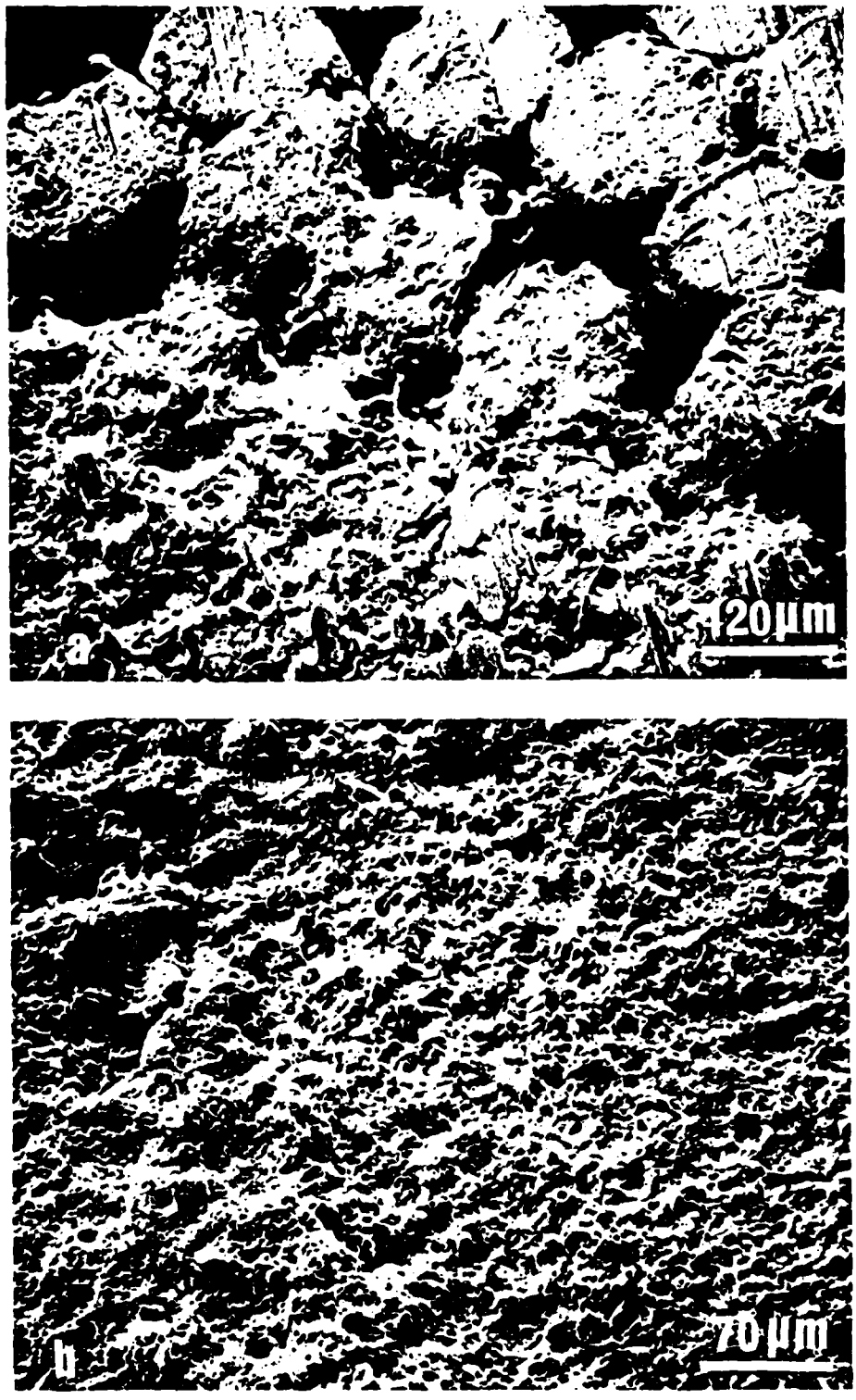

(a) BRUSH END VIEW OF THE 50 A, 150 RPM EXPERIMENT AND
(b) MAGNIFIED PICTURE OF THE FUSED REGION OF (a).

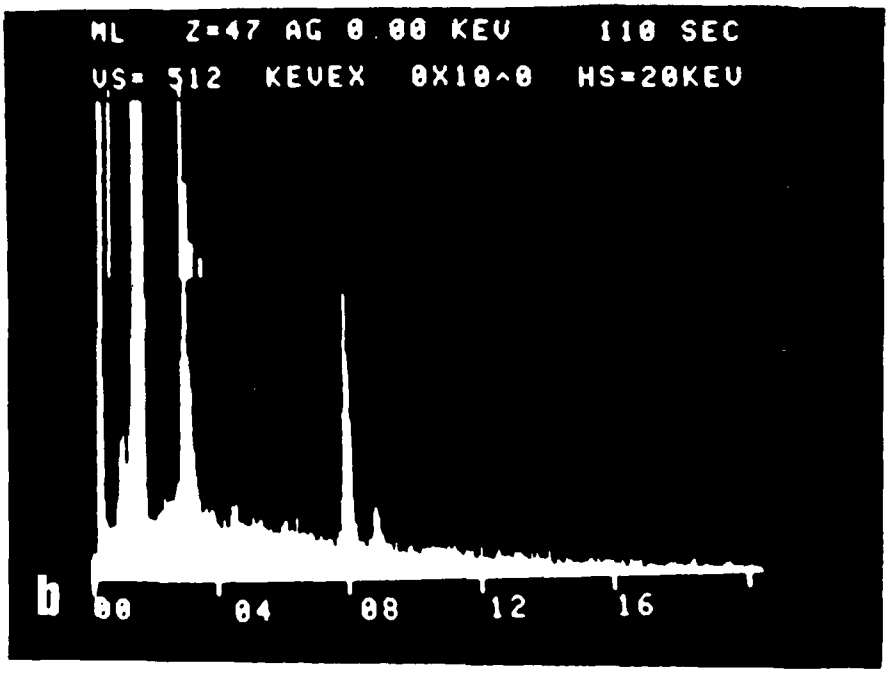

(a) WEAR PARTICLE FORMED IN THE 50 A, 150 RPM EXPERIMENT AND (b) EPM TRACE OF THE PARTICLE SHOWING PRESENCE OF BOTH AG AND CU.

Distribution List

Final Report (Classified/Unlimited and Unclassified/Limited)

1 to Sc Officer
1 to ONR Branch Office
1 to Res. Rep., ONR, Rochester
*6 to NRL Code 2627 **none to 262
*12 to DDC **two to DDC
distributions list to be furnished by Sc Officer

*Unclassified/Unlimited reports only
**Unclassified/Limited and Classified reports

Vincent A. Morano
Office of Naval Research
715 Broadway
New York, New York 10003

Dr. A. W. Ruff, Scientific Officer
Material Sciences Division
Office of Naval Research
800 North Quincy Street
Arlington, VA 22217

NRL Code 2627 (DODAAD Code N00173)
Naval Research Laboratory
Washington, D.C. 20375

DDC (DODAAD Code S47031)
Defense Documentation Center
Building 5, Cameron Station
Alexandria, VA 22314

Office of Naval Research Branch Office (DODAAD Code N62879)
666 Summer Street
Boston, MA 02210